

LETTER

Changes in forest productivity across Alaska consistent with biome shift

Pieter S. A. Beck,^{1*} Glenn P. Juday,²
 Claire Alix,³ Valerie A. Barber,²
 Stephen E. Winslow,² Emily E.
 Sousa,² Patricia Heiser,² James D.
 Herriges⁴ and Scott J. Goetz¹

Abstract

Global vegetation models predict that boreal forests are particularly sensitive to a biome shift during the 21st century. This shift would manifest itself first at the biome's margins, with evergreen forest expanding into current tundra while being replaced by grasslands or temperate forest at the biome's southern edge. We evaluated changes in forest productivity since 1982 across boreal Alaska by linking satellite estimates of primary productivity and a large tree-ring data set. Trends in both records show consistent growth increases at the boreal–tundra ecotones that contrast with drought-induced productivity declines throughout interior Alaska. These patterns support the hypothesized effects of an initiating biome shift. Ultimately, tree dispersal rates, habitat availability and the rate of future climate change, and how it changes disturbance regimes, are expected to determine where the boreal biome will undergo a gradual geographic range shift, and where a more rapid decline.

Keywords

Boreal forests, drought, evergreen forests, global warming, high latitudes, NDVI, productivity, remote sensing, tree rings.

Ecology Letters (2011)

INTRODUCTION

Over the 21st century, dynamic global vegetation models predict that the boreal biome is likely to experience forest conversion and losses resulting in a northward shift in the biome's range, particularly under scenarios of greatest warming (Lucht *et al.* 2006; Scholze *et al.* 2006; Gonzalez *et al.* 2010). As northern high latitude forest ecosystems contain at least 30% of global terrestrial carbon (McGuire *et al.* 2009; Tarnocai *et al.* 2009), such changes could substantially modify future climate (Bonan 2008). Northward and elevational shifts in species distributions over the past decades have been documented across a wide range of taxa (Hickling *et al.* 2006). At high latitudes shrub abundance has increased (Tape *et al.* 2006) and in alpine environments forest communities have recently migrated to higher elevations, apparently in response to environmental warming (Peñuelas & Boada 2003). At regional scales, however, there is little evidence of directional change in the distribution of terrestrial biomes attributable to ongoing climate change.

Model simulations of high latitude ecosystems changes in the last three decades, which experienced rising atmospheric CO₂ concentrations and associated warming (Rahmstorf *et al.* 2007), suggest an increasing vegetation productivity trend (Lucht *et al.* 2002; Kimball *et al.* 2007; Zhao & Running 2010). Analyses of satellite imagery since 1982 have generally supported this view, indicating consistent increases in gross primary productivity estimated using remote sensing (Prs; Myneni *et al.* 1997; Zhou *et al.* 2001). Recent field measured increases in tundra shrub growth over the same period are also in

agreement with model outputs (Forbes *et al.* 2010). Populations of far northern trees in cold marginal environments have sustained positive growth responses to temperature, and in recent decades have grown at their greatest recorded rates (Juday *et al.* 2005). In contrast, spatially restricted field observations have documented anomalously low white spruce (WS) [*Picea glauca* (Moench) Voss] growth in productive stands in interior Alaska in the last three decades of the 20th century (Barber *et al.* 2000). Similar observations at elevational tree line in Canada indicate that once the climate warms beyond a physiological threshold, a divergence of tree growth and air temperature occurs (D'Arrigo *et al.* 2004). A few satellite-based studies report a recent reversal of the initial (1982 through 1991) productivity gains of boreal forest across many high latitude forest areas (Angert *et al.* 2005; Goetz *et al.* 2005), but these observations have not been directly linked to field measurements.

Tree-ring measurements provide a consistent record of past productivity but are traditionally collected at ecosystem transition zones (ecotones) to test for climate sensitivity or to reconstruct climate records (D'Arrigo *et al.* 2004), rather than to capture growth trends in more typical (higher density) forest stands. As a result, comparisons of *in situ* tree growth measurements with more synoptic scale observations across large spatial domains, such as satellite data, are rare (Kaufmann *et al.* 2004). Establishing this link provides a potentially powerful way to extend relatively limited field observations to the spatial domain covered by remote sensing observations, and thus provide a comprehensive view of biome-wide productivity patterns and trends.

¹Woods Hole Research Center, Falmouth, MA 02540, USA

²School of Natural Resources and Agricultural Sciences, University of Alaska Fairbanks, Fairbanks, AK 99775, USA

³Archéologie des Amériques, NRS/Université de Paris 1 – Panthéon Sorbonne, France

⁴Bureau of Land Management, Fairbanks, AK 99709, USA

*Correspondence: E-mail: pbeck@whrc.org

Spruce species dominate the boreal forest biome of North America. We collected an extensive tree-ring width data set from WS and, for the first time, from black spruce [BS, *Picea mariana* (Mill.) B.S.P.] forest stands which, despite their dominance in boreal North America, have rarely been reported in the dendrochronology literature. The WS and BS stands span an east–west gradient from a drier continental to a more mesic maritime climate, and were sampled to capture variations in forest productivity. We compared this data set to satellite remote sensing observations of the normalized difference vegetation index (NDVI), a spectral metric reflecting gross productivity (Prs; Myneni *et al.* 1995; Goetz & Prince 1999). Spatial coherence and temporal covariance of these two very different observational records was assessed along with their interannual variability, to evaluate geographical patterns in changes in vegetation productivity over the period of their coincidence (1982–2008). Here, we investigate these patterns to test the hypothesis that the boreal biome is undergoing a range shift characterized by: (1) productivity increases at the boreal–tundra ecotone and (2) productivity declines at the warmer margin of its current distribution.

MATERIAL AND METHODS

Remotely sensed gross productivity (Prs) 1982–2008

Remotely sensed gross productivity was mapped annually from a gridded time series as the mean NDVI during the growing season, while accounting for spatial variation in the growing season length (GSL). The NASA Global Inventory Modeling and Mapping Studies data set (GIMMS-NDVI version G) spans the period 1982–2008 (<http://glcf.umiaccs.umd.edu/data/gimms/>; Tucker *et al.* 2005) at 0.07° spatial resolution. It was derived from measurements by the Advanced Very High Resolution Radiometers (AVHRRs) carried by the afternoon-viewing NOAA satellite series (NOAA 7, 9, 11, 14, 16 and 17). The data processing includes corrections for atmospheric aerosols effects from the El Chichón and Pinatubo eruptions, solar zenith angle effects and sensor differences and degradation (Tucker *et al.* 2005). GIMMS-NDVI provides 24 global NDVI images per year, with the first image of each month representing the month's first 15 days, and the other image the remainder.

We mapped Prs for each year between 1982 and 2008. First, the GSL was mapped at 30 arc-second (0.0083°) spatial resolution from the Moderate Resolution Imaging Spectroradiometer (MODIS) Land Cover Dynamics product (MOD12Q2; Zhang *et al.* 2006). Here, the GSL was initially estimated as the period between the latest 'start of greening' date, and the earliest 'start of dormancy' date recorded in the MOD12Q2 data between 2001 and 2004. To ensure exceptionally late snow melt or early snow fall events never overlapped with our growing season estimate, the initial GSL estimate was shortened by a third. The resulting maps of GSL were then averaged to the spatial and temporal resolution of the GIMMS-NDVI data to determine the GSL for each GIMMS-NDVI grid cell (see Figure S1). Next, Prs was calculated and mapped annually from GIMMS-NDVI as the mean NDVI during the growing season, using the GSL map to account for spatial variation in the GSL. To account for year-to-year variation in the start and end of the growing season, each year Prs was set to the maximum value output from a time series moving average, with window length set to GSL (Figure S2).

To map trends in Prs, the NDVI data were further filtered to mask anthropogenic changes and non-deterministic (e.g. stochastic) series.

The MODIS Land Cover map for 2005 (MOD12Q1; Friedl *et al.* 2002), with a spatial resolution of 15 arc-seconds (0.0042°), was reclassified from the International Geosphere-Biosphere Programme (IGBP) classification to (1) anthropogenic land cover, be it agricultural (IGBP-12, IGBP-14), or urban (IGBP-13), (2) non-vegetated (IGBP-0, IGBP-15, IGBP-16) or (3) vegetated (other IGBP classes). A GIMMS grid cell was excluded from the analysis if more than 40% of it was classified as non-vegetated or if vegetated land cover was not at least three times larger than anthropogenic land cover.

Patterns in Prs changes were compared with gradients of (1) tree cover as mapped in the MODIS Vegetation Continuous Fields product (MOD44; Hansen *et al.* 2003) and (2) monthly temperatures in the 1982–2008 period (McKenney *et al.* 2006). Both were gridded to match the GIMMS data set.

Burn history

In each GIMMS grid cell in Alaska and Canada, the yearly area burned was calculated from 1950 to 2007 by merging the fire perimeter data produced by the Bureau of Land Management, Alaska Fire Service (AFS; acquired from the Alaska Geospatial Data Clearinghouse, <http://agdc.usgs.gov/data/blm/fire>), and the Fire Research Group at the Canadian Forest Service.

Tree-ring sampling

We measured radial growth in 839 mature trees, of which 627 WS and 212 BS, that were dominant in the current landscape and had no visible signs of fire or insect damage. The trees were pooled to create 46 WS and 42 BS stand-level wood growth (WG) estimates, based on the GIMMS grid cell the trees were located in. The number of trees sampled in a stand varied from 1 to 62, with a median of 6. Mean stand-level growth was calculated from 1982 until the year of sampling, generating 88 series between 6 and 27 years long (median = 20) where growth and GIMMS data could be paired.

Tree-ring data were not de-trended as spruce trees of the age range in this study exhibit little to no age-related growth trend (Barber *et al.* 2000). Furthermore, Barber *et al.* (2000) showed for a subset of the current data set that de-trending had negligible effects on the growth–climate relationships. Mean radial growth was calculated per stand from non-normalized tree-ring series to preserve the greater contribution of larger trees to stand-level WG. An index of topography-related soil wetness was estimated for the tree stands from a 60-m digital elevation model, and calculated as $\ln(\alpha/\tan \beta)$ where α is the local upslope area draining through a certain point per unit contour length and $\tan \beta$ is the local slope (Beven & Kirkby 1979).

Statistical methods

Prior to mapping, temporal trends in Prs were subjected to a Vogelsang test (Vogelsang 1998) to determine if a deterministic temporal trend was present in the data (statistical significance was set at $\alpha = 0.05$). The Vogelsang stationarity test controls for the possibility of strong serial correlation in the data generating spurious trends. It is valid whether errors are stationary or have a unit root, and does not require estimates of serial correlation nuisance parameters. It is useful for masking stochastic changes in Prs in the landscape such as those associated with disturbance (Goetz *et al.* 2005).

The consistency of temporal changes in both tree growth series and Prs since 1982 was quantified and compared using Kendall's τ (Hollander & Wolfe 1973), calculated at each site from the cross-tabulation of time and radial growth (τ_{growth}), and time and Prs (τ_{Prs}). As a result, τ approaches 1 as a series consistently increases with time, and -1 as it consistently decreases with time. Agreement between trends in Prs and growth was quantified using a regression model describing τ_{growth} as a linear function of τ_{Prs} , weighted by the number of available ring width measurements. The regression included both BS and WS sites, but excluded sites with evidence of burning since 1950.

To compare year-to-year variation in Prs and growth in isolation from multi-year trends, the agreement between yearly changes in radial growth (Δgrowth) and Prs (ΔPrs) was calculated at each site using Kendall's τ , denoted as $\tau_{\Delta\text{Prs},\Delta\text{growth}}$. Agreement was calculated separately in years of increasing growth ($\Delta\text{growth} > 0$), and decreasing growth ($\Delta\text{growth} < 0$), and only if 5 years of observations were available. The agreement was then assessed for statistical significance across sites using the Wilcoxon signed rank test ($H_0: \tau_{\Delta\text{Prs},\Delta\text{growth}} = 0$).

RESULTS

Over the satellite record, which begins in 1982, within-stand variation in tree growth trends was present: 48 of 88 stands contained both trees displaying positive ($\tau_{\text{ring width}} > 0$) and negative growth trends ($\tau_{\text{ring width}} < 0$). However, mean interseries correlation of raw ring widths during the reference growth period of 1950 to date of collection was generally high [for stands with 10 trees or more, mean = 0.43 (± 0.14 SD), $N = 31$] indicating that our tree-ring based estimates of stand-level WG are robust, particularly in the larger samples.

Across boreal Alaska both WG and satellite-derived Prs predominantly declined since 1982, except in the more maritime areas of the

West (Fig. 1). Across tree-ring sites where the remote sensing data indicated non-stochastic trends in gross productivity ($N = 30$, Vogelsang test, $\alpha = 0.05$; see Table S1), yearly values of WG and Prs were strongly positively correlated and displayed a negative temporal trend between 1982 and 2008 ($R = 0.69$, $N = 27$ years, $P < 0.001$; Fig. 2). Furthermore, all but 2 of these 30 sites (13 WS and 17 BS), showed an identical direction of change in WG and Prs as measured by the signs of τ_{growth} and τ_{Prs} respectively. Across all sites without traces of fire since 1950, temporal changes in Prs since 1982 reflect commensurate changes in spruce growth [Fig. 3; $\tau_{\text{growth}} = \tau_{\text{Prs}} * 1.06(\pm 0.14 \text{ SEM}) - 0.001(\pm 0.05 \text{ SEM})$, d.f. = 55]. Overall, the best agreement in trends occurred when growth was estimated from a larger number of samples (Figure S3).

Decreases in WG relative to the previous year were weakly correlated with changes in Prs (median $\tau_{\Delta\text{Prs},\Delta\text{growth}} = 0.2$, $P = 0.002$, $N = 21$). By contrast, increases in WG from 1 year to the next were not consistently associated with equivalent increases in Prs (median $\tau_{\Delta\text{Prs},\Delta\text{growth}} = -0.05$, $P = 0.59$, $N = 21$), suggesting that resource allocation to leaf mass and WG is not necessarily regulated at identical time scales.

While the tree-rings used here were collected from mature trees in unburned stands, the satellite Prs time series reflects the legacy of wildfire. The magnitude of that effect is dependent upon the timing, extent and severity of burning (Goetz *et al.* 2006). Consequently, trends in WG and Prs may not agree in some areas characterized by vegetation mortality from fire (sudden decrease in Prs) or rapid vegetation regrowth following fire (steady increase in Prs; Figure S4). After excluding disturbance-related stochastic changes in Prs using the burn history data and the Vogelsang test (Goetz *et al.* 2005), the tundra areas of Alaska show near-ubiquitous increases in Prs (Fig. 1). The coldest boreal areas, which are currently sparsely forested, i.e. those at the boreal-tundra ecotone, also display deterministic increases in productivity over the past three decades (Fig. 4).

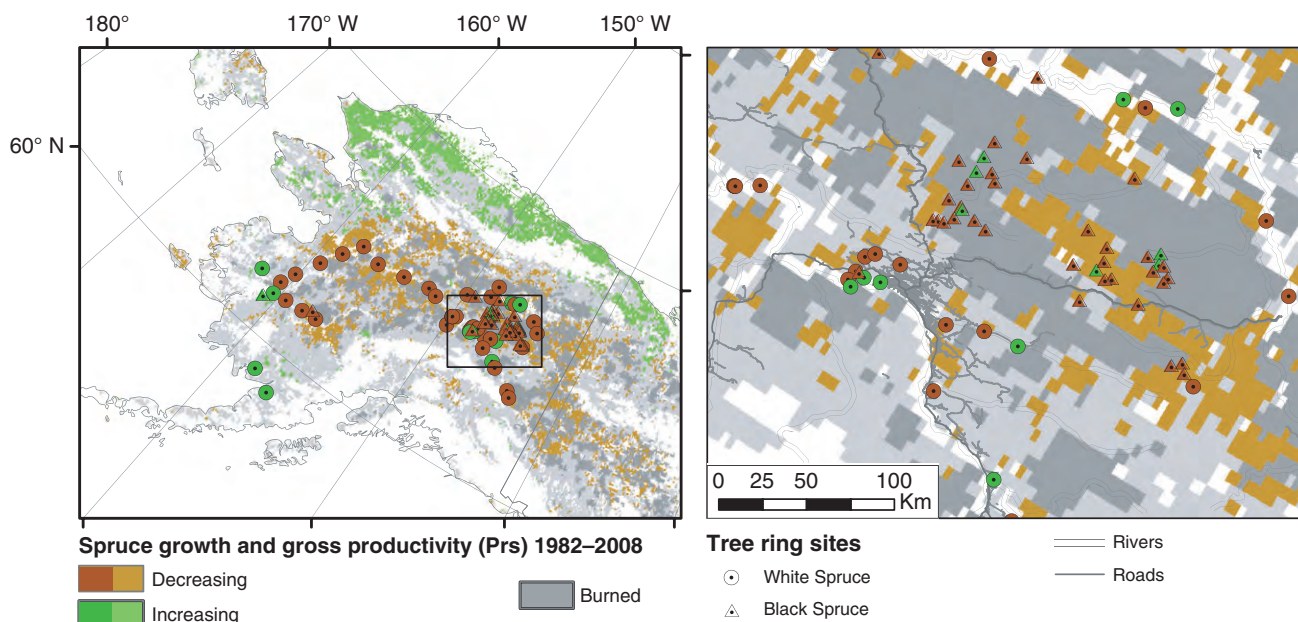


Figure 1 Trends in remotely sensed gross productivity (Prs) between 1982 and 2008 and trends in spruce growth since 1982 in Alaska (left) and the area around Fairbanks (right). White shading indicates sparsely vegetated or human modified land cover. Light grey shading indicates the trend in Prs from 1982 to 2008 was non-deterministic based on a Vogelsang significance test ($\alpha = 0.05$), and dark grey areas had wildfires anywhere between 1982 and 2007. Green and brown shading in the symbols indicate increasing and decreasing ring widths, respectively, in unburned stands from 1982 to the year of sampling which ranged from 1994 to 2008.

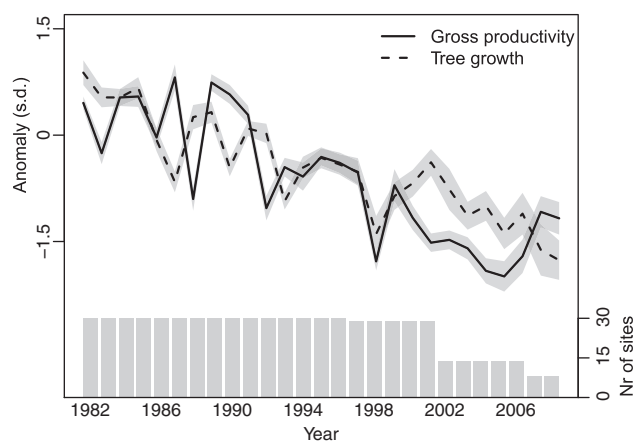


Figure 2 Trends in remotely sensed gross productivity (Prs, solid line) and radial tree growth (dashed line) at the 30 tree-ring sampling sites with deterministic changes in Prs based on a Vogelsang test ($\alpha = 0.05$; Vogelsang 1998). Anomalies are expressed in units of standard deviations (SD) from the respective means calculated over the period 1982–1996. Lines represent yearly mean anomalies across all sites and shaded areas their standard errors, both weighted by the number of trees sampled at each site.

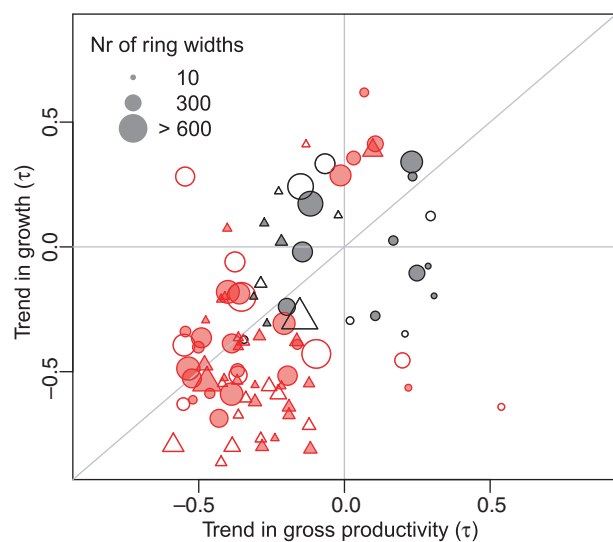


Figure 3 Temporal trends in WG and Prs. Growth is calculated from ring widths of all trees sampled within a single satellite grid cell ($\approx 64 \text{ km}^2$), and point sizes are equivalent to the number of ring widths in the series, which were restricted to years when both Prs and growth data were available. Circles represent white spruce stands and triangles black spruce stands. Open symbols indicate vegetation burning and regrowth after 1950 might have influenced Prs estimates. Red points represent cases where τ of the Prs series or the WG series were statistically different from 0 ($\alpha = 0.05$).

In contrast, all other forested areas in the boreal zone, not only the warmest or most densely forested ones, were dominated by productivity declines (Figs 1 and 4). Topographical wetness (W) did not differ significantly between sites where productivity increased or decreased, whether measured as WG or satellite-derived gross productivity (Kruskal–Wallis rank sum test, $H_0: W_{\tau_{WG}<0} = W_{\tau_{WG}>0}$, $P = 0.3$; $H_0: W_{\tau_{Prs}<0} = W_{\tau_{Prs}>0}$, $P = 0.1$; $N = 88$) and at 8 of the 10 wettest sites both measures indicated declining productivity.

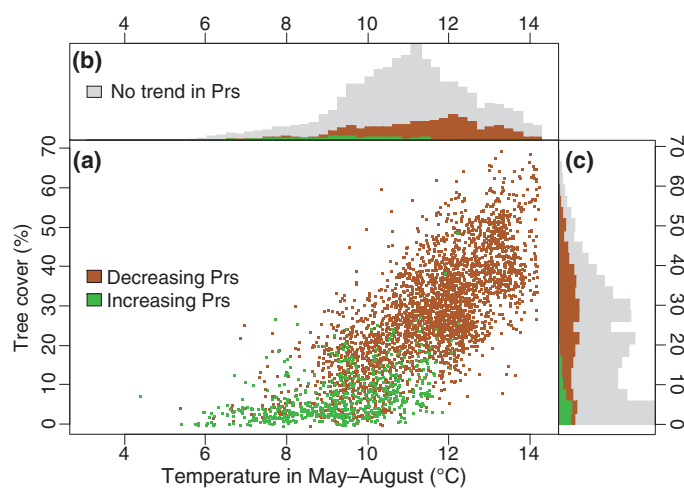


Figure 4 (a) Tree cover (Hansen *et al.* 2003) compared to mean air temperature in May–August in 1982–2007 for non-anthropogenic vegetated areas of interior Alaska, i.e. the mainland north of the Alaska Range and south of the Brooks Range. Only areas where gross productivity (Prs) shows a deterministic trend from 1982 to 2008 and where there were no wildfires between 1982 and 2007 are shown. Histograms represent the distribution of (b) temperature and (c) tree cover and include areas where no trend was detected.

DISCUSSION

Along with temperature, tropospheric ozone, nitrogen deposition and CO_2 concentrations have all increased globally in the last three decades, potentially driving shifts in vegetation productivity (IPCC 2007). Mean ozone concentrations in Alaska are low compared to more populated areas, and are generally considered to be at global 'background levels' (Figure S5; Vingarzan 2004). Because of this and the greater tolerance of needle-leaved trees to elevated ozone concentrations (Sitch *et al.* 2007; Wittig *et al.* 2009) projected increases in ozone over the 21st century are not expected to adversely affect vegetation productivity in Alaska (Sitch *et al.* 2007), and recent increases are unlikely to explain the patterns in productivity documented here. Similarly, the relatively low rates of nitrogen deposition in interior Alaska [at Denali National Park; Jones *et al.* (2005) report $0.3 \text{ kg N ha}^{-1} \text{ year}^{-1}$] are an order of magnitude lower than rates that were experimentally found to limit boreal tree growth (Hogberg *et al.* 2006). This is consistent with recent results from a process-based biogeochemistry model with coupled carbon and nitrogen cycles that indicates that over the past five decades N deposition has had a very small effect on boreal net ecosystem exchange (McGuire *et al.* 2010). These same model simulations indicate that increased atmospheric CO_2 concentrations since 1750 have promoted net uptake of carbon by arctic as well as boreal ecosystems, i.e. a CO_2 fertilization effect. At the pan-arctic scale, however, this effect appears outweighed by a stronger increase of carbon losses from the biosphere to the atmosphere due to shifts in fire disturbance and climate (mediated by combustion and temperature, moisture, and successional controls on photosynthesis and respiration), to the extent that the CO_2 fertilization is not likely to be detectable over the 30-year period investigated here (McGuire *et al.* 2010). Overall, we conclude that the productivity patterns we document in mature unburned forests are driven more by climate (temperature and moisture) than ozone, nitrogen or CO_2 fertilization effects.

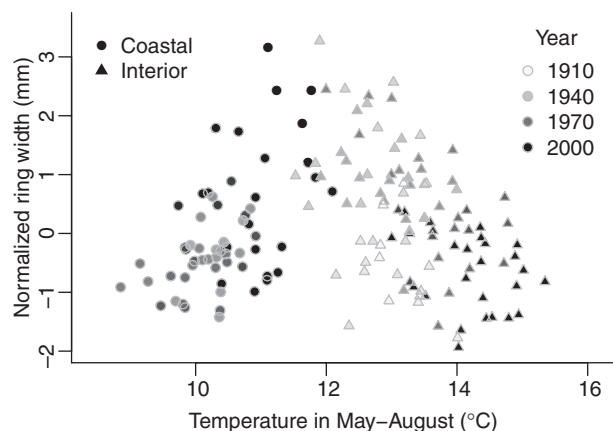


Figure 5 Normalized white spruce mean tree-ring widths at coastal and interior sites where trees were sampled in 2010 vs. mean temperature in May–August of the year of ring growth and 1 and 2 years prior. The coastal trees were sampled at Dillingham ($N = 10$) and King Salmon ($N = 8$; Table S1) and compared with the temperature record at King Salmon Airport (59°N , 157°W) which starts in 1947. The trees from interior Alaska were sampled in the Yukon River Flats ($N = 25$; Table S1) and were compared with the Fairbanks/University Experiment Station (65°N , 148°W) temperature record which is the longest one available in interior Alaska and representative of interannual variation across the region (Barber *et al.* 2000). We note that the choice for the months of May–August as a temperature index represents a compromise since seasonal temperature sensitivity differs between the sites (Figure S6).

The observed spatiotemporal pattern in productivity suggests that in colder areas temperature limitations on spruce growth have been released during the recent decades of warming, while the climate has shifted beyond the optimum for spruce growth in the warmer zones of interior Alaska (Figs 4 and 5). Earlier analysis of carbon isotopes in WS has attributed the growth declines in interior Alaska to temperature-induced drought stress (Barber *et al.* 2000). Additional analysis of BS tissue reveals an equally strong drought-induced shift in isotopic composition since the early 1980s (Fig. 6, Appendix S1), suggesting that water availability is increasingly limiting productivity of the dominant tree species in Alaskan boreal forests.

Drought in boreal forests can originate from a lack of soil moisture or an excessive evaporative demand. Although summer precipitation has been experimentally shown to limit productivity of spruce trees (Yarie 2008), it does not show a directional change in Alaska during the decades investigated here (Hinzman *et al.* 2005). Our finding that recent decreases in productivity are not restricted to upland sites, but are equally prominent in floodplains where ground water could buffer against precipitation-driven water deficits (Viereck *et al.* 1993), further indicates that soil moisture is not the main driver of the widespread declines in productivity. In contrast to soil moisture stress, evaporative demand has grown during the last decades; even during periods when temperatures were relatively stable (Figure S7). This supports our contention that observed decreases in productivity are the result of drought stress stemming from hydraulic limitations imposed by high vapour pressure deficits (VPDs) on photosynthesis during warm summer periods. Furthermore, because plant growth responds nonlinearly to both VPD and temperature, which are coupled, this observation is consistent with the temperature–growth relationship reported here (Fig. 5).

Negative productivity trends in the Alaskan boreal forest are particularly pronounced since the mid-1990s (Fig. 2), in contrast to

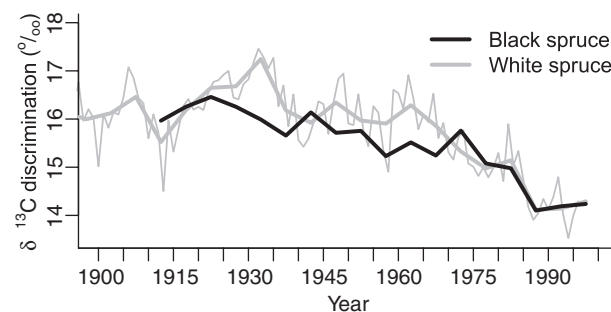


Figure 6 Stable carbon isotope ($\delta^{13}\text{C}$) time series for black spruce and white spruce stands in interior Alaska. Black spruce data were measured in the Zasada Road 8 stand at the Bonanza Creek Long-term Ecological Research (LTER) site (64.8°N , 148.0°W) following the methods described by Barber *et al.* (2000) and at 5-yearly intervals to assure sufficient wood material was available for analysis. Yearly white spruce $\delta^{13}\text{C}$ discrimination (thin grey line) was taken from Barber *et al.* (2000), measured in the Reserve West stand in the same LTER site and averaged at 5-year intervals (bold line). Isotopic discrimination is expressed as the proportional deviation of the measured $^{13}\text{C}/^{12}\text{C}$ ratio from the Peedee belemnite carbonate standard (Craig 1957).

widespread productivity increases in both forest and tundra areas in the preceding decade (Figure S8a; Myneni *et al.* 1997). Since the mid-1990s, we observe a divergent response to climate warming in Arctic tundra and forests, consistent with earlier reported NDVI trends across North America (Goetz *et al.* 2005) and Alaska (Verbyla 2008). Whereas the warmer climate has continued to increase tundra productivity, it appears to constrain photosynthetic activity in boreal forests (Fig. 1; Figure S8a). Recent global ecosystem model simulations showing increased net primary productivity in both forested and tundra areas in Alaska from 2000 to 2009 (Zhao & Running 2010) apparently fail to capture the declines we observe using satellite imagery (Figure S8b). As plant respiration generally increases with temperature, increased net productivity is at odds with the gross productivity declines we observed in undisturbed mature boreal forest. While net productivity increases are consistent with assumed metabolic responses to rising temperature in cold climates, the recent simulation results currently show no moisture limitations on Alaskan vegetation productivity (Zhao & Running 2010). In contrast, our observations indicate that the higher temperatures of recent decades have limited productivity of Alaskan forests owing to coincident increases in evaporative demand (VPD; Figure S7), which is consistent with experimental and *in situ* measurements (Barber *et al.* 2000; Hogg *et al.* 2008; Way & Oren 2010), as well as earlier model simulations (e.g. Angert *et al.* 2005; Zhang *et al.* 2008).

The observed changes in forest productivity during the period of the satellite record (27 years), and their relationship to temperature, indicate that warming has resulted in drought stress exerting an increasingly limiting role on both Prs and tree growth across most of the boreal forest ecosystem of interior Alaska. We observed increasing tree growth and Prs only in the marginal zone of low tree cover in western Alaska, which constitutes the boreal–tundra ecotone, and beyond current tree limits, both areas where 20th century temperatures were sub-optimal for tree growth. An identical pattern of shifts in boreal forest productivity has been projected by global vegetation models to occur over the course of the 21st century, leading to biome-wide changes such as northward forest expansion and regional drought-induced forest recession (Lucht *et al.* 2006; Scholze *et al.* 2006). The confluence of the current observational record with the

latter longer term projections thus provides support for the hypothesis that a biome shift is already underway on a quasi-continental scale. As long as increases in temperature persist, currently forested areas will experience intensified stress, mortality and composition changes, while the transitional ecotones of western and northern Alaska will become climatically more suitable for enhanced tree recruitment and growth associated with forest migration.

Ultimately, the resiliency of the boreal forest to climate change and the possibility for forest migration, as dictated by tree dispersal rates and habitat availability, will shape the extent and speed of a biome shift. Both the *in situ* tree ring and the satellite data presented here suggest that the climate of the last few decades has shifted beyond the physiological optimum for spruce growth throughout the Alaskan boreal ecosystem. Intensified monitoring is needed to document whether the pattern observed here will result in a rapid decline of the boreal biome rather than a more gradual geographical range shift, particularly since direct effects of climate warming on tree growth can amplify its indirect effects, e.g. through increased susceptibility to insect disturbance (Malmström & Raffa 2000). Moreover, forest expansion into tundra areas is expected to vary geographically, since it too is impacted by indirect climate effects, such as thermokarst and fire, and can be physiologically limited by drought (Lloyd *et al.* 2002; D'Arrigo *et al.* 2004). Finally, if the continued shift in the climate optimum for forest growth outpaces tree migration rates, a contraction of the boreal biome in the 21st century is more likely than a northward or elevational shift in its distribution.

ACKNOWLEDGEMENTS

We thank John Little of the Canadian Forest Service for providing the Canadian fire database, Dave McGuire for his responses to queries on biogeochemical cycles in Alaska and the anonymous referees for their constructive comments. We acknowledge support from the National Science Foundation (0902056), the NOAA Carbon Cycle Science program (NA08OAR4310526) and the NASA Carbon program (NNX08AG13G) to SJG, from the McIntire-Stennis Cooperative Forestry Research Program, the US Geological Survey Yukon River Basin program, and the US NSF Long-Term Ecological Research (LTER) Program (DEB 0620579) to GPJ, and from the French Polar Institute Paul Emile Victor (IPEV) programme 402 Anthropobois, the International Arctic Research Center (G1464, NSF ARC-0327664 and G191, NOAA NA17RJ1224), the NSF Office of Polar Programs (0436527) and the Geist Fund of the University of Alaska Museum of the North to CA.

REFERENCES

Angert, A., Biraud, S., Bonfils, C., Henning, C.C., Buermann, W., Pinzon, J. *et al.* (2005). Drier summers cancel out the CO₂ uptake enhancement induced by warmer springs. *Proc. Natl. Acad. Sci. USA*, 102, 10823–10827.

Barber, V.A., Juday, G.P. & Finney, B.P. (2000). Reduced growth of Alaskan white spruce in the twentieth century from temperature-induced drought stress. *Nature*, 406, 668–673.

Beven, K.J. & Kirkby, M.J. (1979). A physically based, variable contributing area model of basin hydrology. *Hydrol. Sci. Bull.*, 24, 43–69.

Bonan, G.B. (2008). Forests and climate change: forcings, feedbacks, and the climate benefits of forests. *Science*, 320, 1444–1449.

Craig, H. (1957). Isotopic standards for carbon and oxygen and correction factors for mass spectrometric analysis of carbon dioxide. *Geochim. Cosmochim. Acta*, 12, 133–149.

D'Arrigo, R.D., Kaufmann, R.K., Davi, N., Jacoby, G.C., Laskowski, C., Myneni, R.B. *et al.* (2004). Thresholds for warming-induced growth decline at elevational tree line in the Yukon Territory, Canada. *Global Biogeochem. Cycles*, 18, GB3021.

Forbes, B.C., Fauria, M.M. & Zetterberg, P. (2010). Russian Arctic warming and 'greening' are closely tracked by tundra shrub willows. *Glob. Change Biol.*, 16, 1542–1554.

Friedl, M.A., McIver, D.K., Hodges, J.C.F., Zhang, X.Y., Muchoney, D., Strahler, A.H. *et al.* (2002). Global land cover mapping from MODIS: algorithms and early results. *Remote Sens. Environ.*, 83, 287–302.

Goetz, S.J. & Prince, S.D. (1999). Modeling terrestrial carbon exchange and storage: evidence and implications of functional convergence in light use efficiency. *Adv. Ecol. Res.*, 28, 57–92.

Goetz, S.J., Bunn, A.G., Fiske, G.J. & Houghton, R.A. (2005). Satellite-observed photosynthetic trends across boreal North America associated with climate and fire disturbance. *Proc. Natl. Acad. Sci. USA*, 102, 13521–13525.

Goetz, S.J., Fiske, G.J. & Bunn, A.G. (2006). Using satellite time-series data sets to analyze fire disturbance and forest recovery across Canada. *Remote Sens. Environ.*, 101, 352–365.

Gonzalez, P., Neilson, R.P., Lenihan, J.M. & Drapek, R.J. (2010). Global patterns in the vulnerability of ecosystems to vegetation shifts due to climate change. *Global Ecol. Biogeogr.*, 19, 755–768.

Hansen, M.C., DeFries, R.S., Townshend, J.R.G., Carroll, M., Dimiceli, C. & Sohlberg, R.A. (2003). Global percent tree cover at a spatial resolution of 500 meters: first results of the MODIS vegetation continuous fields algorithm. *Earth Interact.*, 7, 1–15.

Hickling, R., Roy, D.B., Hill, J.K., Fox, R. & Thomas, C.D. (2006). The distributions of a wide range of taxonomic groups are expanding polewards. *Glob. Change Biol.*, 12, 450–455.

Hinzman, L., Bettez, N., Bolton, W., Chapin, F., Dyrugerov, M., Fastie, C. *et al.* (2005). Evidence and implications of recent climate change in northern Alaska and other arctic regions. *Clim. Change*, 72, 251–298.

Hogberg, P., Fan, H.B., Quist, M., Binkley, D. & Tamm, C.O. (2006). Tree growth and soil acidification in response to 30 years of experimental nitrogen loading on boreal forest. *Glob. Change Biol.*, 12, 489–499.

Hogg, E.H., Brandt, J.P. & Michaelian, M. (2008). Impact of regional drought on the productivity, dieback and biomass of western Canadian aspen forests. *Can. J. For. Res.*, 38, 1373–1384.

Hollander, M. & Wolfe, D.A. (1973). *Nonparametric Statistical Methods*. John Wiley & Sons, New York.

IPCC (2007). *Climate Change 2007: The Physical Science Basis. Contribution of Working Group I to the Fourth Assessment Report of the Intergovernmental Panel on Climate Change*. Cambridge University Press, Cambridge.

Jones, J.B.J., Petrone, K.C., Finlay, J.C., Hinzman, L.D. & Bolton, W.R. (2005). Nitrogen loss from watersheds of interior Alaska underlain with discontinuous permafrost. *Geophys. Res. Lett.*, 32, L02501.

Juday, G.P., Barber, V., Vaganov, E., Rupp, S., Sparrow, S., Yarie, J. *et al.* (2005). Forests, land management, and agriculture. In: *Arctic Climate Impact Assessment* (eds Symon, C., Arris, L. & Heal, B.). Cambridge University Press, Cambridge, pp. 781–862.

Kaufmann, R.K., D'Arrigo, R.D., Laskowski, C., Myneni, R.B., Zhou, L. & Davi, N.K. (2004). The effect of growing season and summer greenness on northern forests. *Geophys. Res. Lett.*, 31, L09205.

Kimball, J.S., Zhao, M., McGuire, A.D., Heinsch, F.A., Clein, J., Calef, M. *et al.* (2007). Recent climate-driven increases in vegetation productivity for the western Arctic: evidence of an acceleration of the northern terrestrial carbon cycle. *Earth Interact.*, 11, 0004.

Lloyd, A.H., Rupp, T.S., Fastie, C.L. & Starfield, A.M. (2002). Patterns and dynamics of treeline advance on the Seward Peninsula, Alaska. *J. Geophys. Res.-Atm.*, 107, 8161, 15 pp.

Lucht, W., Prentice, I., Myneni, R., Stith, S., Friedl, P., Cramer, W. *et al.* (2002). Climatic control of the high-latitude vegetation greening trend and Pinatubo effect. *Science*, 296, 1687–1689.

Lucht, W., Schaphoff, S., Erbrect, T., Heyder, U. & Cramer, W. (2006). Terrestrial vegetation redistribution and carbon balance under climate change. *Carbon Balance Manage.*, 1, 6, 7 pp.

Malmström, C.M. & Raffa, K.F. (2000). Biotic disturbance agents in the boreal forest: considerations for vegetation change models. *Glob. Change Biol.*, 6, 35–48.

- McGuire, A.D., Anderson, L.G., Christensen, T.R., Dallimore, S., Guo, L., Hayes, D.J. *et al.* (2009). Sensitivity of the carbon cycle in the Arctic to climate change. *Ecol. Monogr.*, 79, 523–555.
- McGuire, A.D., Ruess, R.W., Lloyd, A., Yarie, J., Klein, J.S. & Juday, G.P. (2010). Vulnerability of white spruce tree growth in interior Alaska in response to climate variability: dendrochronological, demographic, and experimental perspectives. *Can. J. For. Res.*, 40, 1197–1209.
- McKenney, D.W., Pedlar, J.H., Papadopol, P. & Hutchinson, M.F. (2006). The development of 1901–2000 historical monthly climate models for Canada and the United States. *Agr. Forest Meteorol.*, 138, 69–81.
- Myneni, R.B., Hall, F.G., Sellers, P.J. & Marshak, A.L. (1995). The interpretation of spectral vegetation indices. *IEEE Trans. Geosci. Remote Sens.*, 33, 481–486.
- Myneni, R.B., Keeling, C.D., Tucker, C.J., Asrar, G. & Nemani, R.R. (1997). Increased plant growth in the northern high latitudes from 1981–1991. *Nature*, 386, 698–702.
- Peñuelas, J. & Boada, M. (2003). A global change-induced biome shift in the Montseny mountains (NE Spain). *Glob. Change Biol.*, 9, 131–140.
- Rahmstorf, S., Cazenave, A., Church, J.A., Hansen, J.E., Keeling, R.F., Parker, D.E. *et al.* (2007). Recent climate observations compared to projections. *Science*, 316, 709.
- Scholze, M., Knorr, W., Arnell, N.W. & Prentice, I.C. (2006). A climate-change risk analysis for world ecosystems. *Proc. Natl. Acad. Sci. USA*, 103, 13116–13120.
- Sitch, S., Cox, P.M., Collins, W.J. & Huntingford, C. (2007). Indirect radiative forcing of climate change through ozone effects on the land-carbon sink. *Nature*, 448, 791–794.
- Tape, K., Sturm, M. & Racine, C. (2006). The evidence for shrub expansion in Northern Alaska and the Pan-Arctic. *Glob. Change Biol.*, 12, 686–702.
- Tarnocai, C., Canadell, J.G., Schuur, E.A.G., Kuhry, P., Mazhitova, G. & Zimov, S. (2009). Soil organic carbon pools in the northern circumpolar permafrost region. *Global Biogeochem. Cycles*, 23, GB2023.
- Tucker, C.J., Pinzon, J., Brown, M., Slayback, D., Pak, E., Mahoney, R. *et al.* (2005). Extended AVHRR 8-km NDVI data set compatible with MODIS and SPOT vegetation NDVI data. *Int. J. Remote Sens.*, 26, 4485–4498.
- Verbyla, D. (2008). The greening and browning of Alaska based on 1982–2003 satellite data. *Global Ecol. Biogeogr.*, 17, 547–555.
- Viereck, L.A., Dyrness, C.T. & Foote, M.J. (1993). An overview of vegetation and soils of the floodplain ecosystem of the Tanana River, interior Alaska. *Can. J. For. Res.*, 23, 889–898.
- Vingarzan, R. (2004). A review of surface ozone background levels and trends. *Atmos. Environ.*, 38, 3431–3442.
- Vogelsang, T.J. (1998). Trend function hypothesis testing in the presence of serial correlation. *Econometrica*, 66, 123–148.
- Way, D.A. & Oren, R. (2010). Differential responses to changes in growth temperature between trees from different functional groups and biomes: a review and synthesis of data. *Tree Physiol.*, 30, 669–688.
- Wittig, V.E., Ainsworth, E.A., Naidu, S.L., Karnosky, D.F. & Long, S.P. (2009). Quantifying the impact of current and future tropospheric ozone on tree biomass, growth, physiology and biochemistry: a quantitative meta-analysis. *Glob. Change Biol.*, 15, 396–424.
- Yarie, J. (2008). Effects of moisture limitation on tree growth in upland and floodplain forest ecosystems in interior Alaska. *For. Ecol. Manage.*, 256, 1055–1063.
- Zhang, X., Friedl, M.A. & Schaaf, C.B. (2006). Global vegetation phenology from Moderate Resolution Imaging Spectroradiometer (MODIS): evaluation of global patterns and comparison with *in situ* measurements. *J. Geophys. Res.*, 111, G04017.
- Zhang, K., Kimball, J.S., Hogg, E.H., Zhao, M., Oechel, W., Cassano, J.J. *et al.* (2008). Satellite-based model detection of recent climate-drive changes in northern high-latitude vegetation productivity. *J. Geophys. Res.*, 113, G03033, 13 pp.
- Zhao, M. & Running, S.W. (2010). Drought-induced reduction in global terrestrial net primary production from 2000 to 2009. *Science*, 329, 940–943.
- Zhou, L., Tucker, C.J., Kaufmann, R.K., Slayback, D., Shabanove, N.V. & Myneni, R.B. (2001). Variations in northern vegetation activity inferred from satellite data of vegetation index during 1981 and 1999. *J. Geophys. Res.*, 106, 20069–20083.

SUPPORTING INFORMATION

Additional Supporting Information may be found in the online version of this article:

Appendix S1 Background on the use of stable carbon isotopes in wood as indicators of drought conditions.

Figure S1 Map of growing season length in Alaska derived from Moderate Resolution Imaging Spectroradiometer (MODIS) data.

Figure S2 Theoretical example of gross productivity (Prs) calculation from yearly NDVI time series.

Figure S3 Absolute difference in trends in radial growth and remotely sensed gross productivity ($|\tau_{RG} - \tau_{Prs}|$) as a function of tree-ring sample size and area burned.

Figure S4 Time series of mean tree-ring widths and growing season NDVI for individual stands.

Figure S5 Daily tropospheric ozone measurements at Denali National Park since 1998.

Figure S6 Correlation between mean tree-ring width and monthly temperature.

Figure S7 Summer temperature and vapour pressure deficit from 1988 to 2008 at the Bonanza Creek Long Term Ecological Research site.

Figure S8 (a) Comparison of linear trends in Prs over the periods 1982–1991 and 1994–2008, and (b) the linear trend in Prs over the period 2000–2008.

Table S1 Overview of tree-ring sampling sites and observed trends in Prs.

As a service to our authors and readers, this journal provides supporting information supplied by the authors. Such materials are peer-reviewed and may be re-organized for online delivery, but are not copy edited or typeset. Technical support issues arising from supporting information (other than missing files) should be addressed to the authors.

Editor, Josep Penuelas

Manuscript received 20 September 2010

First decision made 27 October 2010

Second decision made 6 January 2011

Manuscript accepted 26 January 2011

Preliminary Report

Projected Vegetation and Fire Regime Response to Future Climate Change in Alaska



Principal Investigator

T. Scott Rupp, University of Alaska Fairbanks



Prepared for U.S. Fish and Wildlife Service

National Wildlife Refuge System

May 1, 2008



Project Overview

This project is part of a statewide model analysis of future vegetation and fire regime response to projected future climate. This work is supported by grants from the National Science Foundation and the Joint Fire Science Program. Additional support has been provided by the UA Scenarios Network for Alaska Planning (SNAP) initiative and from the University of Alaska Fairbanks, US Fish and Wildlife Service, and the National Park Service.

This document provides a summary of preliminary simulation results and a discussion of ongoing modeling activities aimed at providing definitive statewide simulation results. In addition, simulation model details and references are included.

Model Simulations Design

The model simulations design (Fig. 1) provides for the analysis of historical fire activity by (1) simulating historic fires (1860-2007) based on an empirically derived relationship between climate and fire (Duffy et al. 2005), and (2) linking simulated historic fires (1860-1949), based on the empirical climate-fire relationship, with known fire perimeters (1950-2007; <http://agdc.usgs.gov/data/blm/fire/index.html>). The historical simulation results for both methodologies will then be applied to a suite of 6 future climate scenarios (2008-2099) and three emission scenarios (A1B, A1, and B2; see IPCC 2007). This report presents preliminary results for only the A1B emission scenario.

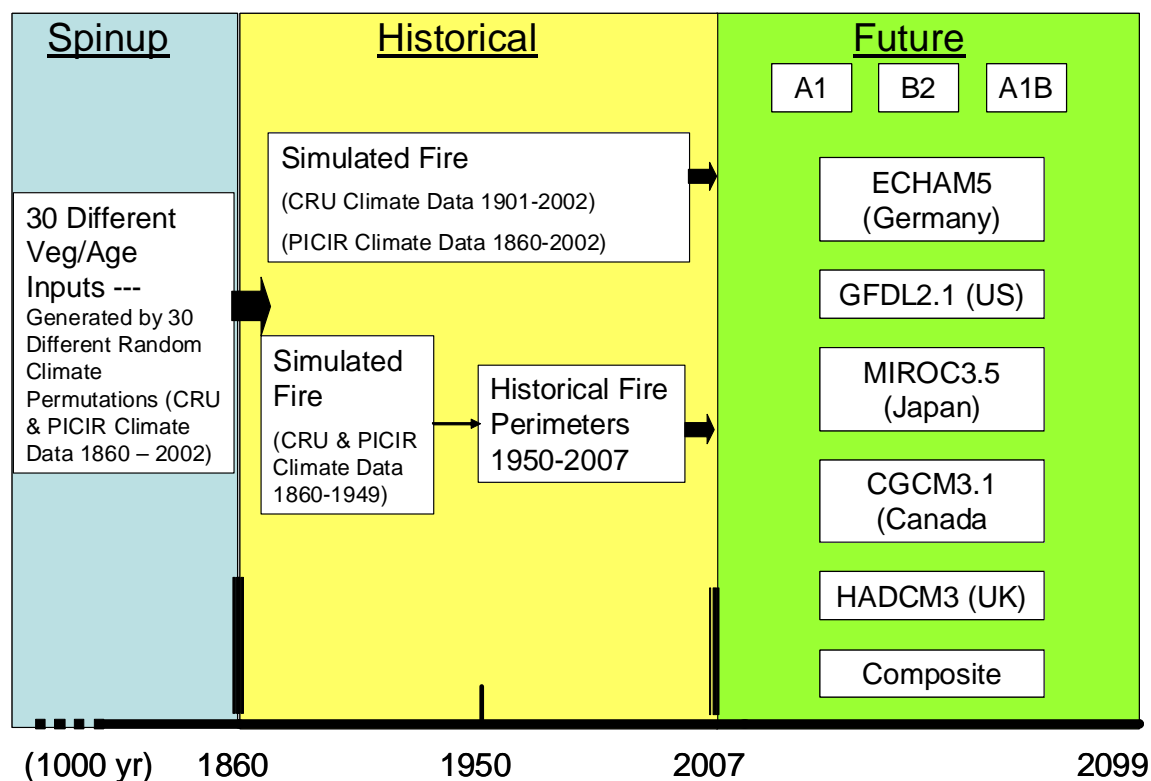


Figure 1 – Schematic showing the model simulation design.

The simulation design ultimately allows for statewide simulations (Fig. 2) of both historical simulation methodologies (2x) to be driven by 6 future climate scenarios (6x) for each of 3 emissions scenarios (3x) for a total of 36 (2x6x3) ensemble runs. Each preliminary ensemble run contains 8 replicated simulations (30 replications to be completed in the final analysis). In all simulations historic climate (1860-2002) was generated using spatially explicit input data from the Climate Research Unit (CRU; <http://www.cru.uea.ac.uk/>) and the Potsdam Institute for Climate Impact Research (PICIR). The PICAR dataset is a modified version of that presented in Leemans and Cramer (1991). The modification is presented in McGuire et al. (2001).

The 'spin-up' phase of the modeling generated 30 different initial landscape conditions (vegetation distribution and age structure) at 1860 by using 30 random permutations of historic climate observations from the CRU and PICIR datasets. These landscapes provide the starting-point (1860) conditions that ALFRESCO uses as input for the simulations. The purpose of the 'spin-up' phase is to produce a simulation landscape with realistic patch size and age-class distributions that are generated over multiple fire cycles.

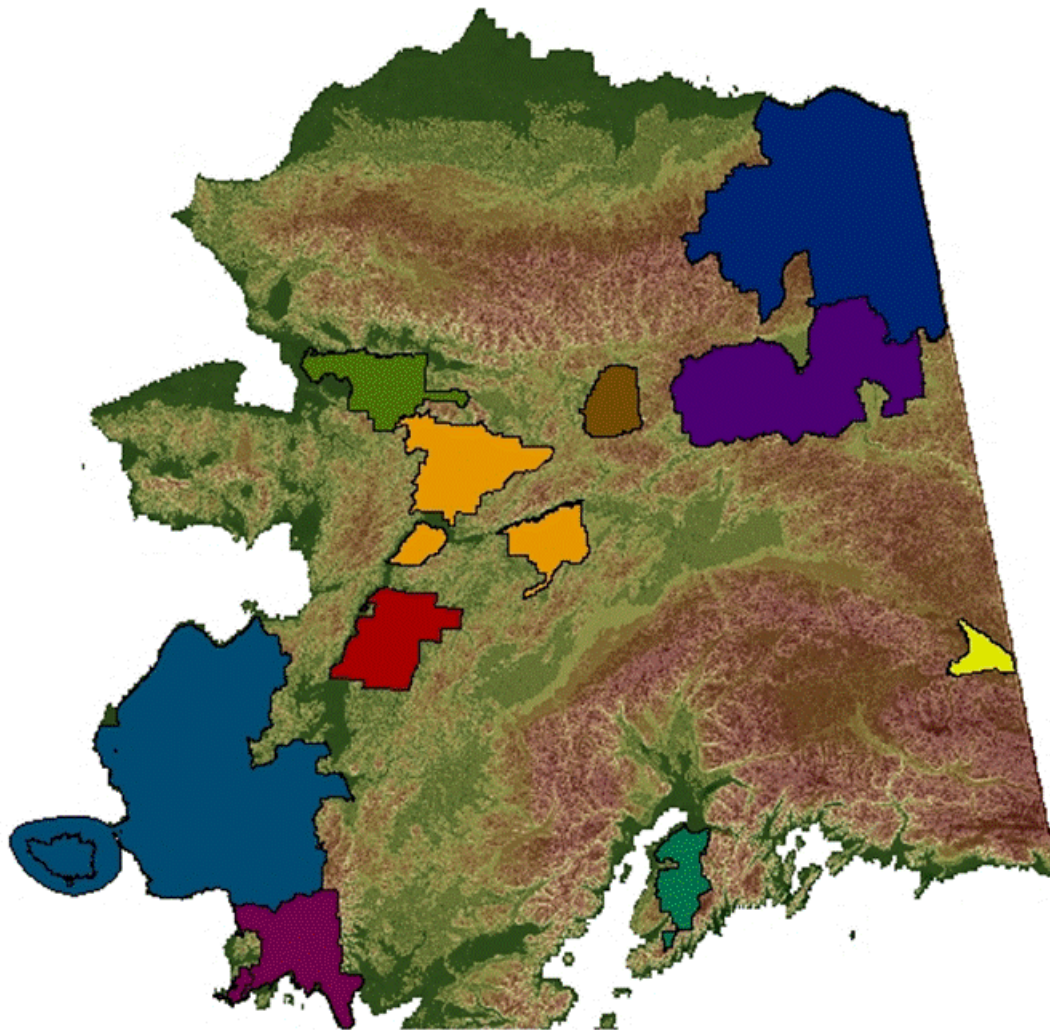


Figure 2 – Statewide simulation domain with refuge boundaries identified.

ALFRESCO Model Overview

ALFRESCO was originally developed to simulate the response of subarctic vegetation to a changing climate and disturbance regime (Rupp et al. 2000a, 2000b). Previous research has highlighted both direct and indirect (through changes in fire regime) effects of climate on the expansion rate, species composition, and extent of treeline in Alaska (Rupp et al. 2000b, 2001, Lloyd et al. 2003). Additional research, focused on boreal forest vegetation dynamics, has emphasized that fire frequency changes – both direct (climate-driven or anthropogenic) and indirect (as a result of vegetation succession and species composition) – strongly influence landscape-level vegetation patterns and associated feedbacks to future fire regime (Rupp et al. 2002, Chapin et al. 2003, Turner et al. 2003). A detailed description of ALFRESCO can be obtained from the literature (Rupp et al. 2000a, 2000b, 2001, 2002). The boreal forest version of ALFRESCO was developed to explore the interactions and feedbacks between fire, climate, and vegetation in interior Alaska (Rupp et al. 2002, 2007, Duffy et al. 2005, 2007) and associated impacts to natural resources (Rupp et al. 2006, Butler et al. 2007).

ALFRESCO is a state-and-transition model of successional dynamics that explicitly represents the spatial processes of fire and vegetation recruitment across the landscape (Fig. 3; Rupp et al. 2000a). ALFRESCO does not model fire behavior, but rather models the empirical relationship between growing-season climate (e.g., average temperature and total precipitation) and total annual area burned (i.e., the footprint of fire on the landscape). ALFRESCO also models the changes in vegetation flammability that occur during succession through a flammability coefficient that changes with vegetation type and stand age (Chapin et al. 2003).

The fire regime is simulated stochastically and is driven by climate, vegetation type, and time since last fire (Rupp et al. 2000a, 2007). ALFRESCO employs a cellular automaton approach, where an ignited pixel may spread to any of the eight surrounding pixels. 'Ignition' of a pixel is determined using a random number generator and as a function of the flammability value of that pixel. Fire 'spread' depends on the flammability of the receptor pixel and any effects of natural firebreaks including non-vegetated mountain slopes and large water bodies, which do not burn.

The ecosystem types modeled were chosen as the simplest possible representation of the complex vegetation mosaic occupying the circumpolar arctic and boreal zones and ignore the substantial variation in species composition within these and other intermediate vegetation types. Detailed descriptions of the vegetation states and classification methodology can be found in Rupp et al. (2000a, 2000b, 2001, 2002). The vegetation data used in the model spinup process was derived by reclassifying the 1990 AVHRR vegetation classification (<http://agdcftp1.wr.usgs.gov/pub/projects/fhm/vegcls.tar.gz>) and the 2001 National Land Cover Database vegetation classification (<http://www.mrlc.gov>) into the five vegetation classes represented in ALFRESCO (tundra, black spruce, white spruce, deciduous, and dry grassland). Currently, the dry grassland ecosystem type represented in ALFRESCO occurs only locally and at a scale masked by the model's 1 x 1 km pixel resolution. Differences among tundra vegetation types recognized in the vegetation classifications were ignored, and all tundra types were lumped together as a single tundra class. Tundra types that identified some level of spruce canopy on site were indicated. The actual spruce-canopy level was determined using growing-season climate thresholds.

Remotely sensed satellite data is currently unable to distinguish species-level differences between black and white spruce. We therefore stratified spruce forest using deterministic rules related to topography (i.e., aspect, slope position, and elevation) and growing-season climate. Aspect and slope were used to identify ‘typical’ black spruce forest sites (i.e., poorly drained and northerly aspects) throughout the study region. Growing-season climate and elevation were used primarily to distinguish treeline white spruce forest. In addition, we used growing-season climate thresholds to distinguish young deciduous forest stands from tall shrub tundra. These deterministic rules were also used to denote the climax vegetation state (i.e., black or white spruce forest) for each deciduous pixel. In other words, the rules were used to predetermine the successional trajectory of each deciduous pixel. In this manner, we were able to develop an input vegetation data set that best related the original remotely sensed data into the five vegetation types represented by ALFRESCO, based on a sensible ecological foundation.

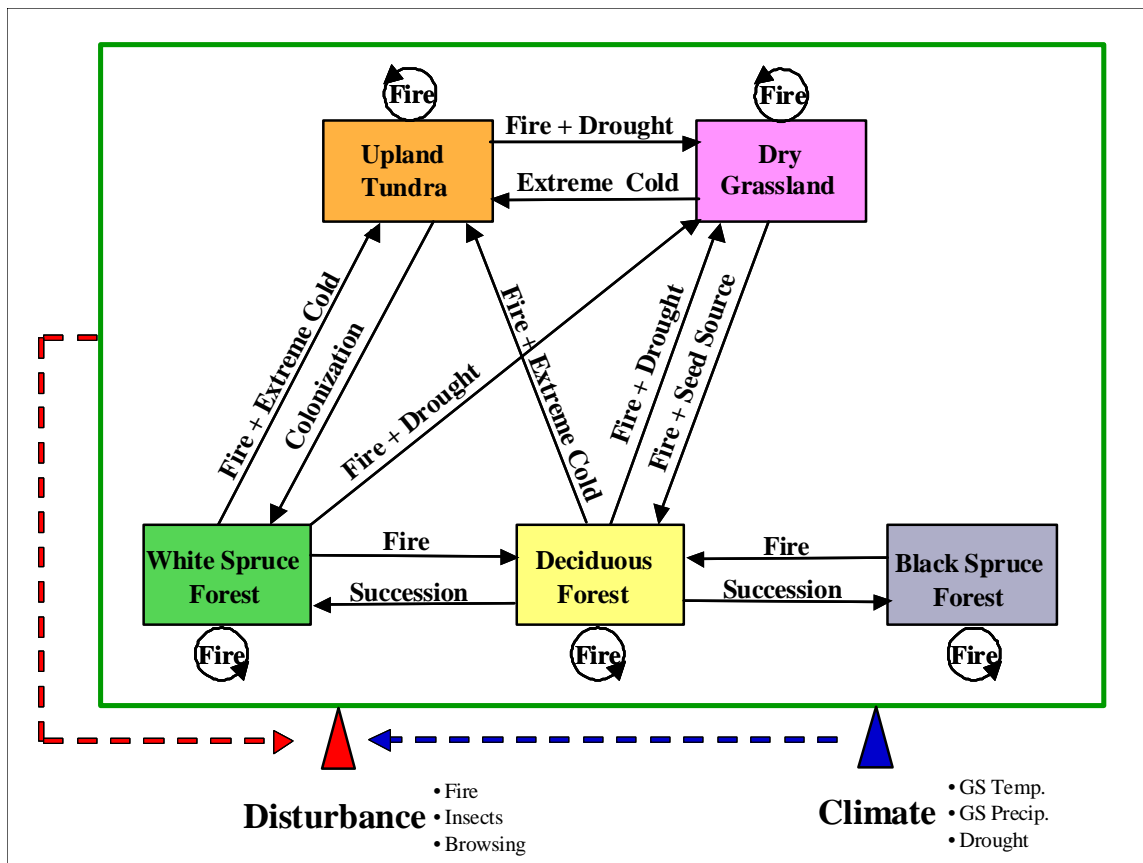


Figure 3 – Conceptual model of vegetation states (colored boxes), possible transitions (arrows), and driving processes/factors responsible for the rate and direction of transitions (arrow labels). **Dynamic treeline transitions and the dry grassland state were not activated for the preliminary simulations.**

Version 1.0.1 can operate at any time step and pixel resolution, however the current model calibration and parameterization was conducted at an annual time step and 1 km² pixel resolution. A 30 m² calibration and parameterization is currently underway. Other model developments include refined tundra transition stages, fire suppression effects on fire size, simulated fire severity patterns and fire severity effects on successional rates and trajectories. New iterations of the boreal ALFRESCO simulation model with these developments will be available beginning in 2009.

Driving Climate Products

The simulation design for this project utilizes climate projections that have been assessed and downscaled by the UA Scenarios Network for Alaska Planning (SNAP).

Use of GCMs to model future climate

General Circulation Models (GCMs) are the most widely used tools for projections of global climate change over the timescale of a century. Periodic assessments by the Intergovernmental Panel on Climate Change (IPCC) have relied heavily on global model simulations of future climate driven by various emission scenarios.

The IPCC uses complex coupled atmospheric and oceanic GCMs. These models integrate multiple equations, typically including surface pressure; horizontal layered components of fluid velocity and temperature; solar short wave radiation and terrestrial infra-red and long wave radiation; convection; land surface processes; albedo; hydrology; cloud cover; and sea ice dynamics.

GCMs include equations that are iterated over a series of discrete time steps as well as equations that are evaluated simultaneously. Anthropogenic inputs such as changes in atmospheric greenhouse gases can be incorporated into stepped equations. Thus, GCMs can be used to simulate the changes that may occur over long time frames due to the release of greenhouse gases into the atmosphere.

Greenhouse gas-driven climate change represents a response to the radiative forcing associated with increases of carbon dioxide, methane, water vapor and other gases, as well as associated changes in cloudiness. The response varies widely among models because it is strongly modified by feedbacks involving clouds, the cryosphere, water vapor and other processes whose effects are not well understood. Changes in the radiative forcing associated with increasing greenhouse gases have thus far been small relative to existing seasonal cycles. Thus, the ability of a model to accurately replicate seasonal radiative forcing is a good test of its ability to predict anthropogenic radiative forcing.

Model Selection

Different coupled GCMs have different strengths and weaknesses, and some can be expected to perform better than others for northern regions of the globe.

SNAP principle investigator Dr. John Walsh and colleagues evaluated the performance of a set of fifteen global climate models used in the Coupled Model Intercomparison Project. Using the outputs for the A1B (intermediate) climate change scenario, they calculated the degree to which each model's output concurred with actual climate data for the years 1958-2000 for each of three climatic variables (surface air temperature, air pressure at sea level, and precipitation) for three overlapping regions (Alaska only, 60-90 degrees north latitude, and 20-90 degrees north latitude.)

The core statistic of the validation was a root-mean-square error (RMSE) evaluation of the differences between mean model output for each grid point and calendar month, and data from the European Centre for Medium-Range Weather Forecasts (ECMWF) Re-Analysis, ERA-40. The ERA-40 directly assimilates observed air temperature and sea level pressure observations into a product spanning 1958-2000. Precipitation is

computed by the model used in the data assimilation. The ERA-40 is one of the most consistent and accurate gridded representations of these variables available. To facilitate GCM intercomparison and validation against the ERA-40 data, all monthly fields of GCM temperature, precipitation and sea level pressure were interpolated to the common 2.5° × 2.5° latitude–longitude ERA-40 grid. For each model, Walsh and colleagues calculated RMSEs for each month, each climatic feature, and each region, then added the 108 resulting values (12 months x 3 features x 3 regions) to create a composite score for each model (Table 1). A lower score indicated better model performance.

Overall Rank	Model	Alaska temperature	Greenland temperature	60-90° N temperature	20-90° N temperature	Alaska precipitation	Greenland precipitation	60-90° N precipitation	20-90° N precipitation	Alaska sea level pressure	Greenland sea level pressure	60-90° N sea level pressure	20-90° N sea level pressure	Integrated Rank Index
1	MPI_ECHAM5	13	02	01	01	05	03	03	03	01	02	01	01	36
2	GFDL_CM2_1	06	01	03	05	02	01	01	02	05	04	04	02	39
3	MIROC3_2_MEDRES	02	03	04	03	07	04	06	08	10	01	03	05	56
4	UKMO_HADCM3	11	04	08	06	03	02	02	09	04	05	06	07	67
5	CCCMA_CGCM3_1	12	11	11	10	04	13	08	02	08	03	02	04	88
6	GFDL_CM2_0	06	09	09	14	01	09	10	06	04	08	08	04	88
7	MRI_CGM2_3_2A	11	14	13	07	06	06	05	04	02	10	11	06	95
8	NCAR_CCSM3_0	08	06	02	02	09	05	08	07	15	11	15	13	101
9	CNRM_CM3	01	07	05	05	12	08	12	13	07	12	12	11	105
10	NCAR_PCM1	14	10	13	14	08	10	05	10	06	06	05	12	113
11	CSIRO_MK3_0	06	12	14	12	11	12	11	05	11	07	09	09	119
12	INMCM3_0	07	13	06	10	10	14	13	12	09	09	07	09	119
13	IPSL_CM4	11	08	07	12	13	07	09	11	14	14	11	15	139
14	GISS_MODEL_ER	06	05	10	10	14	11	14	15	13	15	14	14	141
15	IAP_FGOALS1_0_G	15	15	15	15	15	15	15	14	12	13	13	10	167

Table 1 – Component and overall ranking of the 15 GCMs evaluated from the IPCC 4th assessment. The top five models were chosen as performing best over Alaska.

The specific models that performed best over the larger domains tended to be the ones that performed best over Alaska. Although biases in the annual mean of each model typically accounted for about half of the models' RMSEs, the systematic errors differed considerably among the models. There was a tendency for the models with the smaller errors to simulate a larger greenhouse warming over the Arctic, as well as larger increases of Arctic precipitation and decreases of Arctic sea level pressure when greenhouse gas concentrations are increased.

Since several models had substantially smaller systematic errors than the other models, the differences in greenhouse projections implied that the choice of a subset of models might offer a viable approach to narrowing the uncertainty and obtaining more robust estimates of future climate change in regions such as Alaska. Thus, SNAP selected the five best-performing models out of the fifteen: MPI_ECHAM5, GFDL_CM2_1, MIROC3_2_MEDRES, UKMO_HADCM3, and CCCMA_CGCM3_1. These five models are used to generate climate projections independently, as well as in combination (i.e.,

composite), in order to further reduce the error associated with dependence on a single model.

Downscaling model outputs

Because of the mathematical complexity of GCMs, they generally provide only large-scale output, with grid cells typically 1°-5° latitude and longitude. For example, the standard resolution of HadCM3 is 1.25 degrees in latitude and longitude, with 20 vertical levels, leading to approximately 1,500,000 variables.

Finer scale projections of future conditions are not directly available. However, local topography can have profound effects on climate at much finer scales, and almost all land management decisions are made at much finer scales. Thus, some form of downscaling is necessary in order to make GCMs useful tools for regional climate change planning.

Historical climate data estimates at 2 km resolution are available from PRISM (Parameter-elevation Regressions on Independent Slopes Model), which was originally developed to address the lack of climate observations in mountainous regions or rural areas. PRISM uses point measurements of climate data and a digital elevation model to generate estimates of annual, monthly and event-based climatic elements. Climatic elements for each grid cell are estimated via multiple regression using data from many nearby climate stations. Stations are weighted based on distance, elevation, vertical layer, topographic facet, and coastal proximity.

PRISM offers data at a fine scale that is useful to land managers and communities, but it does not offer climate projections. Thus, SNAP needed to link PRISM to the GCM outputs. This work was also performed by PI Walsh and colleagues. They first calculated mean monthly precipitation and mean monthly surface air temperature for PRISM grid cells for 1961-1990, creating PRISM baseline values. Next, they calculated GCM baseline values for each of the five selected models using mean monthly outputs for 1961-1990. They then calculated differences between projected GCM values and baseline GCM values for each year out to 2099 and created “anomaly grids” representing these differences. Finally, they added these anomaly grids to PRISM baseline values, thus creating fine-scale (2 km) grids for monthly mean temperature and precipitation for every year out to 2099. This method effectively removed model biases while scaling down the GCM projections.

Statewide Driving Climate Summary

Climate data can soon be accessed through SNAP (www.snap.uaf.edu) in tabular form, as graphs, or as maps (GIS layers and KML files) depicting the whole state of Alaska or part of the state. Currently, tables or graphs of mean monthly temperature and precipitation projections by decade are available for 353 communities in Alaska. Statewide GIS layers of mean monthly temperature and total precipitation for each year out to 2099 are also currently available and were used to develop the input data sets used in this project.

The following time series graphs and maps provide examples of the types of summary information that can be generated for any defined region within the state.

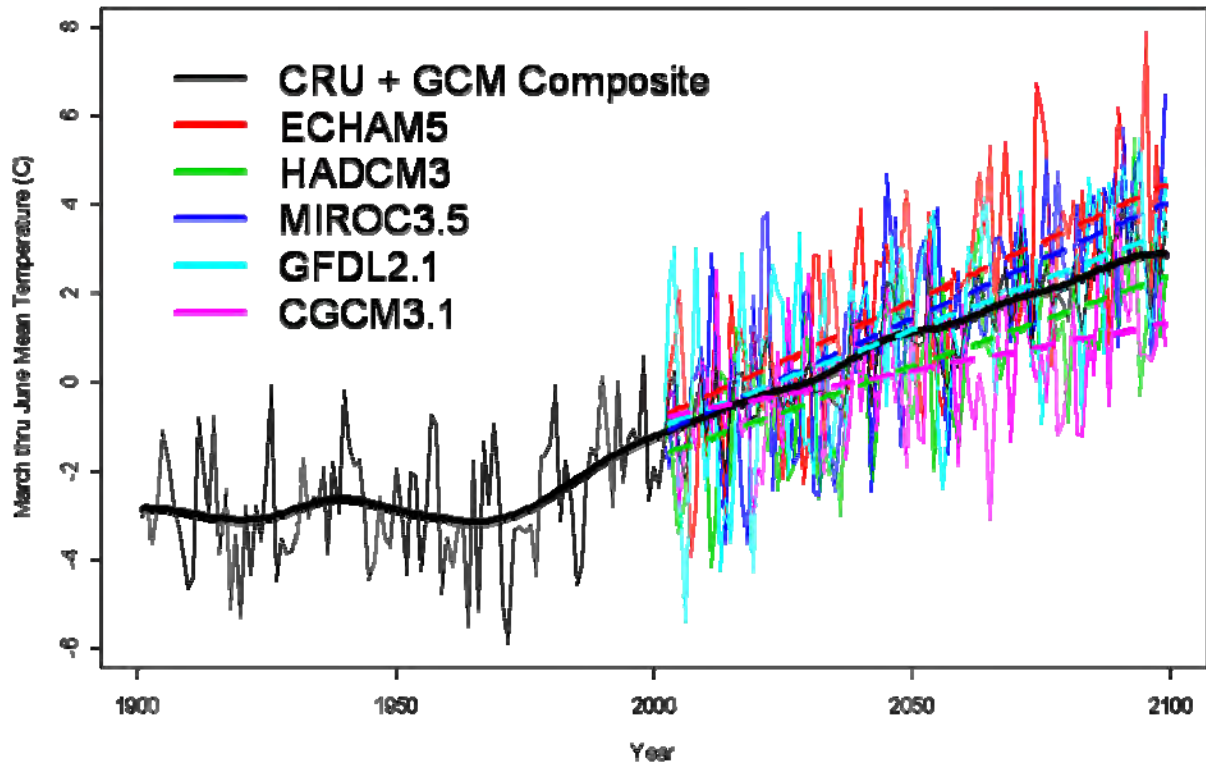


Figure 4 – Time series of average March thru June temperature (C°) integrated across the statewide simulation domain for the historical climate (CRU), the five downscaled GCMs, and the composite GCM.

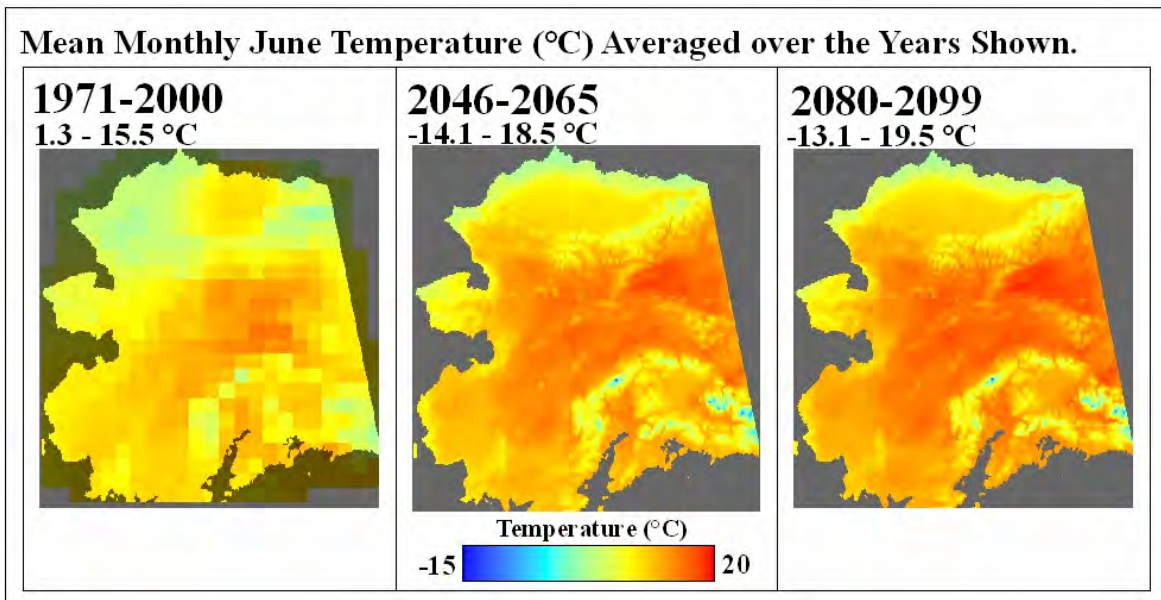


Figure 5 – Map of average June temperature (C°) for the composite GCM model. Historical (1971-2000) is CRU data at 0.5 x 0.5 degree resolution. Downscaled data at 2 x 2 km resolution averaged over two future time periods.

Total Monthly June Precipitation (mm) Averaged over the Years Shown.

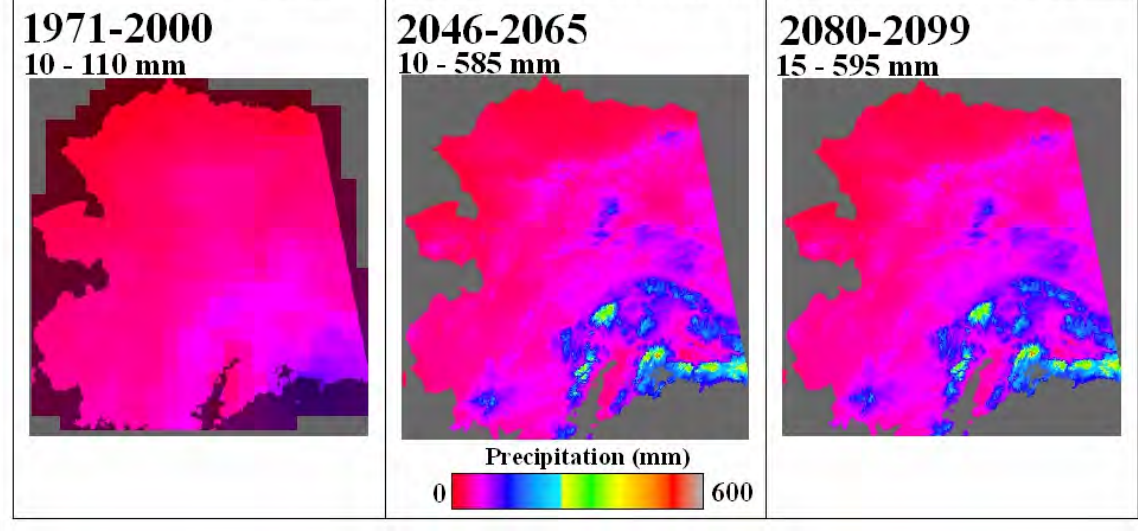


Figure 6 – Map of average June temperature (C°) for the composite GCM model. Historical (1971-2000) is CRU data at 0.5 x 0.5 degree resolution. Downscaled data at 2 x 2 km resolution averaged over two future time periods.

Model Simulation Results

The results presented here represent **preliminary** results. Although we are confident in the overall statewide simulations and their trends, there are several additional refinements that are currently underway. These refinements will be discussed within the report. Final simulation results that incorporate these refinements will be presented in a peer-reviewed journal article scheduled to be submitted summer 2008.

Empirical Climate-Fire Relationship

The ALFRESCO model was driven by spatially explicit datasets of observed and projected monthly temperature and precipitation (see *Model Simulation Design* section) – March through June monthly average temperature and June and July total precipitation. Based on future projections we expect climatic effects alone to result in substantial increases (as much as 50%) in landscape flammability across all 5 climate scenarios (Fig. 7).

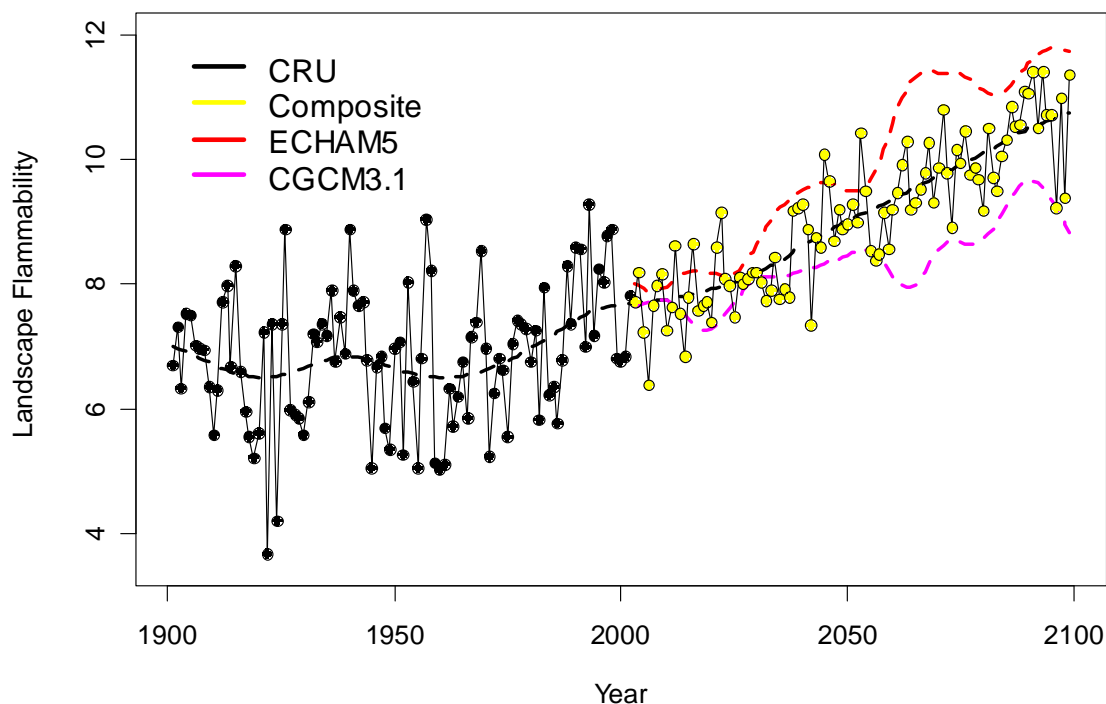


Figure 7 – Time series showing climatic influence on landscape flammability across all vegetation types. CRU observational data (black circles) and the composite future climate (yellow circles); ECHAM5 (red dashed line) represents the greatest warming scenario; CGCM3.1 (purple dashed line) represents the least warming scenario. Black dashed line is 10-yr running average.

One factor that may potentially confound the interpretation of these future results is the potential for the boreal forest ecosystem to dramatically change. For example, one of the likely consequences of future climate change appears to be a significant increase in the amount of burning. This elevated burning results in a shift from conifer dominance to deciduous dominance across interior Alaska. Since the regression linking climate to fire was developed based on a forest structure that was dominated by coniferous vegetation, it is likely that the form of this relationship will change following a shift in the dominant forest vegetation type. This shift will take several decades to develop and one

way to mitigate this impact is to periodically revise the model linking climate and fire. We are currently working on characterizing changes in this linkage between climate and fire through time. One of the limiting factors for this type of analysis is the limited amount of data that are available to explore these changes through time. However, we are moving forward using the available data to characterize and implement potential changes in the linkage between climate and fire that essentially represent a feedback between the forest structure and the climate-fire linkage. Overall, these impacts will be greatest for the latter half of the future simulation period (2050-2099). Given that it will likely take at least several decades for these changes in the structure of the forest to take effect, we feel confident that this current set of ALFRESCO simulation output realistically depicts the average landscape response to each of the down-scaled IPCC climate scenarios.

Historical Simulations

The preliminary results presented in this report cover only simulated historic fires (1860-2007) based on an empirically derived relationship between climate and fire (Duffy et al. 2005; see *Empirical Climate-Fire Relationship* section). The ALFRESCO model performed well simulating historical landscape dynamics that closely followed observed fire regime and vegetation cover characteristics. This assessment is made based on a number of different calibration metrics that compare simulated data to various aspects of the fire regime (e.g. fire size distribution, frequency-area distribution, cumulative area burned). Cumulative area burned is consistent with observed area burned from 1950-2007 (Fig. 8). In general, ALFRESCO underestimates cumulative area burned. Differences in simulated and observed cumulative area burned occur primarily because (1) we are unable to accurately simulate the 1950 fire season, and (2) ALFRESCO simulated fire perimeters contain inclusions of unburned areas whereas the observed fire perimeters disregard inclusions.

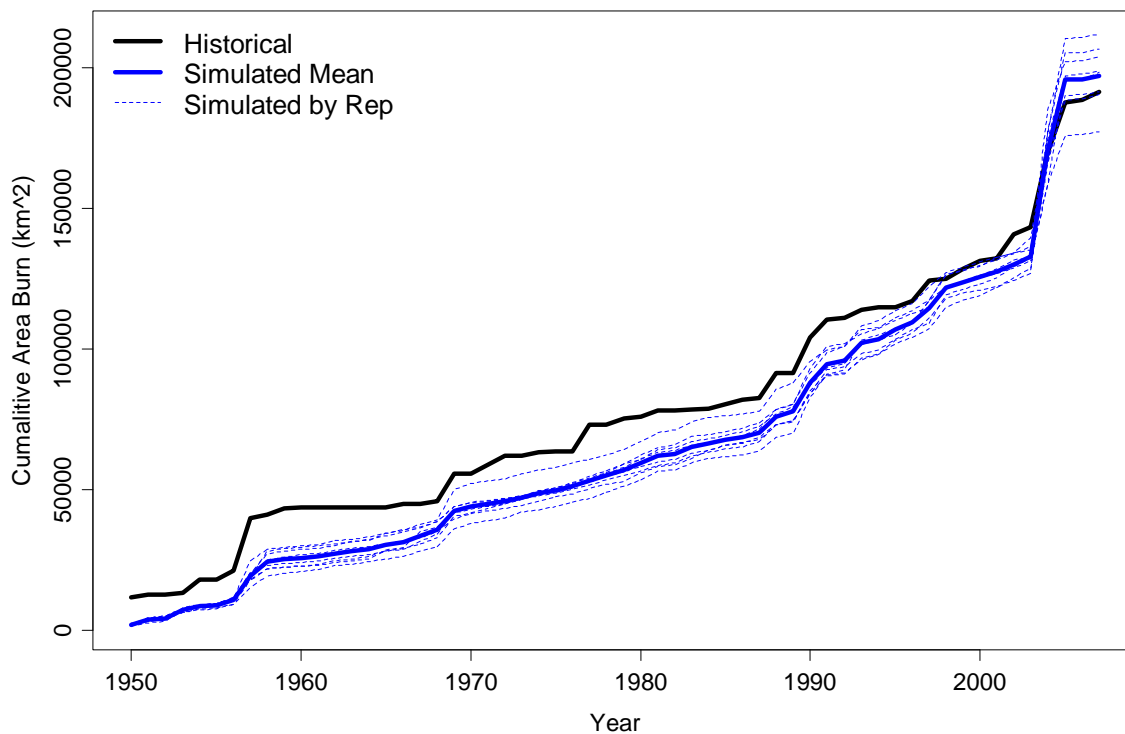


Figure 8 – Comparison of historical (black line) and simulated (blue line) cumulative area burned (km²) from 1950-2007. Solid blue line represents mean (x=8) and the dashed blue lines represent individual replicate results.

The individual replicate simulations also captured well the interannual variability in total area burned (Fig. 9) and the spatial distribution of fires across the landscape (Fig. 10). ALFRESCO performed well simulating fire activity from 1860-1949 relative to the statistically backcast estimates. These backcast estimates were generated by taking the statistical model linking climate and fire and applying it to historical data. The validity of this backcast is dependent on the relative stability of the structure of the boreal forest from 1859-2007; however, there is currently no strong evidence suggesting that the vegetation dynamics of the boreal forest in Alaska have been radically altered from 1859-2007. Although the model performed well overall, correlations ranged from 0.51-0.58, simulating observed historical fire activity (1950-2007), ALFRESCO performed better over the second half of the observation period.

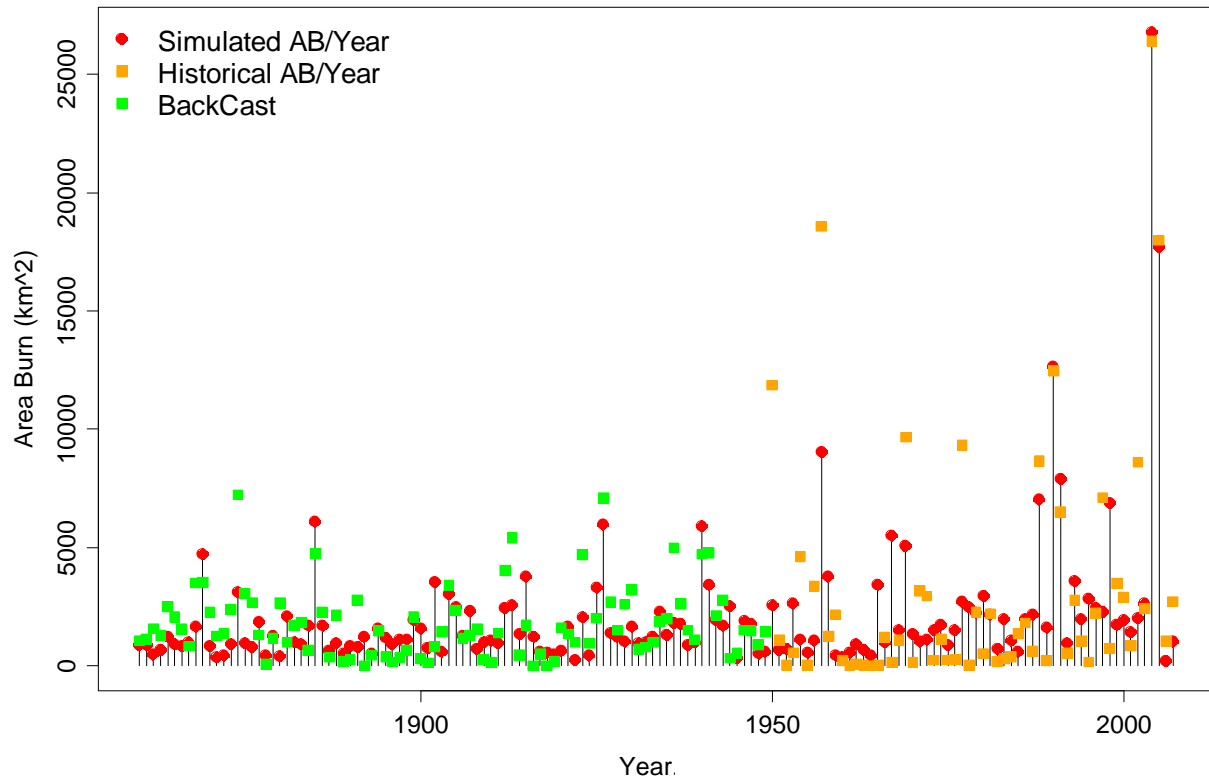


Figure 9 – Historical observed (orange boxes) and statistical backcast (green boxes) versus simulated (red circles) total annual area burned. Simulation results from the best single replicate (replicate 6).

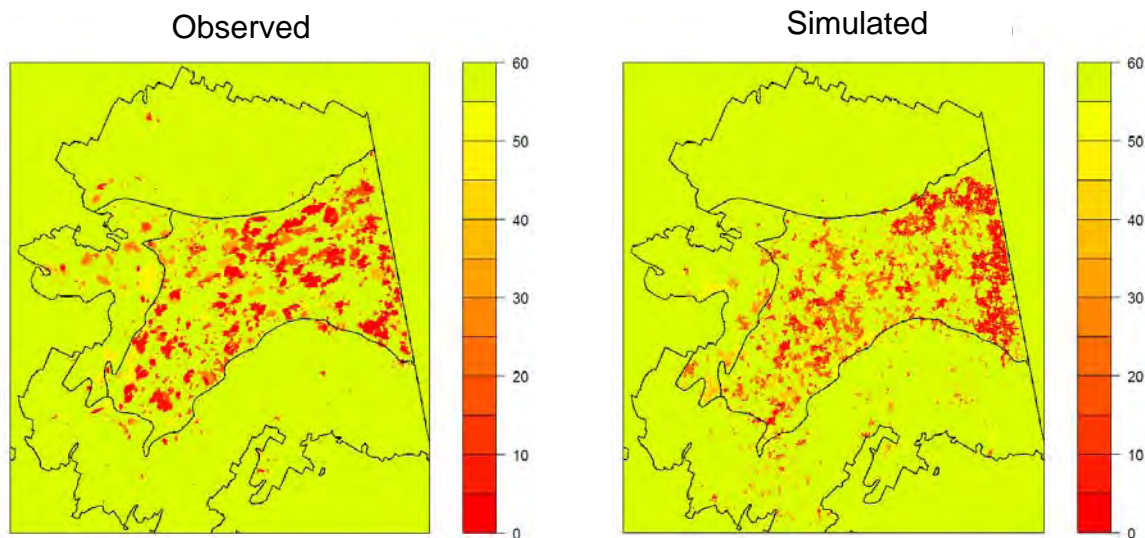


Figure 10 – Map showing observed fire perimeters (left panel) and simulated fire perimeters (right panel). Color scale indicates time since last fire (darker red equals more recent fires). Simulated results from the best single replicate (replicate 6). The four regions identified by black outlines identify major ecoregion delineations.

We parameterized the model using major ecoregion delineations (Fig. 10) to account for the distinct differences in observed fire history between the North Slope, Seward Peninsula, interior Alaska, and southcentral Alaska; each ecoregion has a different set of fire-climate-vegetation parameters developed during the calibration phase of the simulations.

Currently, we hold the most confidence in the simulation results for the interior Alaska region. We are in the process of further development and refinement of the tundra vegetation state, which will increase our confidence in the North Slope and Seward Peninsula regions. Further development and implementation of the grassland frame in southcentral Alaska will also improve our confidence in the simulation results. Interpretation of the simulation results should consider two major sources of uncertainty: (1) the GCM projections and validity of ALFRESCO model assumptions regarding successional trajectories become less certain the farther into the future we consider, and (2) due to the stochastic nature of ALFRESCO it is not possible to simulate the exact geographic location of future fire occurrence or vegetation type.

The ALFRESCO model also performed well simulating general vegetation composition across the landscape. Model simulations suggest a long-term dominance of conifer forest relative to deciduous vegetation (Fig. 11). However, since approximately 1990 the difference in proportion of conifer to deciduous has decreased substantially as a direct result of increased fire activity and conversion of conifer forest to early successional deciduous vegetation. Remotely sensed data provides two snapshots in time, 1990 and 2001, from which we can directly compare proportion of conifer to deciduous. At both time slices ALFRESCO was consistent (1990 observed ratio = 2.3 versus 1990 average (x=8) simulated ratio = 1.6; 2001 observed ratio = 1.5 versus 2001 average (x=8) simulated ratio = 1.5) with the classified remote sensing data (Fig. 11 and Fig. 12).

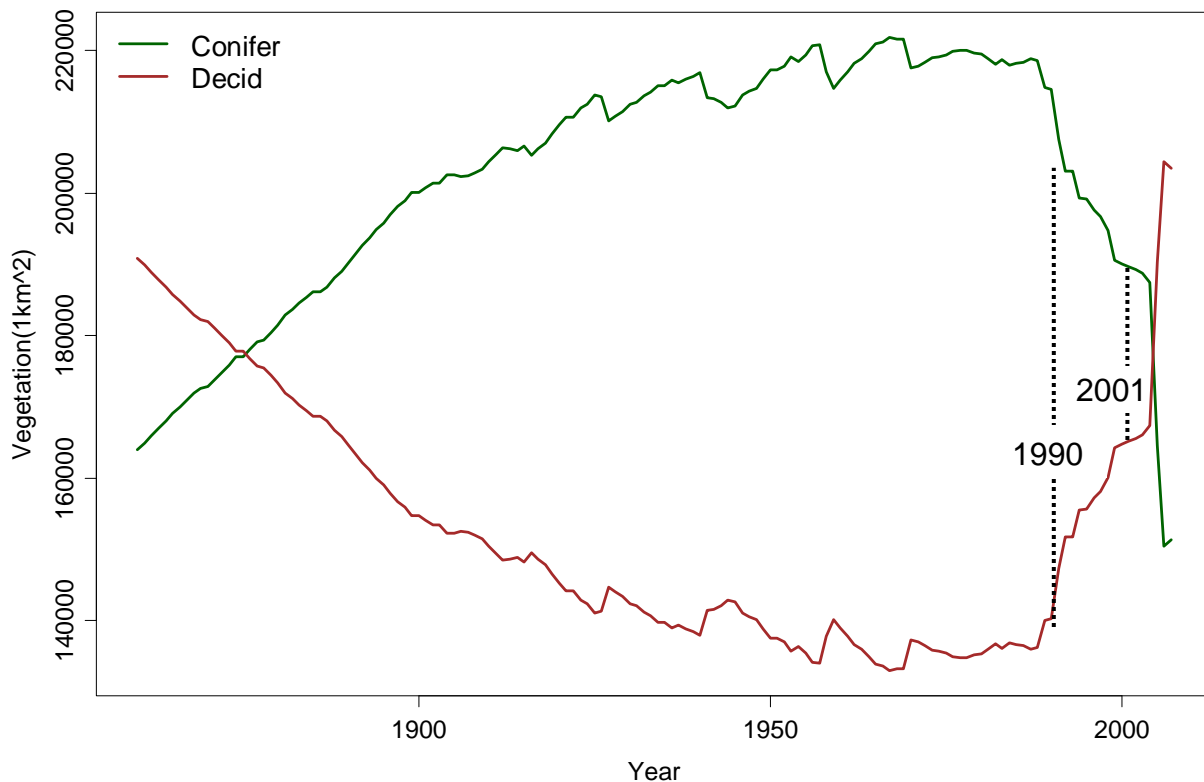


Figure 11 – Time series showing the total simulated amount of conifer (green line) versus deciduous (brown line) vegetation 1860-2007 across interior Alaska. AVHRR classification (<http://agdcftp1.wr.usgs.gov/pub/projects/fhm/vegcls.tar.gz>) at 1990 and the National Land Cover Database (<http://www.mrlc.gov>) at 2001.

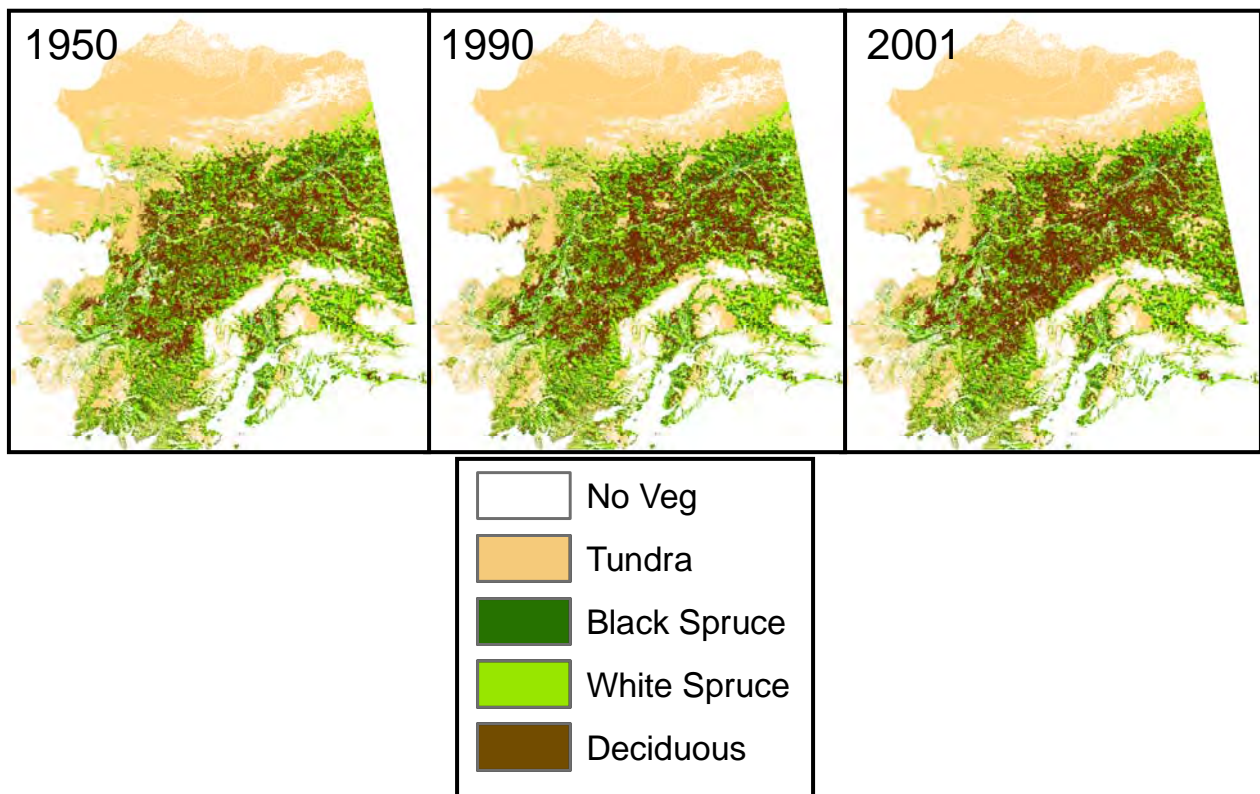


Figure 12 – Vegetation map from a single replicate showing the simulated distribution of vegetation types across the landscape.

Future Projections

The success of ALFRESCO in simulating historical observations when driven with historical climate provides a degree of confidence that allows us to simulate into the future, driving the simulations with projected climate scenarios, and to use that information to make inferences about future landscape structure and function.

ALFRESCO simulations suggest in general an increase in cumulative area burned through 2099 (Fig. 13). Changes in the slope of cumulative area burned suggest that the next 20-30 years will likely produce rapid change in fire activity and subsequent landscape dynamics. However, individual climate scenarios produced substantial differences in simulated fire activity. ECHAM5 and MIROC3.5 GCM scenarios produced the largest simulated changes in fire activity, whereas GFDL2.1 and HADCM3 produced more moderate simulated fire activity. CGCM3.1 produced the least simulated future fire activity. Individual replicate simulations also identify continued interannual variability in total area burned, but with less frequent periods of low fire activity (Figs. 14-16).

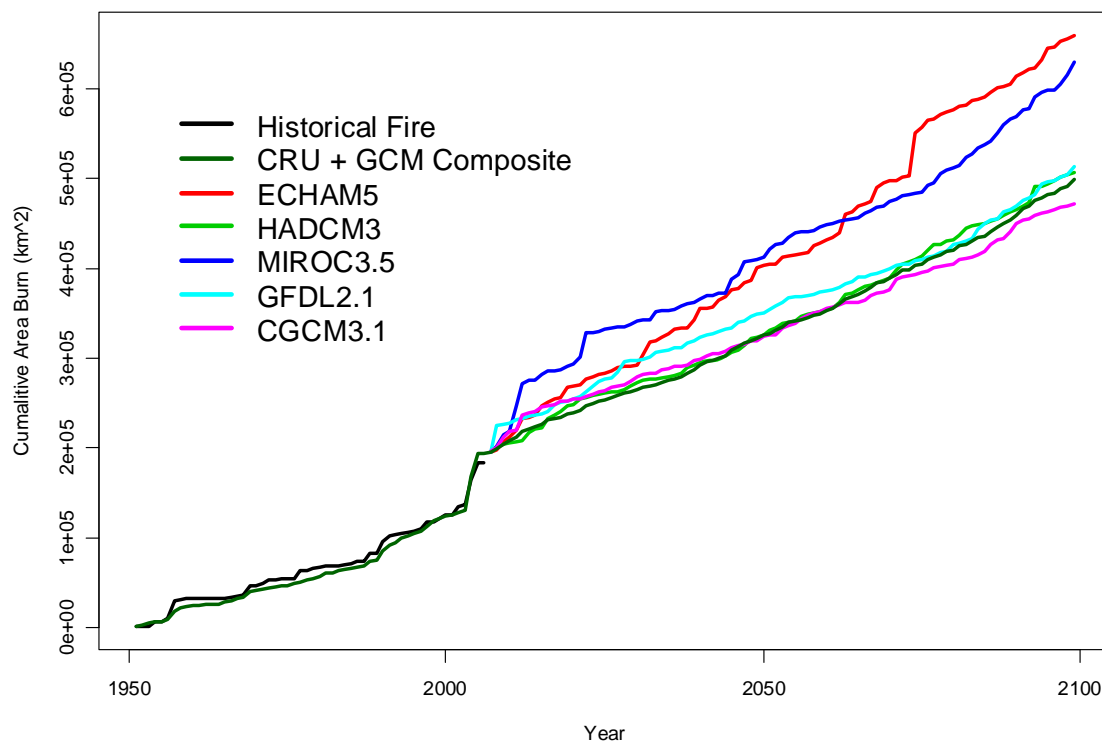


Figure 13 – Time series graph showing simulated cumulative area burned (km²) through 2099 for historical observations (black line), simulated historical (dark green line), and the five GCM scenarios plus the composite scenario (also dark green line).

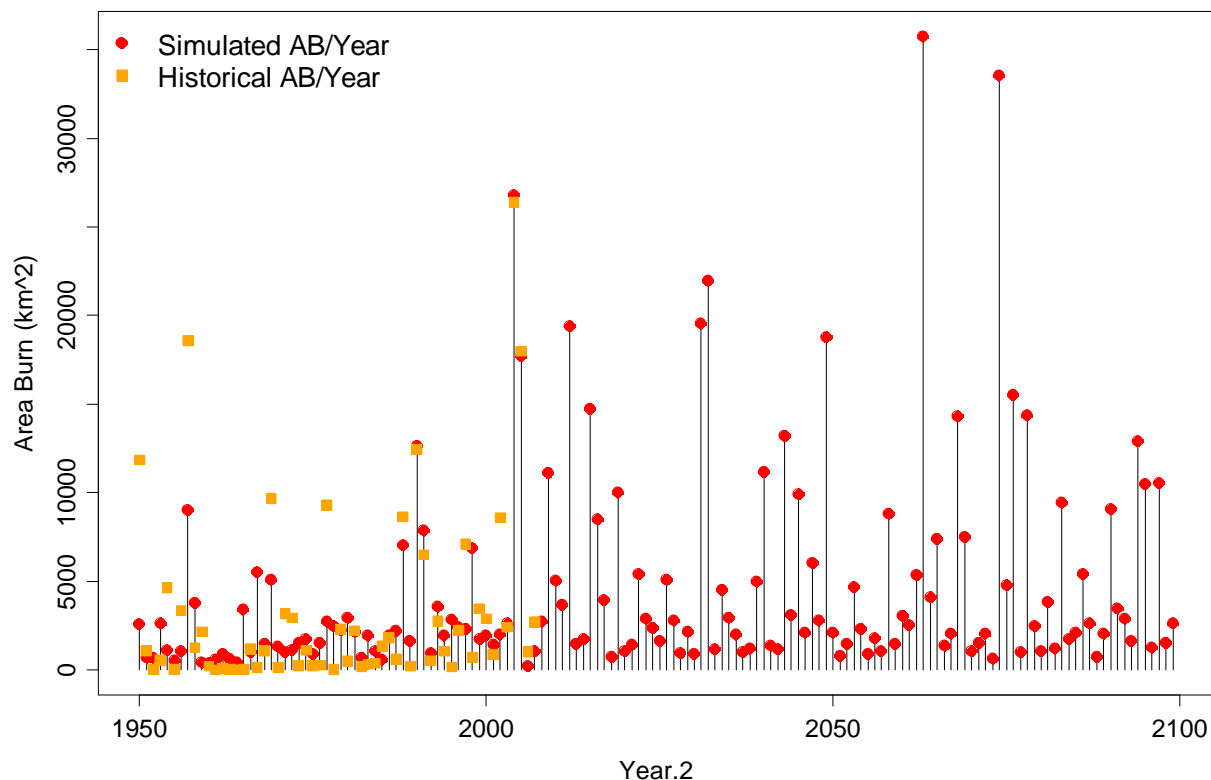


Figure 14 – Time series graph showing simulated fire activity for a single replicate simulation of the ECHAM5 climate scenario. The ECHAM5 climate scenario produced the largest increase in fire activity.

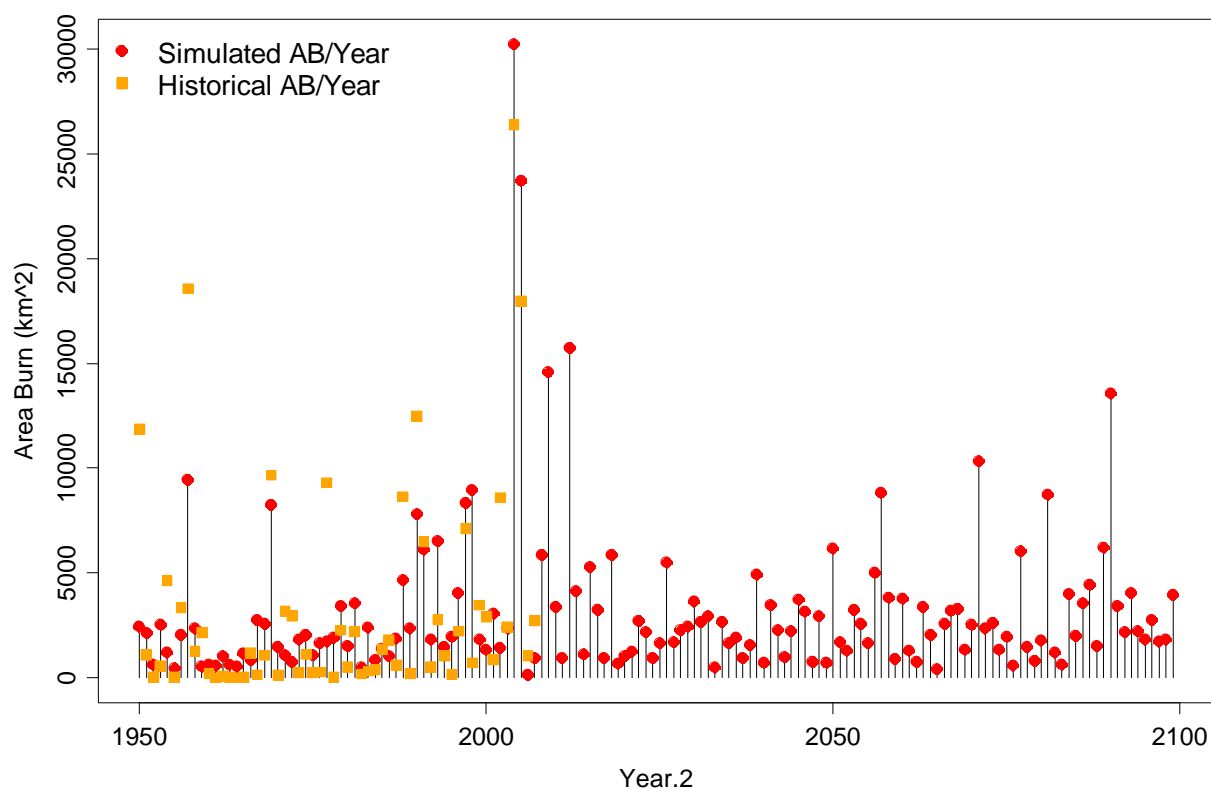


Figure 15 – Time series graph showing simulated fire activity for a single replicate simulation of the CGCM3.1 climate scenario. The CGCM3.1 climate scenario produced the smallest increase in fire activity.

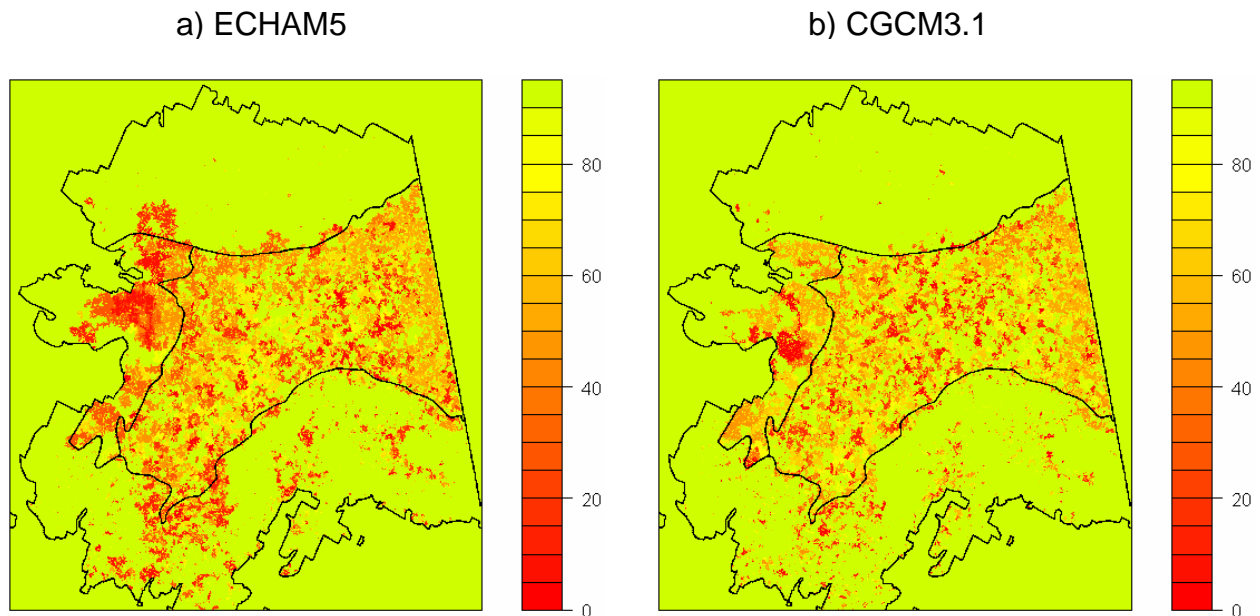


Figure 16 – Map showing time since last fire (TSLF) for the period 2008-2099 for (a) the ECHAM5 climate scenario, and (b) the CGCM3.1 scenario.

The simulated response of vegetation to increased burning suggests the potential for a substantial shift in the future proportion of conifer and deciduous forest on the landscape (Fig. 17). Although there is variability in the simulated response of vegetation across climate scenarios all scenarios simulate a shift in dominance. The magnitude of the shift differs from the most warming scenario (ECHAM5; Fig. 18 and 19) to the least warming scenario (CGCM3.1; Fig. 20 and Fig. 21).

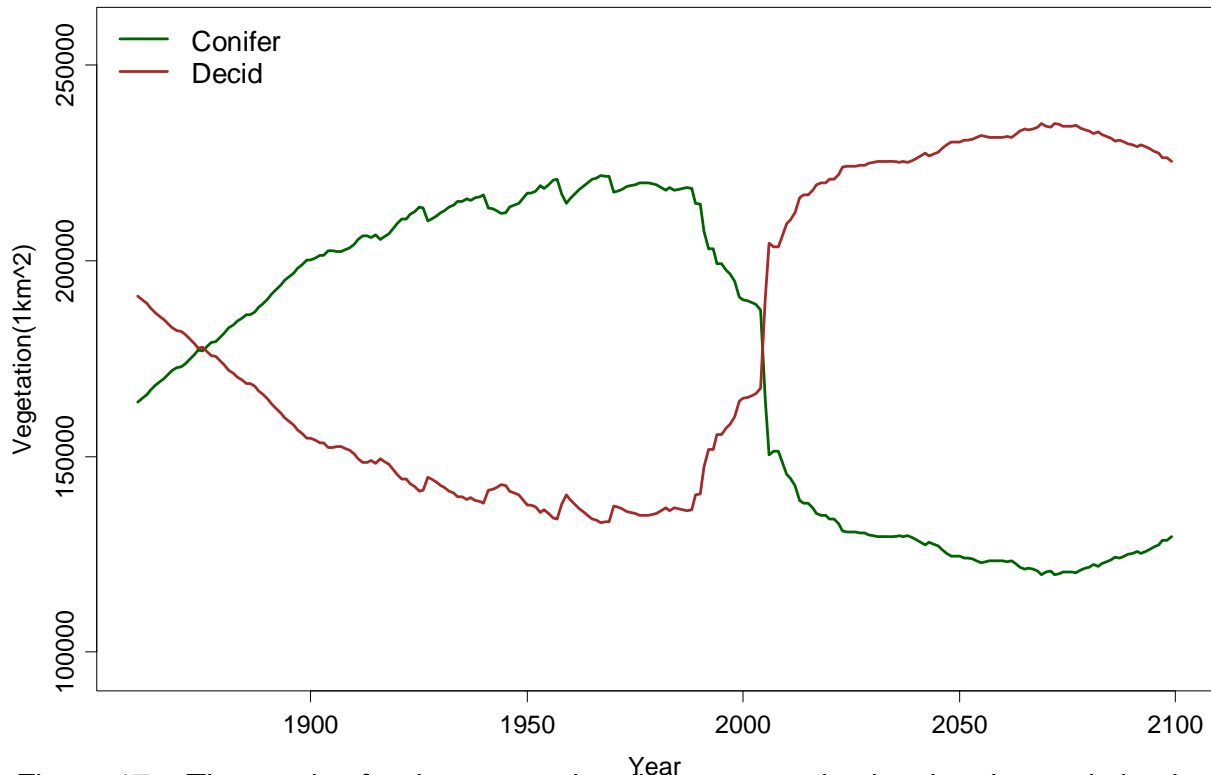


Figure 17 – Time series for the composite climate scenario showing the total simulated amount of conifer (green line) versus deciduous (brown line) vegetation 1860-2099 across interior Alaska.

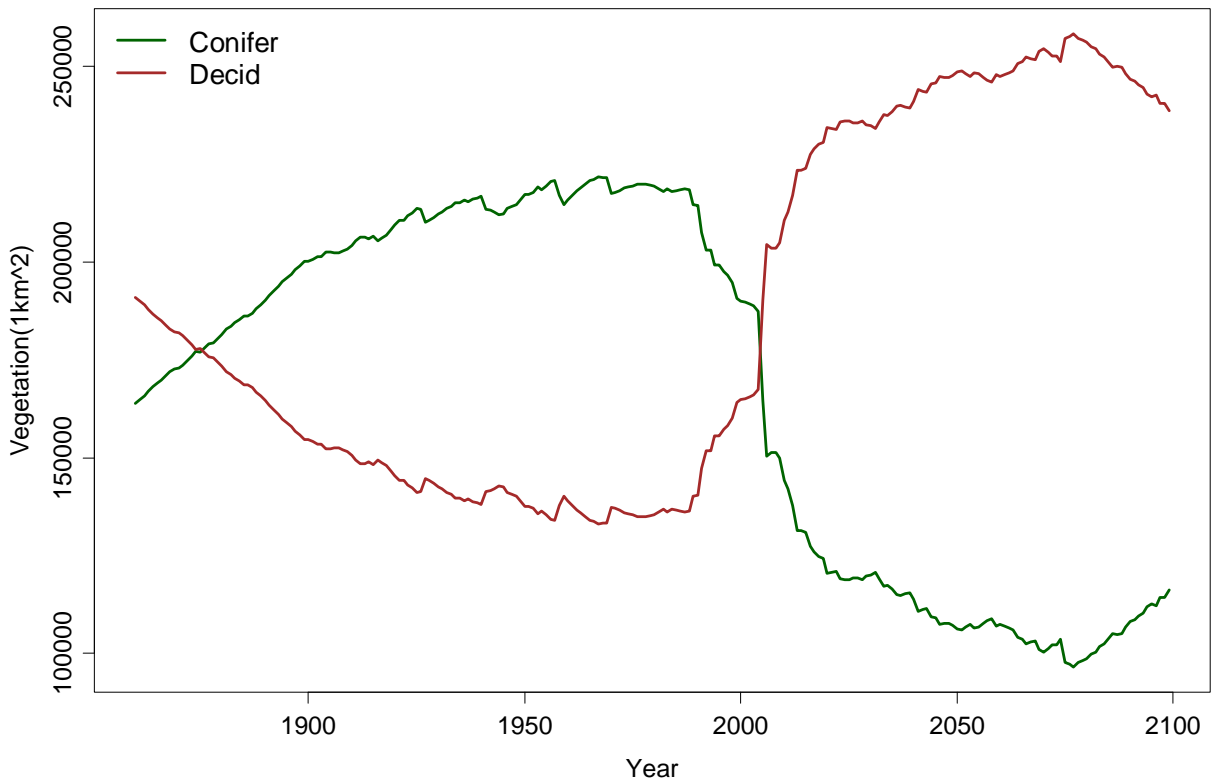


Figure 18 – Time series for the ECHAM5 climate scenario showing the total simulated amount of conifer (green line) versus deciduous (brown line) vegetation 1860-2099 across interior Alaska.

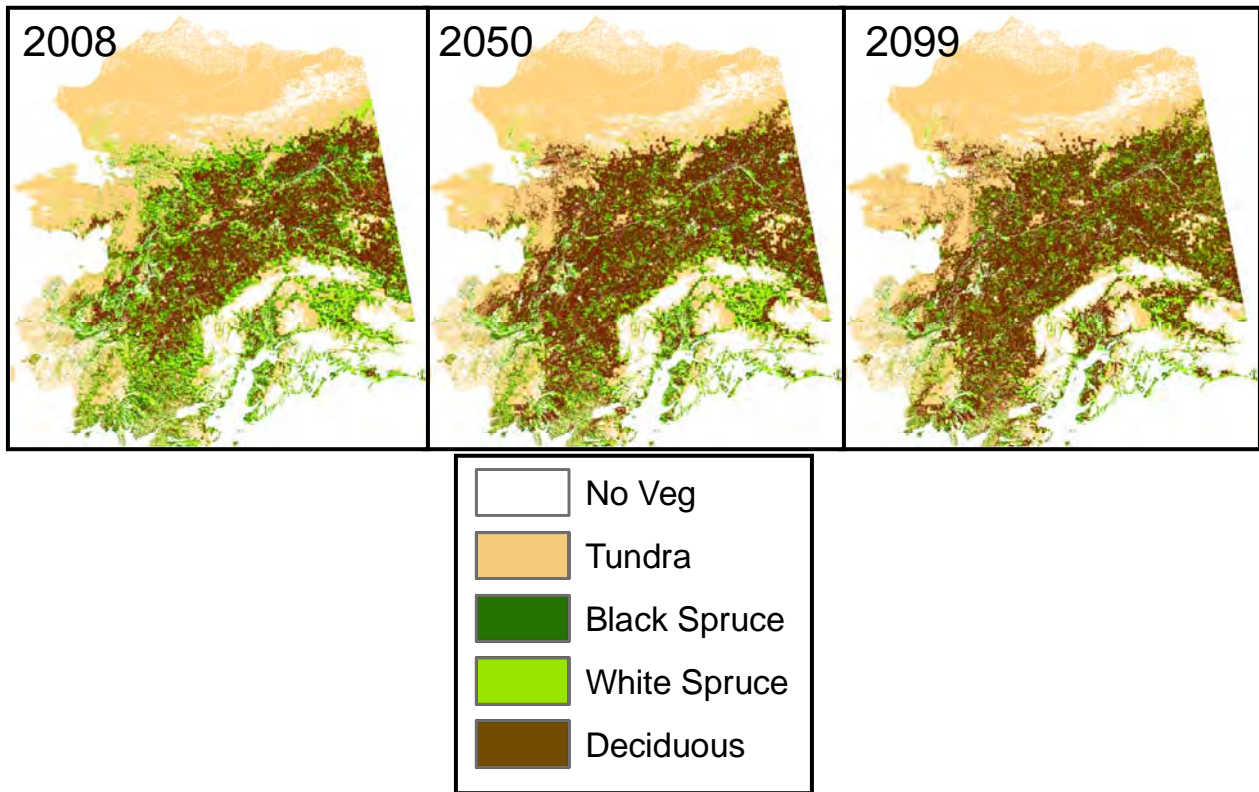


Figure 19 – Vegetation map from a single replicate of the ECHAM5 climate scenario showing the simulated distribution of vegetation types across the landscape.

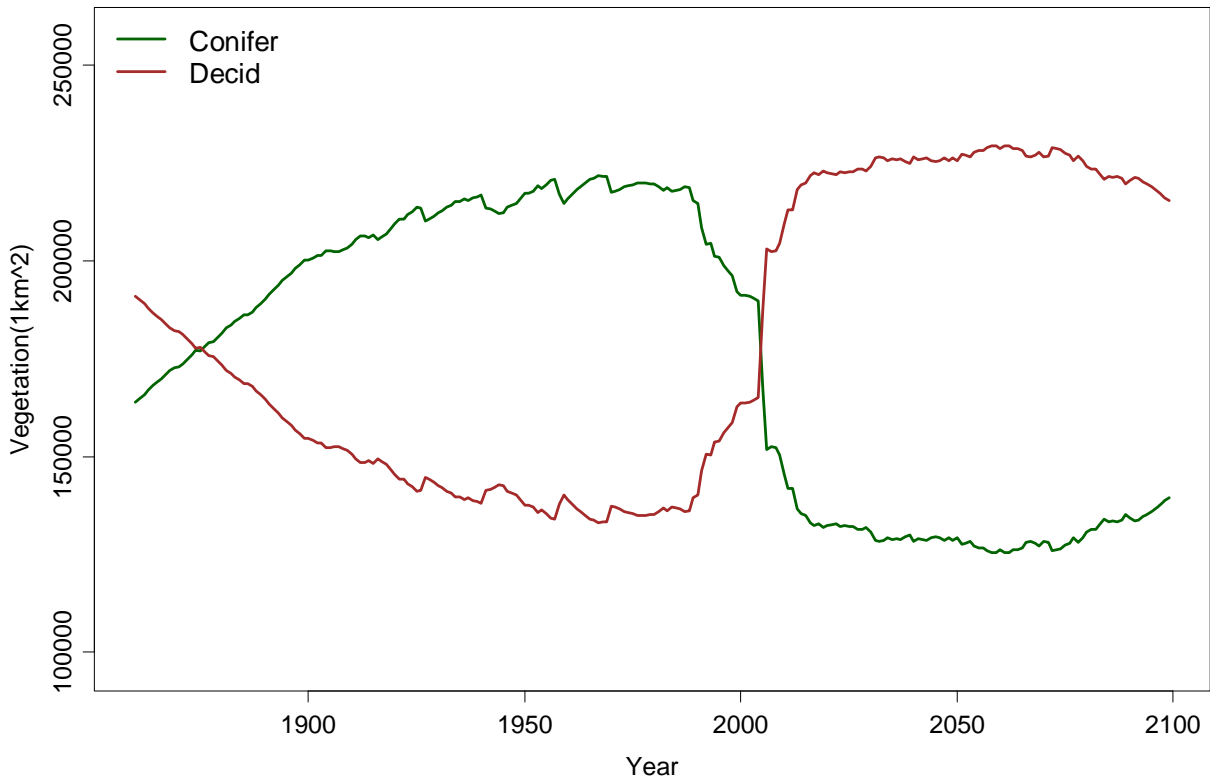


Figure 20 – Time series for the CGCM3.1 climate scenario showing the total simulated amount of conifer (green line) versus deciduous (brown line) vegetation 1860-2099 across interior Alaska.

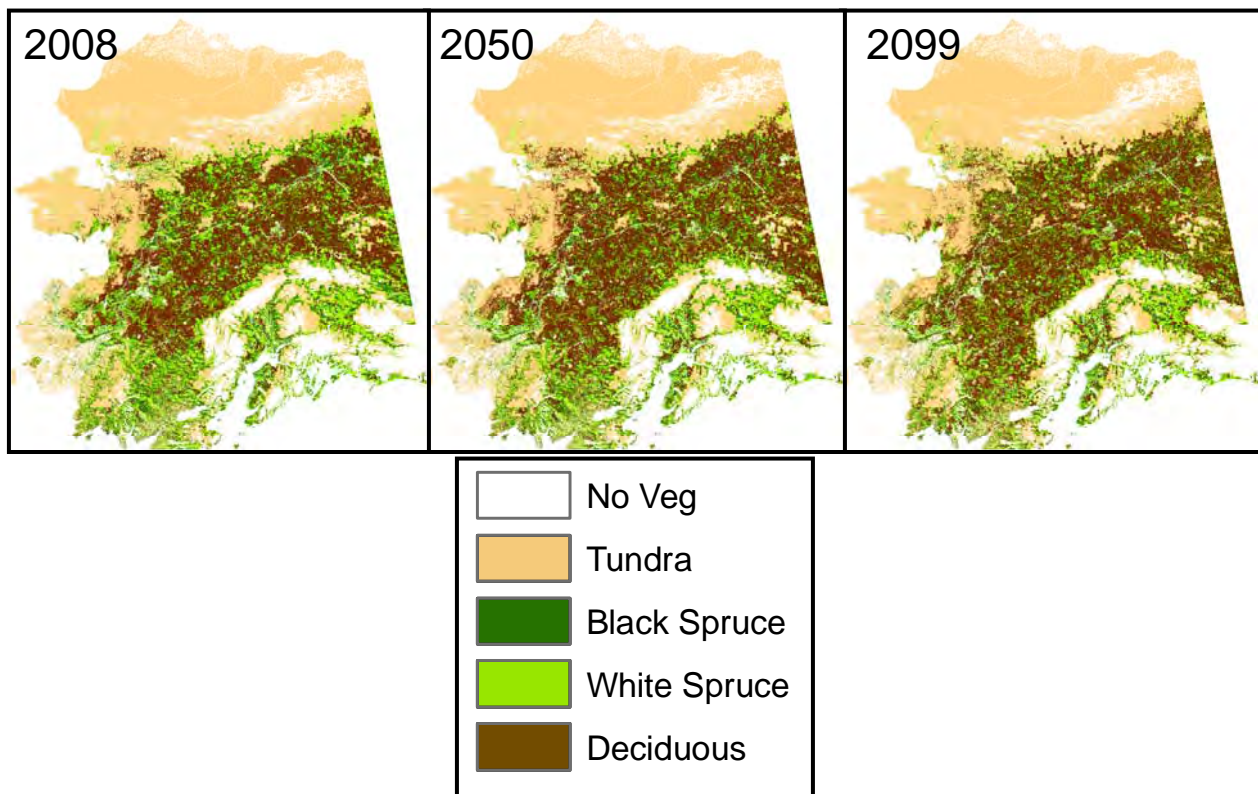


Figure 21 – Vegetation map from a single replicate of the CGCM3.1 climate scenario showing the simulated distribution of vegetation types across the landscape.

Summary of Preliminary Simulation Results and Management Implications

Preliminary results from the statewide simulations identify consistent trends in projected future fire activity and vegetation response. The simulation results strongly suggest that boreal forest vegetation will change dramatically from the spruce dominated landscapes of the last century. While Figures 17 through 21 identify a range of potential responses between the different climate scenarios, all model results show a shift in landscape dominance from conifer to deciduous vegetation within the next 50 years.

The ALFRESCO model simulations suggest a general increase in fire activity through the end of this century (2099) in response to projected warming temperatures and less available moisture. Changes in the projected cumulative area burned suggest the next 20-30 years will experience the most rapid change in fire activity and the associated changes in vegetation dynamics. Future fire activity suggests more frequent large fire seasons and a decrease in magnitude and periodicity of small fire seasons. Large differences do exist among climate scenarios providing multiple possible futures that must be considered within the context of land and natural resource management.

Increased deciduous dominance on the landscape will contribute to a probable change in the patch dynamics between vegetation types and age. The large regions of mature unburned spruce will likely be replaced by a more patchy distribution of deciduous forests and younger stages of spruce. The simulation results suggest that this change will occur over the next few decades, in response to simulated increases in fire activity, and will then reach an equilibrium stage where the patch dynamics may self-perpetuate for many decades if not centuries. In spite of the shift towards less flammable age classes and towards deciduous species, the simulation results indicate that there will be more frequent fires burning; resulting in an overall increase in acres burned annually. These two results appear to drive the simulated change in landscape dynamics where increased landscape flammability, driven by climate change, modifies landscape-level vegetation (i.e., fuels) distribution and pattern, which in turn feeds back to future fire activity by reducing vegetation patch size (i.e., fuel continuity).

Decisions made by fire and land managers during this current period of rapid change, will influence the structure and pattern of vegetation across the boreal forest in Alaska. Fire managers should consider how land management objectives may be affected by the predicted changes to natural fire on the landscape. The Boreal ALFRESCO model can be used to simulate how changes in fire management may change the potential future landscape, it can also be used to assess how particular vegetation age classes (i.e., deciduous forest 10-30 years old) that may represent habitat conditions for important wildlife resources may be affected by the fire, vegetation and climate interactions predicted into the future.

Acknowledgements

I want to thank Mark Olson, Dr. Paul Duffy, Tim Glaser, and Anna Springsteen for their determined work and attention to detail in parameterizing and analyzing the statewide simulations and assisting in the preparation of this report. Karen Murphy (USFWS) provided critical input throughout this project.

ALFRESCO Model References

- BUTLER, L.G., K. KIELLAND, T.S. RUPP, AND T.A. HANLEY. 2007. Interactive controls by herbivory and fluvial dynamics over landscape vegetation patterns along the Tanana River, interior Alaska. *Journal of Biogeography*. 34:1622-1631.
- DUFFY, P., J. EPTING, J.M. GRAHAM, T.S. RUPP, AND A.D. McGUIRE. 2007. Analysis of Alaskan fire severity patterns using remotely sensed data. *International Journal of Wildland Fire*. 16:277-284.
- RUPP, T.S., X. CHEN, M. OLSON, AND A.D. McGUIRE. 2007. Sensitivity of simulated land cover dynamics to uncertainties in climate drivers. *Earth Interactions*. 11(3):1-21.
- HU, F.S., L.B. BRUBAKER, D.G. GAVIN, P.E. HIGUERA, J.A. LYNCH, T.S. RUPP, AND W. TINNER. 2006. How climate and vegetation influence the fire regime of the Alaskan boreal biome: the Holocene perspective. *Mitigation and Adaptation Strategies for Global Change (MITI)*. 11(4):829-846.
- RUPP, T.S., OLSON, M., HENKELMAN, J., ADAMS, L., DALE, B., JOLY, K., COLLINS, W., and A.M. STARFIELD. 2006. Simulating the influence of a changing fire regime on caribou winter foraging habitat. *Ecological Applications*. 16(5):1730-1743.
- CHAPIN, F.S., III, M. STURM, M.C. SERREZE, J.P. McFADDEN, J.R. KEY, A.H. LLOYD, A.D. McGUIRE, T.S. RUPP, A.H. LYNCH, J.P. SCHIMEL, J. BERINGER, W.L. CHAPMAN, H.E. EPSTEIN, E.S. EUSKIRCHEN, L.D. HINZMAN, G. JIA, C.L. PING, K.D. TAPE, C.D.C. THOMPSON, D.A. WALKER, and J.M. WELKER. 2005. Role of Land-Surface Changes in Arctic Summer Warming. *Science*. Published online September 22 2005; 10.1126/science.1117368 (Science Express Reports).
- DUFFY, P.A., J.E. WALSH, J.M. GRAHAM, D.H. MANN, and T.S. RUPP. 2005. Impacts of the east Pacific teleconnection on Alaskan fire climate. *Ecological Applications*. 15(4):1317-1330.
- LLOYD, A., T.S. RUPP, C. FASTIE, and A.M. STARFIELD. 2003. Patterns and dynamics of treeline advance on the Seward Peninsula, Alaska. *Journal of Geophysical Research - Atmospheres*. 108(D2):8161, DOI: 10.1029/2001JD00852.
- CHAPIN, F.S., III, T.S. RUPP, A.M. STARFIELD, L. DeWILDE, E.S. ZAVALETA, N. FRESCO, J. HENKELMAN, and A.D. McGUIRE. 2003. Planning for resilience: modeling change in human-fire interactions in the Alaskan boreal forest. *Frontiers in Ecology and the Environment*. 1(5):255-261.
- TURNER, M.G., S.L. COLLINS, A.L. LUGO, J.J. MAGNUSON, T.S. RUPP, and F.J. SWANSON. 2003. Disturbance Dynamics and Ecological Response: The Contribution of Long-term Ecological Research. *BioScience*. 53(1)46-56.
- RUPP, T.S., A.M. STARFIELD, F.S. CHAPIN III, and P. DUFFY. 2002. Modeling the impact of black spruce on the fire regime of Alaskan boreal forest. *Climatic Change* 55: 213-233.
- RUPP, T.S., R.E. KEANE, S. LAVOREL, M.D. FLANNIGAN, and G.J. CARY. 2001. Towards a classification of landscape-fire-succession models. *GCTE News* 17: 1-4.
- RUPP, T.S., F.S. CHAPIN III, and A.M. STARFIELD. 2001. Modeling the influence of topographic barriers on treeline advance of the forest-tundra ecotone in northwestern Alaska. *Climatic Change* 48: 399-416.
- RUPP, T.S., A.M. STARFIELD, and F.S. CHAPIN III. 2000. A frame-based spatially explicit model of subarctic vegetation response to climatic change: comparison with a point model. *Landscape Ecology* 15: 383-400.
- RUPP, T.S., F.S. CHAPIN III, and A.M. STARFIELD. 2000. Response of subarctic vegetation to transient climatic change on the Seward Peninsula in northwest Alaska. *Global Change Biology* 6: 451-455.

Long-term Monitoring of 1977 Tundra Fires in the Northwest Alaska Parks

By Charles Racine, Jennifer Barnes, Randi Jandt, and John Dennis

The frequency and size of lightning-caused tundra fires could increase with climate warming and may result in major ecosystem changes in vegetation, soils, and wildlife habitat over large areas of the arctic. Two of the longest monitored sites (28-32 years) in Arctic Alaska for vegetation change and post-fire tundra succession are located in Bering Land Bridge (BELA) and Noatak (NOAT) National Preserves in northwestern Alaska. These permanent vegetation plots were established following widespread tundra and forest fires in 1977, when one million acres burned during an extremely dry year in northwestern Alaska (Racine *et al.* 1987, 2004). Recently the NPS Arctic Network Inventory and Monitoring Program has supported re-measurements of these sites.

The BELA site on the Seward Peninsula is located where a large 1977 tundra fire burned a west facing slope along Imuruk Lake (Nimrod Hill). Pre-fire vegetation and soils along this slope ranged from moist tussock-shrub tundra on the lower slopes to dwarf shrub tundra on the steeper upper-slope (12%) and wet sedge meadow on the ridge top. We sampled vegetation before the fire in 1973 and at eight sites following the fire at irregular time intervals from one year to 32 years. Over the monitoring period we have seen dramatic changes in vegetation on Nimrod Hill

(Figure 1), particularly on the severely burned upper-slope. Immediately after the fire, the upper-slope sites were dominated by pioneering mosses and liverworts (Figure 2), followed by sedges and grasses within a decade (Figure 3). Twenty to 30 years after the fire, both deciduous and evergreen shrubs expanded dramatically at all sites on the hill; particularly on the upper slope where fast growing willows (*Salix pulchra*) now up to 5 ft (1.5 m) tall, currently cover 30-40% of the slope (Figure 4). The thaw depths and active layer thickness have recovered to pre-fire levels at the lower-slope tussock tundra sites; however, there is evidence for major permafrost thawing and surface subsidence on the well-drained slope in the area colonized by willows. We have seen slow recovery of Sphagnum moss and lichens 32 years after fire. The loss of Sphagnum moss could change the hydrologic and water retention capacity of tussock tundra and the loss of lichens could reduce winter forage for caribou and reindeer. This long-term record of change provides valuable documentation of fire effects on vegetation, permafrost, and wildlife habitat during an era of rapid climate warming in the Alaska Arctic.

REFERENCES

- Racine, C., R. Jandt, C. Meyers, and J. Dennis. 2004. *Tundra fire and vegetation change along a hillslope on the Seward Peninsula, Alaska, USA*. Arctic, Antarctic and Alpine Research 26:1-10.
- Racine, C.H., L.A. Johnson, and L.A. Viereck. 1987. *Patterns of vegetation recovery after tundra fires in northwestern Alaska*. Arctic and Alpine Research 19:461-469.



Photograph courtesy of Charles Racine

1



Photograph courtesy of Charles Racine

2



Photograph courtesy of Charles Racine

3



NPS photograph by Jennifer Barnes

4

Figure 1. 1973 pre-fire view downslope to Imuruk Lake from the upper face of Nimrod Hill dominated by dry dwarf shrub tundra mat.

Figure 2. 1978 one year post-fire on the severely burned upper slope. Cover was dominated by early successional mosses and liverworts with bare frost boils and exposed rock.

Figure 3. 1983 six years post-fire, this site was dominated by sedges (*Carex*) and grasses (*Calamagrostis*) that overgrew the mosses and liverworts. Gary Ahlstand, former AKRO NPS Research Ecologist, shown in photo.

Figure 4. 2009 thirty-two years post fire, what once was dwarf shrub tundra at this site is now tall willow. Randi Jandt, BLM Fire Ecologist, shown in photo.



The Bering Land Bridge: a moisture barrier to the dispersal of steppe–tundra biota?

Scott A. Elias*, Barnaby Crocker

Geography Department, Royal Holloway, University of London, Egham, Surrey TW20 0EX, UK

ARTICLE INFO

Article history:

Received 14 April 2008

Received in revised form 9 September 2008

Accepted 11 September 2008

ABSTRACT

The Bering Land Bridge (BLB) connected the two principal arctic biological refugia, Western and Eastern Beringia, during intervals of lowered sea level in the Pleistocene. Fossil evidence from lowland BLB organic deposits dating to the Last Glaciation indicates that this broad region was dominated by shrub tundra vegetation, and had a mesic climate. The dominant ecosystem in Western Beringia and the interior regions of Eastern Beringia was steppe–tundra, with herbaceous plant communities and arid climate. Although Western and Eastern Beringia shared many species in common during the Late Pleistocene, there were a number of species that were restricted to only one side of the BLB. Among the vertebrate fauna, the woolly rhinoceros was found only to the west of the BLB, North American camels, bonnet-horned musk-oxen and some horse species were found only to the east of the land bridge. These were all steppe–tundra inhabitants, adapted to grazing. The same phenomenon can be seen in the insect faunas of the Western and Eastern Beringia. The steppe–tundra beetle fauna of Western Beringia was dominated by weevils of the genus *Stephanocleonus*, a group that was virtually absent from Eastern Beringia. The dry-adapted weevils, *Lepidophorus lineaticollis* and *Vitavitus thulius* were important members of steppe–tundra communities in Eastern Beringia, but were either absent or rare in Western Beringia. The leaf beetles *Chrysolina arctica*, *C. brunnicornis bermani*, and *Galeruca interrupta circumdata* were typical members of the Pleistocene steppe–tundra communities of Western Beringia, but absent from Eastern Beringia. On the other hand, some steppe tundra-adapted leaf beetles managed to occupy both sides of the BLB, such as *Phaedon armoraciae*. Much of the BLB remains unstudied, but on biogeographic grounds, it appears that there was some kind of biological filter that blocked the movements of some steppe–tundra plants and animals across the BLB.

© 2008 Elsevier Ltd. All rights reserved.

1. Introduction

The concept of a land connection between northeast Asia and the Americas began more than 400 years ago (Hoffecker and Elias, 2007). The existence of a northern land connection between Asia and America was first proposed in AD 1590 by the Spanish missionary Fray Jose de Acosta. He suggested that a land bridge had allowed people to enter the New World (Wilmsen, 1965). Some naturalists, including Charles Darwin (1859, pp. 365–382), believed that the entire circumpolar region had been ice-covered during Pleistocene glaciations, but G.M. Dawson (1894) suggested that much of Alaska had been unglaciated and joined to Northeast Asia by a “wide terrestrial plain”. Dawson noted the shallow depths of the Bering and Chukchi seas, and was impressed by the discovery of mammoth remains on the Aleutian and Pribilof Islands (Dall and

Harris, 1892). The fact that the flora and fauna of the Eurasian and American Arctic zone were nearly identical prompted biogeographers such as Wallace (1876) to argue for a land bridge linking the two regions. The biogeographic evidence eventually formed the primary basis for the concept of Beringia.

The term ‘Beringia’ was first proposed by the Swedish botanist Eric Hultén in 1937. Since his pioneering work, scientists have continued to speculate on the role of the Bering Land Bridge as a biotic migration route between North America and Asia. In his monumental work describing the Alaskan flora, Hultén (1968, p. xiv) observed that “the present ranges of Alaskan plants seemed to demonstrate that Beringia had been a pathway for the interchange of biota and that its Asian and American remnants lie at the center of many present distributional patterns”. In these early writings, Hultén used the term ‘Beringia’ only to mean the Bering Land Bridge (BLB). Beringia has since taken on far broader geographic meaning, as Quaternary scientists discovered that the vast lowland regions of northeast Asia and northwest North America remained ice-free during Pleistocene glaciations. The eastern and western sectors

* Corresponding author. Tel.: +44 1784 443647; fax: +44 1784 472836.
E-mail address: s.elias@rhul.ac.uk (S.A. Elias).

were linked together by the BLB each time sea level dropped by more than about 70 m below the modern level.

Alaskan geologist David Hopkins (1967) broadened the geographic definition of Beringia to include unglaciated regions of Alaska and Northeast Asia, as far west as the Kolyma River. Hopkins et al. (1981) later expanded the eastern boundary to the lower Mackenzie River in the Northwest Territories of Canada, thus aligning the eastern edge of Beringia with the western margin of the Laurentide ice sheet. Russian palaeobotanist Boris Yurtsev (1984) also proposed extending the western boundary of Beringia to the Lena Basin, based on the distribution of relict flora. Archaeologists working in Beringia also argued for the extension of this boundary to the Verkhoyansk Mountains, along the eastern margin of the lower Lena Basin (Hoffecker et al., 1993) (Fig. 1).

Thus we see that from the beginning, Beringia has been of vital interest to biogeographers, palaeoecologists, glacial geologists, and archaeologists. The idea that the BLB may have served as the primary pathway for people to enter the New World has always added interest and vitality to Beringian research. As far as we can tell, humans did not enter the New World deliberately. They merely crossed the broad, low plains of the land bridge in search of game animals, eventually climbing up a bank to enter what we know as Alaska. If this otherwise unremarkable lowland region between the continents really was the conduit for the entry of humans and other arctic biota into the New World, then we want to know what it was like.

2. Palaeoenvironments of the Bering Land Bridge

In this review, we focus mainly on the environments of the Last Glacial Maximum (LGM). LGM ice in Western Beringian highlands reached its maximum extent between 27,000 and 20,000 cal yr BP (Brigham-Grette et al., 2003). The vegetation cover of the land bridge was undoubtedly some mixtures of various kinds of tundra. Brief definitions of Alaskan tundra types are provided in Table 1. The timing of the LGM in Eastern Beringia (the unglaciated regions of

Alaska and the Yukon Territory) is not as well defined, but climatic cooling towards the LGM began by 32,000 cal yr BP (Elias and Brigham-Grette, 2007). Late Wisconsin ice began to advance in the mountains of southwestern Yukon by 31,000 cal yr BP (Tom Hamilton, personal communication, October, 2008), and mountain glaciers expanded in the Alaska Range by about 29,000 cal yr BP. Deglaciation was likewise time-transgressive. Hughes (1983) suggested that the western limit of the Cordilleran ice sheet began retreating in the Yukon Territory by about 19,000 yr BP. Mann and Hamilton (1995) suggested that the retreat of ice in southern Alaska began about 16,000 cal yr BP. The LGM is generally thought to have been the coldest, possibly driest interval of the last 100,000 years in many parts of Beringia. During this interval the regions of the Chukchi and Bering Seas above about 120 m below modern sea level were exposed, forming a BLB of considerable size. This land bridge effectively blocked moisture from entering much of interior Alaska and the Yukon. Given this moisture barrier, the LGM should have been the last interval of time in which steppe–tundra vegetation was able to flourish at the expense of mesic tundra in Eastern Beringia.

Various lines of evidence have been used to reconstruct the environments of the BLB. Palaeoecological reconstructions have largely been based on fossil pollen studies, but a considerable body of evidence has been developed from plant macrofossil and insect fossil analyses. Another approach to the reconstruction of BLB environments, indeed the approach taken by Hultén when he coined the term *Beringia*, was to examine the modern distributional patterns of species across the regions that were formerly part of Beringia. This biogeographic approach can also shed light on the role of the BLB in either facilitating or limiting the spread of flora and fauna from one side of the land bridge to the other.

2.1. Fossil evidence

Starting in the 1960s, palaeobotanists began attempting to reconstruct the vegetation cover of the BLB, based on pollen spectra

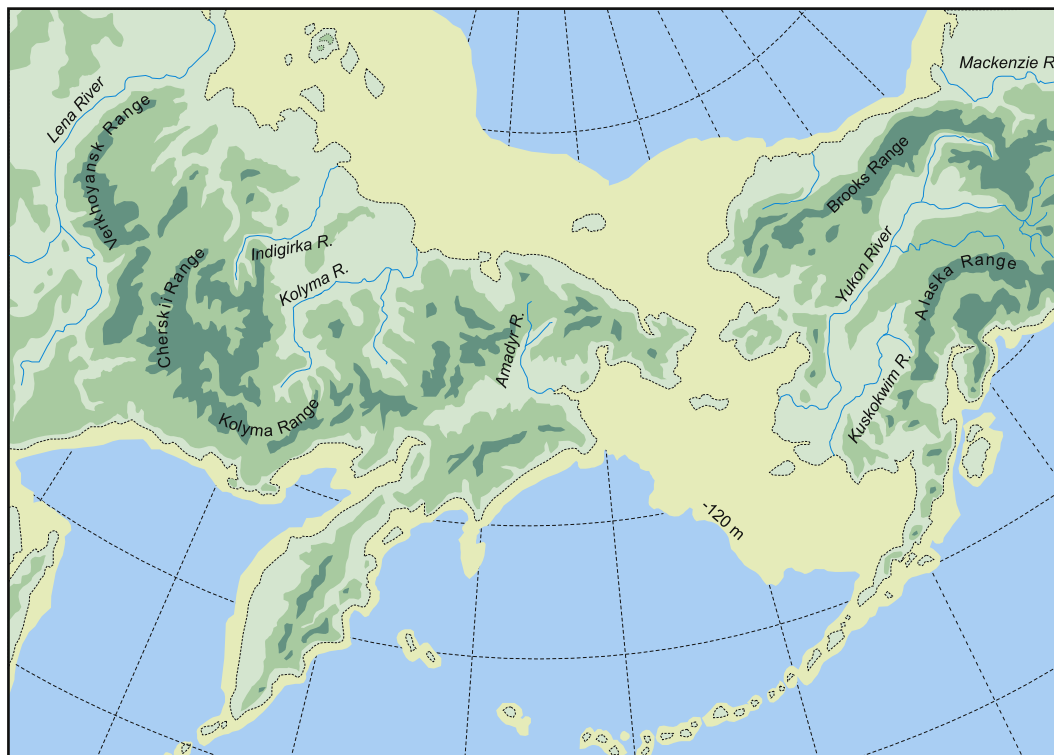


Fig. 1. Relief map of northeast Asia and northwest North America, showing proposed boundaries of Beringia (from the Lena River in the west to the Mackenzie River in the east) and the maximum extent of the Bering Land Bridge during the Last Glaciation (after Hoffecker and Elias, 2007).

Table 1
Alaskan tundra vegetation communities (after Hoffercker and Elias, 2007)

Tundra type	Brief definition
Alpine tundra	Tundra vegetation growing above the elevational limit of trees on mountains. In the Alaska Range, for instance, dwarf scrub communities grow on well-drained, windswept sites. More protected slopes provide moist to mesic sites that support low or tall scrub communities.
Dry herbaceous tundra	Tundra vegetation dominated by herbs (grasses, sedges, and other non-woody tundra plants), growing in relatively dry soils, such as uplands with sandy substrates.
Lichen tundra	Tundra vegetation dominated by lichens, including <i>Cladina</i> and <i>Stereocaulon</i> , with dwarf shrubs and mosses.
Mesic tundra	Tundra vegetation growing in mesic (medium moisture) conditions.
Shrub tundra	Tundra dominated by dwarf shrubs, such as dwarf birch, dwarf willow, narrow-leaf Labrador-tea, mountain-cranberry, and crowberry. This type of vegetation requires mesic (medium moisture) to moist conditions.
Steppe-tundra	A mixture of plant species found today in steppe regions (mid- to high-latitude grasslands) and in Arctic tundra regions. This once-widespread vegetation type is now restricted to relict patches on south-facing slopes of mountains in both Eastern and Western Beringia. The vegetation included a wide variety of herbs and dwarf shrubs. The herbs included tufted grasses, sedges, and tufted sedges. The tufted grasses included several species of fescue (<i>Festuca</i>), grasses, including <i>Poa botryoides</i> , <i>P. stepposa</i> , <i>P. arctosteporum</i> , <i>P. glauca</i> , <i>Calamagrostis purpurascens</i> , and <i>Helictotrichon krylovii</i> , <i>Koeleria cristata</i> and <i>K. asiatica</i> , and wheatgrasses (<i>Elytrigia</i>). The sedges included true steppe species, such as <i>Carex duriuscula</i> , meadow-steppe species such as <i>C. obtusata</i> and <i>C. rupestris</i> , and tufted sedges, such as <i>Carex pediformis</i> , <i>C. filifolia</i> , <i>C. rossii</i> , and <i>C. aenea</i> (Yurtsev, 2001).
Tussock tundra	Tundra vegetation growing in the form of tussocks, compact mounds of grasses or sedges, held together by root masses, growing in mesic to moist environments.
Wet herbaceous tundra	Tundra dominated by moisture-tolerant sedges and grasses, often with standing pools of shallow water. On the Alaskan North Slope, wet herbaceous tundra is dominated by sedge communities with <i>Carex aquatilis</i> and <i>Eriophorum angustifolium</i> . Grass communities are generally dominated by <i>Dupontia fischeri</i> and <i>Alopecurus alpinus</i> , but <i>Arctophila fulva</i> dominates where surface water is 15–200 cm deep (Gallant et al., 1995).

from sediment cores and exposures in western Alaska. The first of these efforts was by Paul Colinvaux (1964), who cored sediments from Imuruk Lake on Seward Peninsula (Fig. 2, No. 1). He concluded that the BLB must have been covered in 'cold Arctic tundra' during glacial intervals. The Imuruk lake site is more than 300 m above sea level, and Colinvaux conceded that even though his full glacial-age pollen spectra were dominated by grasses, the BLB itself might have had a slightly less severe climate, and therefore might have supported tussock tundra vegetation.

In 1967 Colinvaux cored a lake on St Lawrence Island, a former highland region in the middle of the BLB. He reckoned that the study site, Flora Lake (Fig. 2, No. 2), would have been about 100 m above the surrounding plains of the BLB during the Last Glaciation. He interpreted the pollen spectra from last-glacial sediments as representing cold arctic tundra, dominated by grasses and sedges. He went on to say that "there was probably much bare ground, and dwarf birches (*Betula nana*) were scarce".

In 1974 Matthews published an extensive study of pollen, plant macrofossils and insect fossils from a suite of organic deposits exposed at Cape Deceit on the northeast coast of the Seward Peninsula (Fig. 2, No. 7). One sample, S-1, dates to the LGM interval (ca 21,500 cal yr BP). This sample is an intriguing mixture of mesic tundra beetles and steppe-tundra plant remains. The beetle assemblage contains five species in the *Cryobius* group of *Pterostichus*. All of these species are associated with mesic tundra today. The other abundantly preserved species in this assemblage include two highly cold-tolerant species: the ground beetle *Amara alpina*

(MNI = 37) and the rove beetle *Micralymma brevilingue* (MNI = 89). *Amara alpina* is the most northerly distributed ground beetle today, ranging north to the Canadian Arctic archipelago and Greenland. Lindroth (1968) describes it as an insect of "open, rather dry country, notably on the true tundra". While this generalization is accurate, Elias has certainly collected numerous specimens of *A. alpina* in mesic tundra habitats, both in Arctic Alaska and in the alpine tundra of the Rocky Mountains. *Micralymma brevilingue* is a rove beetle most often associated with coastal habitats. It is often found today under stones on beaches, close to the high water mark. However, it has also been found well away from the shore, for instance under moss-covered rocks, in snow beds, and shaded gorges in Greenland. Böcher (1988) described its habitat as "both the upper tidal zone and in damp situations in different plant communities further inland". It has been found as a fossil in numerous sites well away from ancient shorelines in Eastern Beringia. However, it can survive in extreme environments, such as the polar desert regions of Severnaya Zemlya in arctic Siberia. Here it has been collected throughout the archipelago of islands. Makarova et al. (2007) concluded that this tiny rove beetle "should be considered as the most cold-tolerant beetle species of the Northern Hemisphere". Another highly cold-adapted beetle was identified from this assemblage, the leaf beetle *Chrysolina sub-sulcata*. This is an Arctic species that ranges north to the polar desert regions of Siberia today. It was a common member of Siberian steppe-tundra faunas in the Pleistocene (Kuzmina et al., 2008).

Interestingly, no specimens of the typical steppe-tundra pill beetles *Byrrhus* or *Morychus* were found in sample S-1 from Cape Deceit. Only four specimens of the characteristic steppe-tundra weevil *Lepidophorus lineaticollis* were recovered. Although the steppe-tundra 'signal' is relatively weak in the Cape Deceit LGM beetle fauna, the palaeobotanical record from this sample gives clear indications of herbaceous vegetation. Matthews (1974) noted the abundance of macrofossils of *Potentilla* and Cruciferae. Based on various lines of evidence, Matthews considered that the LGM soils at Cape Deceit were not acidic, as are found in most tundra regions today. Rather, they had the higher pH levels associated with modern grassland and steppe soils. He reconstructed the LGM vegetation cover at the site as "grassy tundra with shrub birches".

In 1981 Colinvaux published the results of another study attempting to reconstruct the vegetation cover of the BLB during the Last Glaciation. This time he took a sediment core from a lake on St Paul Island, near the southern edge of the BLB region (Fig. 2, No. 11). His interpretation of the pollen spectra from the last glacial interval was that the southern sector of the BLB was covered by herb tundra without trees or shrubs. Dwarf birch was "at best a rare plant and may have been completely absent". Likewise Colinvaux considered that tussock vegetation was lacking from this region. Colinvaux does not provide the elevation of the lake from which the sediment core was taken, but he mentions that the modern island would have been a hill that was 150–300 m above the BLB plain during intervals of lowered sea level.

Anderson (1985) described herb tundra from LGM lake sediments in northwest Alaska. The Squirrel Lake site is in the Kallarichuk Hills region, northeast of the Baldwin Peninsula (Fig. 2, No. 9). Kaiyak Lake is in the Kugoruk River valley of the Baird Mountains (Fig. 2, No. 6). While neither of these sites is near enough to the BLB to shed much light on land bridge environments, they do provide evidence concerning LGM environments in western Alaska. Both sites yielded pollen spectra from the LGM interval (Table 1); these pollen assemblages are dominated by grasses and sedges. Poaceae pollen percentage values range from about 20–50% through the LGM at Kaiyak Lake; Cyperaceae pollen percentages range from about 10–35%; there is also about 20% sage, and 10% birch and willow pollen in most LGM spectra. Anderson (1985) interpreted

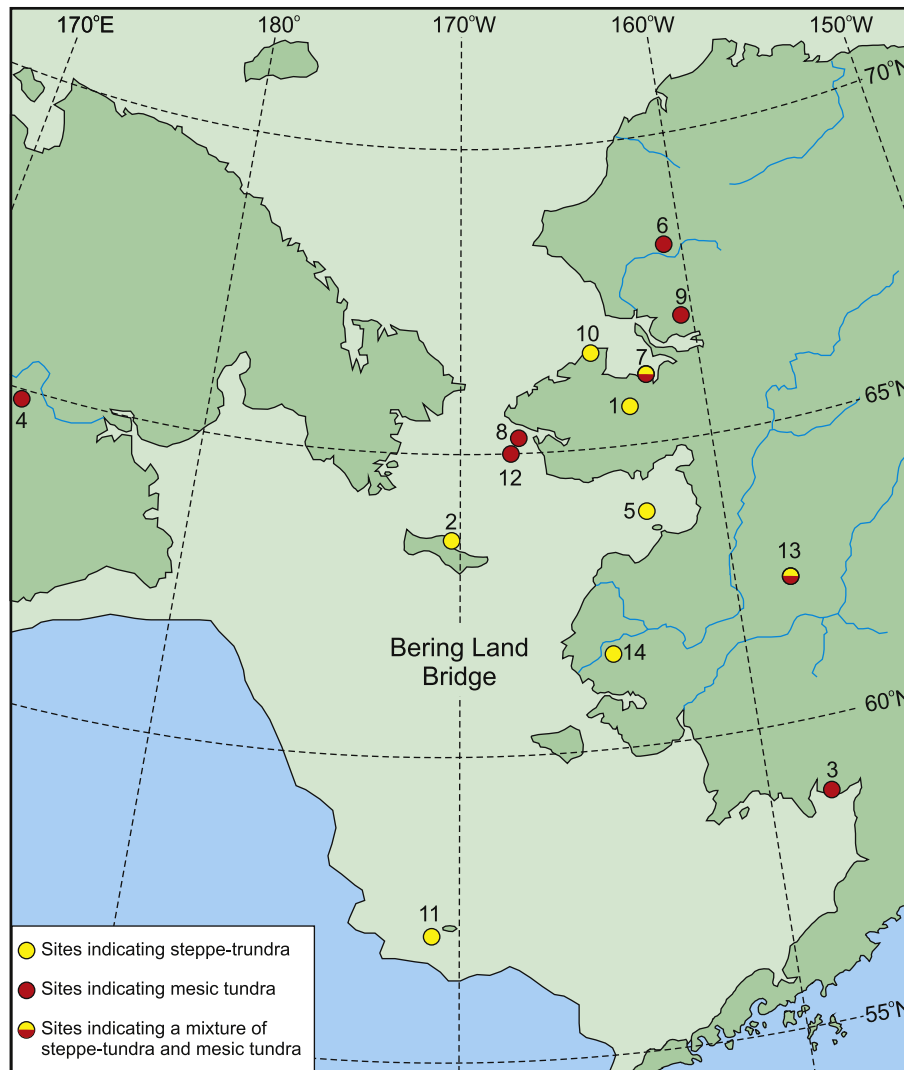


Fig. 2. Map showing fossil sites discussed in text, and the approximate margin of the Bering Land Bridge during the Last Glacial Maximum. 1, Imuruk Lake; 2, Flora Lake, St Lawrence Island; 3, Flounder Flat; 4, Chukotka site ChM-B21; 5, Zagoskin Lake, St Michael Island; 6, Kaiyak Lake; 7, Cape Deceit; 8, Bering Sea shelf core 78-15; 9, Squirrel Lake; 10, Cape Espenberg; 11, Cagaloq Lake, St Paul Island; 12, Bering Sea shelf core 76-101; 13, Colorado Creek; 14, Tungak Lake.

the LGM vegetation cover of this valley as meadow-like tundra with dwarf birch forming a local shrub component in the vegetation.

Elias led a research team that analysed pollen, plant macrofossils, and insect fossils from a series of sediment cores taken from the Bering and Chukchi shelves by the U.S. Geologic Survey in the 1970s. The cores contained sediments associated with the lowland surfaces of the BLB, and our team focussed on sampling organic-rich sediments, in order to maximize the recovery of plant macrofossils and insects. We obtained organic sediments from 20 cores, but only a few sampling horizons yielded ^{14}C ages associated with the LGM. These included samples from the Bering shelf region off the coast of the Seward Peninsula, near Port Clarence (Fig. 2, Nos. 8 and 12). The team's LGM-age samples were dated $20,725 \pm 165$ yr BP and $16,540 \pm 200$ yr BP. It could be argued that the latter of these post-dated the full glacial interval, but most studies in Alaska have shown that regional climates did not begin to warm significantly until about 13,000 yr BP (Elias, 2001). Ager (2003) drew the boundary between LGM and Lateglacial pollen zones at about 14,500 ^{14}C yr BP for the BLB region.

This study of Bering shelf sediments yielded different results than what Colinvaux and others predicted would be found on the lowland surfaces of the land bridge. Instead of evidence for dry, herb-dominated tundra, we found evidence for mesic shrub tundra,

such as is found today in Arctic Alaska. All three lines of evidence (pollen, plant macrofossils and insects) indicate shrub tundra. It might be possible to explain away the plant macrofossil and insect evidence for mesic habitats, as our samples undoubtedly represent local wetland localities, where organic detritus accumulated. However, the pollen spectra from our samples also indicate mesic tundra, and the pollen rain certainly represents regional vegetation, not just local environments. These pollen samples contain about 20% birch pollen, 10% Ericales, 15% willow, and 40% grasses (Poaceae) (Elias et al., 1997). There is only about 1% *Artemisia* pollen in these samples. This is the signature of mesic shrub tundra, not of steppe-tundra.

In 2001, Goetcheus and Birks published the results of their study of plant macrofossils from the LGM at a site on Cape Espenberg, on the north coast of the Seward Peninsula (Fig. 2, No. 10). This region was buried by tephra from a volcanic eruption that has been radiocarbon dated at 18,000 yr BP (Table 1). The site is a geological Pompeii, with plant and invertebrate life extinguished by the tephra, then frozen and preserved *in situ* by the permafrost until its discovery by David Hopkins in 1968 (discussed in Hopkins, 1988). Goetcheus and Birks were able to recover patches of vegetation from the former land surface, thereby documenting the regional vegetation cover in a way that is essentially unique to this region.

They found that the vegetation cover was dominated by *Kobresia myosuroides*, a dry-adapted sedge that grows today on dry mountain slopes and lichen tundra in Alaska (Hultén, 1968). There were a few remains of dwarf willow, but no other dwarf shrub remains were found. The mosses and herbs that made up most of the flora are all dry-adapted species that do best on calcareous soils. There was a second set of plant species identified from their samples: plants with high moisture requirements that most likely represent snow-bank communities or wet hollows. These included arctic willow (*Salix arctica*), mock wallflower (*Eutrema edwardsii*), and alpine mountain sorrel (*Oxyria digyna*). Under glacial-stage climates, the regular deposition of calcareous loess is interpreted by the authors to have been an important source of calcium in regional soils. The calcium-enriched soils played an important role in determining the composition of plant species in the regional vegetation (Goetcheus and Birks, 2001).

Kuzmina et al. (2008) have described fossil insect assemblages collected from the 18k buried surface at Cape Espenberg. The insect fossil assemblages from these samples are dominated by beetle species associated with steppe–tundra environments, such as the weevils *Lepidophorus lineaticollis* and *Coniocleonus*, and the pill beetle *Morychus*. The palaeoenvironmental reconstruction from these fossil assemblages is in close agreement with the plant macrofossil interpretation: steppe–tundra vegetation growing in cold, dry environments.

While the reconstruction of cold, dry environments at Cape Espenberg matches the evidence from the LGM sample at Cape Deceit (Matthews, 1974), the two beetle faunas are very different. The Cape Deceit (S-1) fauna is dominated by mesic tundra species and contains very few steppe–tundra indicators. The Cape

Espenberg faunas are just the opposite: dominated by steppe–tundra species with a much small mesic tundra component. Yet both sites are at essentially the same latitude on the modern north coast of the Seward Peninsula. While the Cape Espenberg flora is dominated by *Kobresia*, Matthews (1974) did not find any *Kobresia* plant remains in his LGM sample.

Ager (2003) set out to test the reconstructions of BLB vegetation of Elias et al. (1996, 1997) by analysing the pollen from a sediment core taken from St Michael Island, in the southern Norton Sound region of the Bering Sea (Fig. 2, No. 5). The core was taken from Zagoskin Lake, situated 7 m above modern sea level. St Michael Island, like St Paul Island and St Lawrence Island in the Bering Sea, would have constituted a highland region, perched above the plains of the BLB. The core yielded fossil pollen spanning the LGM interval, with radiocarbon dates from about 26,000–15,000 yr BP (Table 2). The LGM pollen assemblages were dominated by grasses and sage (*Artemisia*). Ager (2003) interpreted the LGM vegetation as “grassy herbaceous tundra”. He went on to conclude that this kind of vegetation probably dominated the BLB, and that mesic shrub tundra was “largely restricted to stream banks, ponds, lakeshores, and sites that trapped windblown snow”. He rejected the arguments made by Dale Guthrie (2001) that the BLB contained a broad belt of mesic tundra vegetation that served as an ecological filter, preventing some megafaunal species from crossing the land bridge.

Additional evidence for herbaceous tundra comes from LGM pollen assemblages from Tungak Lake, near the Yukon River delta in southwestern Alaska (Fig. 2, No. 14). Ager (1982) described an herb zone in the basal section of a lake core. The upper boundary of this zone was radiocarbon dated at $14,230 \pm 350$ yr BP. The pollen spectra in this zone are dominated by Gramineae (15–30%) and

Table 2

Summary of radiocarbon ages and palaeoenvironmental reconstructions for fossil sites discussed in text

Site	¹⁴ C age (yr BP)	Fossil evidence	Vegetation reconstruction	Reference
1 Imuruk Lake, central Seward Peninsula	LGM—undated	Pollen dominated by grasses and sedges, with sage and birch	Herb tundra vegetation with minor birch shrub component	Colinvaux, 1964
2 Flora Lake, St Lawrence Island	LGM—undated	Pollen dominated by grasses and sedges	Cold arctic tundra dominated by grasses and sedges	Colinvaux, 1967
3 Flounder Flat, Bristol Bay	LGM—undated	Mesic tundra beetles, no steppe–tundra species present	Cold mesic tundra environments	Elias, 1992b
4 Chukotka ChM-B21	LGM—undated	Arctic tundra beetles, aquatic and riparian beetles, no steppe–tundra species	Cold, mesic tundra	Kuzmina et al., 2008
5 St Michael Island	25,690 ± 420 to 14,970 ± 170	Pollen dominated by grasses and sage; mesic plant pollen only a minor component	Herb tundra	Ager, 2003
6 Kaiyak Lake, Baird Mountains	21,690 ± 330 to 14,300 ± 140	Pollen dominated by grasses and sedges with sage, birch and willow	Meadow-like tundra	Anderson, 1985
7 Cape Deceit Sample S-1	ca 21,500	Mesic tundra beetles; steppe–tundra beetles a minor component; plant macrofossils indicate calcareous soils	Grassy tundra with shrub birches	Matthews, 1974
8 Bering Sea shelf off Port Clarence	20,725 ± 165	Mesic tundra beetles; pollen dominated by grasses, birch, sedge, <i>Sphagnum</i> spores	Birch–graminoid tundra with small ponds choked with aquatic plants; no evidence of steppe–tundra vegetation or insects	Elias et al., 1996, 1997
9 Squirrel Lake, north of Kotzebue	20,300 ± 380 to 17,360 ± 200	Pollen dominated by grasses and sedges with sage, birch and willow	Meadow-like tundra	Anderson, 1985
10 Cape Espenberg	18,070 ± 60	Plant macrofossils dominated by <i>Kobresia</i> , other sedges, and occasional dwarf willow; steppe–tundra beetle fauna	Herb-rich tundra grassland with a continuous moss layer	Goetcheus and Birks, 2001
11 Cagaloq Lake, St Paul Island	17,800 ± 700	Pollen dominated by grasses, sedges, and sage	Herb tundra	Colinvaux, 1981
12 Bering Sea shelf off Port Clarence	16,540 ± 200	Pollen dominated by grasses, birch, sedge, <i>Sphagnum</i> spores	Birch–graminoid tundra with small ponds choked with aquatic plants; no evidence of steppe–tundra	Elias et al., 1996a,b
13 Colorado Creek	16,150 ± 230	Mixture of mesic tundra and steppe–tundra beetles	Mosaic of steppe–tundra and mesic tundra habitats	Elias, 1992a; Thorson and Guthrie, 1992
14 Tungak Lake	>14,230 ± 350	Pollen dominated by Cyperaceae and Poaceae, willow and sage, smaller amounts of Ericaceae and birch pollen	Herb tundra with some mesic to wet habitats locally	Ager, 1982

Cyperaceae (10–40%), *Salix* (2–10%) and *Artemisia* (5–20%). While Ager interpreted the dominant vegetation cover of the site as “herb-dominated tundra”, he noted that the presence of Ericaceae and birch (probably dwarf-birch) pollen in the samples meant that mesic to wet habitats persisted there during the LGM.

At Colorado Creek in west-central Alaska (Fig. 2, No. 13), fossil insect assemblages associated with woolly mammoth remains have been dated at $16,150 \pm 230$ yr BP (Elias, 1992a; Thorson and Guthrie, 1992). Because of its interior continental locality, this fossil locality bears no relation to BLB environments, but it sheds light on LGM environments in western Alaska. The small fossil insect fauna identified from this site (Table 3) is an intriguing mixture of steppe-tundra and mesic tundra beetle taxa. The steppe-tundra elements include the pill beetle *Morychus* and the weevil *Lepidophorus lineaticollis*. However, there is a strong mesic-tundra component in this fauna, including the ground beetles *Pterostichus brevicornis* and *P. caribou*, and the rove beetles *Holoboreaphilus nordenskiöldi*, *Micralymma brevilingue*, and *Tachinus brevipennis*. All of these ground beetle and rove beetle species are found today in mesic tundra habitats on the Alaskan North Slope. The dung beetle *Aphodius congregatus* was found in association with a mammoth dung bolus. This species is found today in the highlands of the Pacific Northwest, and at lower elevations farther north in Alaska (R. Gordon, personal communication cited in Bain et al., 1997). The carrion beetle *Thanatophilus coloradensis* is known today from alpine tundra regions in the Rocky Mountains, northern British Columbia, and central Alaska (Anderson and Peck, 1985). This beetle was probably feeding on mammoth remains at Colorado Creek. Elias has collected modern specimens that were feeding on

carrion in *Kobresia* meadows in the alpine tundra of northern Colorado.

The Colorado Creek fauna thus presents almost an equally balanced combination of steppe-tundra and mesic tundra insects—a mixture unique among Beringian fossil insect assemblages. The steppe-tundra beetles may well have lived on upland surfaces surrounding the gully containing the mammoth carcasses. The mesic tundra beetles may have lived along a moist stream bank or adjacent to perennial snow banks in the gully. The mixed palaeoenvironmental signal from Colorado Creek is in some ways similar to the ‘mixed’ signal obtained from the LGM sample from Cape Deceit (Matthews, 1974). The former site has a mixture of steppe-tundra and mesic tundra beetles, while the latter site has predominantly mesic tundra beetles, combined with botanical indicators for grass-dominated vegetation. The ‘mixed signal’ quality of these two sites is indicated in Fig. 2 by showing them with circles filled half with black and half with white.

At Flounder Flat in the Nushagak Lowland region (Fig. 2, No. 3) of southwestern Alaska, LGM beetle assemblages contained only mesic tundra taxa. No steppe-tundra beetles were found at this site during the LGM (Elias, 1992b). Faunal diversity declined in this region during the LGM, but the species that persisted through the glacial interval, such as the rove beetle *Tachinus brevipennis* and several species of ground beetles in the *Cryobius* group of the genus *Pterostichus*, are associated with cold mesic tundra habitats today. Elias (1992b) went as far as proposing that southwest Alaska had served as a refugium for mesic and hygrophilous insects during the Late Pleistocene.

The study of LGM environments near the eastern edge of Western Beringia (i.e., on Chukotka and further south along the Siberian coast of the Bering Sea) has only recently begun. Kuzmina et al. (2008) reported briefly on an LGM beetle fauna from a site on the Main River (Fig. 2, No. 4). The sediments sampled from this site are ice-rich sandy silts called ‘Yedoma’ by Russian researchers. The exact origins of Yedoma deposits remain unknown, but in this case the organic silts are thought to represent a flood plain deposit (Svetlana Kuzmina, written communication, August 2008). The fauna is dominated by beetle taxa found today in arctic tundra regions of northeast Asia. There are also substantial numbers of aquatic and riparian species. The fauna contains few species associated with dry tundra environments, and no steppe indicators, in spite of the fact that steppe-tundra taxa are dominant in assemblages from other time intervals at this site. The authors interpreted the LGM environment of the site to be cold mesic tundra. Ironically, it may have been too cold in this region during the LGM to support the Western Beringian steppe-tundra insect fauna. As discussed below, during warmer intervals of the Pleistocene, steppe-associated beetle species from southern Siberia were able to invade northeastern Siberia. Many of these relatively warm-adapted steppe species must have died out during glacial intervals. Alfimov and Berman (2001) examined the thermal requirements of the species that composed the Pleistocene steppe beetle fauna in northeastern Asia, and determined that these species require mean summer temperature (TMAX) values of at least 10–11 °C, even when they live in extremely continental climate where winter temperatures are very low. If TMAX values in some regions of Beringia were only 7–9 °C during the Late Wisconsin interval (Elias, 2001), this may have favoured the development of mesic tundra insect communities at the expense of steppe-adapted species (Elias et al., 2000).

2.2. Biogeographic evidence

The modern distribution patterns of plants, insects, and vertebrates have all been used by biogeographers to reconstruct environmental conditions on the BLB during the Late Pleistocene.

Table 3
Fossil insects identified from the Colorado Creek site, Alaska

Taxon	Sample	Habitat
DIPTERA		
CALLIPHORIDAE (Blow flies)		
Genus indet.	Mammoth bone (nasal cavities)	N/A
HOMOPTERA		
CICADELLIDAE (Leaf hoppers)		
Genus indet.	Hair horizon	S-T
HYMENOPTERA		
CHALCIDOIDEA (Chalcid Wasps)		
Genera indet.	Hair horizon	N/A
COLEOPTERA		
CARABIDAE (Ground beetles)		
<i>Carabus</i> sp.	Hair horizon	N/A
<i>Pterostichus brevicornis</i> Kby.	Hair horizon	MT
<i>Pterostichus caribou</i> Ball	‘Mammoth Site’	MT
<i>Pterostichus (Cryobius)</i> sp.	Hair horizon	MT
STAPHYLINIDAE (Rove beetles)		
<i>Holoboreaphilus nordenskiöldi</i> Mäkl.	Hair horizon	MT
<i>Micralymma brevilingue</i> Schiodt	Hair horizon	MT
<i>Lathrobium</i> sp.	Hair horizon	MT
<i>Tachinus brevipennis</i> Sahlb.	Hair horizon	MT
<i>Aleocharinae</i> gen. et sp. indet.	Hair horizon	MT
SILPHIDAE (Carrion beetles)		
<i>Thanatophilus coloradensis</i> (Wickh.)	Hair horizon, ‘Mammoth Site’	AT
SCARABAEIDAE (Dung beetles, chafers)		
<i>Aphodius congregatus</i> Mannh.	Dung bolus, Hair horizon	MT
BYRRHIDAE (Pill beetles)		
<i>Morychus</i> sp.	Hair horizon	S-T
CHRYSOMELIDAE (Leaf beetles)		
<i>Chrysolina</i> sp.	Hair horizon, ‘Mammoth Site’	S-T?
Chrysomelidae gen. et sp. indet.	‘Mammoth Site’	
CURCULIONIDAE (Weevils)		
<i>Lepidophorus lineaticollis</i> Kby.	Hair horizon, ‘Mammoth Site’	S-T

Habitat abbreviations: AT, alpine tundra; MT, mesic tundra; S-T, steppe-tundra; N/A, habitat not defined at the generic level.

Yurtsev (2001) noted that even though the BLB may have functioned as a filter for the migrations of cold- and dry-adapted steppe and montane plants, more than 40 dry-adapted plant species that presently occur on both sides of the Bering Strait managed to cross over the BLB during the Pleistocene. Among these are the dry-adapted sedges, *Kobresia myosuroides* and *Carex rupestris*. Yurtsev (2001) considers these to have been of Central-Asian origin. Today, the vegetation cover of the alpine tundra zones in both northern Mongolia (Miehe, 1996) and the easternmost Rocky Mountains is dominated by *Kobresia myosuroides* (Cooper and Sanderson, 1997). It also occurs on dry, calcareous slopes up to 1800 m elevation in Alaska (Hultén, 1968).

If the BLB served as a mesic 'filter' that slowed or stopped the migration of dry-adapted insect species, it was a leaky filter, at best. It apparently prevented some species from spreading between the continents, but not others. Several groups of steppe–tundra beetles have distributional patterns limited to either the western or eastern side of Bering Strait. Among these are some cold-adapted leaf beetles (Chrysomelidae), including *Chrysolina arctica* and *C. brunnicornis wrangeliana*. Both of these leaf beetles are found only west of Bering Strait, both today and in the Pleistocene fossil record (Elias and Kuzmina, 2008). Today they are limited to patches of relict steppe habitat in northeastern Siberia, such as on Wrangel Island (Lozhkin et al., 2001). Table 4 shows other species of leaf beetles found either on both sides of Bering Strait today, or isolated on only one side. The Siberian steppe-associated fauna includes *Galeruca interrupta*, *Hydrothassa hannoveriana*, *Phaedon concinnus*, and two species of *Phratora* (Fig. 3). The only steppe-associated leaf beetle species common to both sides of the Bering Strait is *Phaedon armoraciae* (Fig. 3). The Western Beringian beetle faunas were richer in steppe-associated species than were the Eastern Beringian faunas. Elias and Kuzmina (2008) point out that the steppe–tundra fauna played a dominant role in Western Beringian Pleistocene assemblages, even through interglacial intervals. In contrast to the situation in most of arctic North America, most of northeast Asia's lowlands were free from ice cover during Pleistocene glaciations, allowing unbroken biotic communication between southern and northern Siberia. This, in turn, allowed northern Siberia to be repeatedly invaded by southern steppe species during warm intervals.

There are relict patches of steppe-like habitats on both sides of the Bering Strait today. The modern insect fauna of relict steppe patches in the mountains of the Yukon Territory has been studied by Berman et al. (2001). They found that some species of steppe weevils (family Curculionidae) have managed to survive in these relict patches, such as *Coniocleonus zherichini*. This is a cold-adapted weevil that is mainly found today only in relict steppe localities of northeast Siberia, along the upper Yana and Indigirka river basins. It has also survived in relict steppe environments on south facing slopes of mountains in the Yukon (Fig. 4). Other typical steppe weevils from northeast Siberia, such as *Hypera ornata* and all members of the genus *Stephanocleonus* are absent from North America. These weevils, including *Coniocleonus*, dominated steppe–tundra faunas of Western Beringia during the Pleistocene, but failed

to become established east of the BLB. So some Asian steppe weevils made it across the BLB, while others did not.

The same phenomenon can be observed in the steppe-adapted weevil fauna of Eastern Beringia. The North American weevil *Vitavitus thulius*, a typical steppe–tundra beetle in Eastern Beringia, became established in the Kolyma Lowland and Anadyr River basin of Western Beringia during the Pleistocene, but is not found in Asia today (Fig. 4). Berman et al. (2001) note that this weevil has managed to disperse into formerly glaciated regions of northern Canada in postglacial times, and that it is associated with dry mountain tundra slopes and steppes of the Yukon, although it has not ventured into similar habitats in Alaska during the Holocene, even though it was present there during the Pleistocene. Much of the interior and northern Yukon regions today are quite dry. A total of 19 out of 30 meteorological stations in the Yukon record less than 350 mm of annual precipitation (Environment Canada, 1982), and the average mean annual precipitation (MAP) of these stations is 268 mm. The remaining sites are either situated in mountainous regions, or near the southern boundary, where they are closer to sources of Pacific moisture. However, the same could be said for the interior lowland regions of Alaska, where the MAP for 11 stations is 291 mm (NOAA, 2002).

Other predominantly Eastern Beringian weevils, such as *Lepidophorus lineaticollis*, which dominates many steppe–tundra beetle assemblages from this region, managed to establish a 'beach head' in the easternmost regions of Western Beringia (i.e., coastal Chukotka), but never made it any farther west in Asia (Fig. 4).

2.3. The dispersal of the woolly rhinoceros

The Pleistocene woolly rhinoceros (*Coelodonta antiquitatis* Blumenbach, 1799) was a cold-adapted rhinoceros first known from the Wucheng Formation of northern China 2.5 Mya (Deng, 2008). From here, it migrated northwest across the Palaeartic, reaching western Europe by MIS 12 (Bad Frankenhausen, Germany; Kahlke and Lacomat, 2007). The extent of the woolly rhinoceros' range waxed and waned with the glacial-temperate episodes that characterized the Pleistocene, with its greatest distributions corresponding to the glacial episodes of the late Pleistocene. Perhaps strangely, given the origins of the woolly rhinoceros in northern China and Transbaikalia, woolly rhinoceros is only known from northeastern Siberia during the Last Glaciation (Valdai). The woolly rhinoceros appears to have been relatively unhindered in moving west across the Palaeartic during the Pleistocene, but some form of barrier prevented colonization of northeastern Siberia until the Last Glaciation. In addition to this delay, the woolly rhinoceros also appears to have been prevented from crossing the BLB and colonizing Eastern Beringia at all. It would appear that despite finally colonizing Western Beringia, and being in a position to cross the BLB and migrate onto the North American landmass, a filter restricted the distribution of this taxon to Western Beringia.

The work of Kahlke (1999) shows the distribution of the woolly rhinoceros at the Last Glaciation to be widespread across the Palaeartic region, but never conquering the Scandinavian region or North America. More recently, finds have been recorded from Chukotka, Kamchatka and Wrangel Island in northeastern Siberia (Tikhonov et al., 1999; Boeskorov, 2001). These eastern populations put the woolly rhinoceros on the doorstep of the BLB, yet still it failed to cross despite other members of the same faunal assemblage (*Mammuthus–Coelodonta* faunal complex; Kahlke, 1999) being successful. Chief among these taxa are the previously mentioned woolly mammoth and Pleistocene horses. Proboscideans had their origins firmly in the Old World, yet migrated into the New World via the BLB approximately 1.8 Ma BP (as *Archidiskodon meridionalis*). A second pulse of mammoth migration pushed *Mammuthus primigenius* (woolly mammoth) into North America

Table 4
Comparative species of Western and Eastern Beringian leaf beetles (after Elias and Kuzmina, 2008)

Western Beringia	Eastern Beringia
<i>Chrysolina arctica</i> Medv.	<i>Chrysolina basilaris</i> (Say)
<i>Chrysolina brunnicornis wrangelia</i> Vor.	
<i>Chrysolina septentrionalis</i> (Men.)	<i>Chrysolina septentrionalis</i> (Men.)
<i>Phratora vulgatissima</i> L.	<i>Phratora hudsonia</i> Brown
<i>Phratora polaris</i> Schn.	
<i>Phaedon armoraciae</i> L.	<i>Phaedon armoraciae</i> L.
<i>Phaedon concinnus</i> Steph.	<i>Phaedon cyanescens</i> Stal.
<i>Hydrothassa hannoverana</i> F.	<i>Hydrothassa boreala</i> Sch.

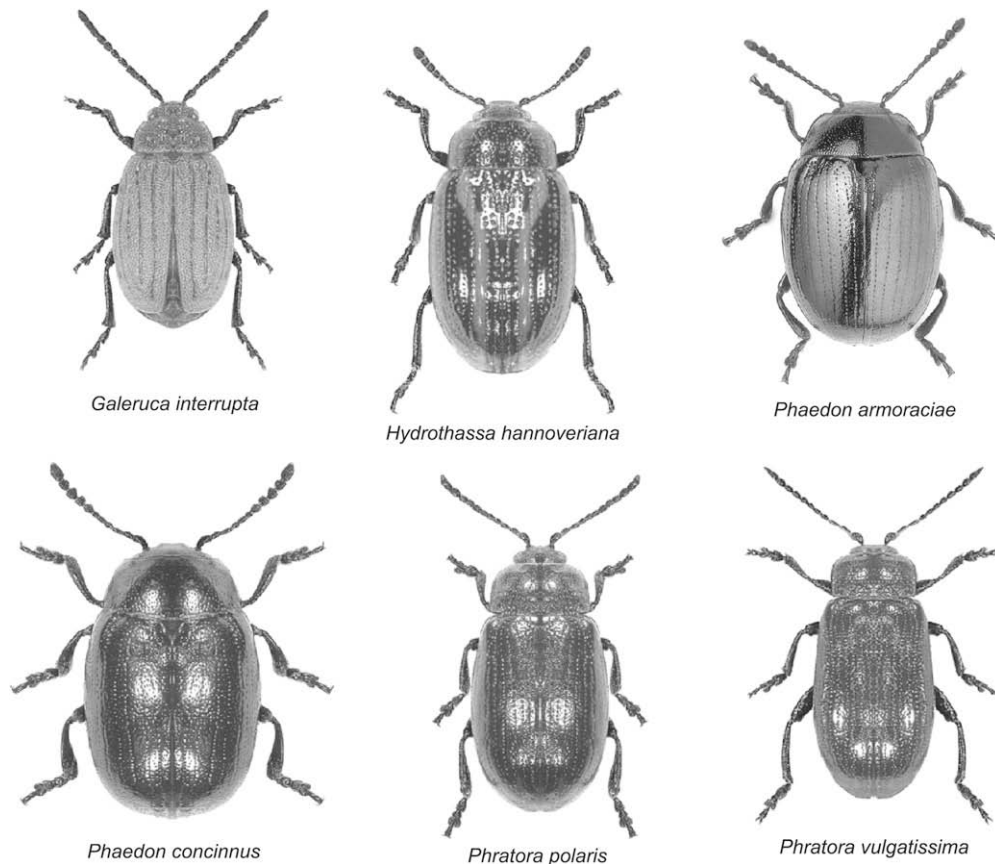


Fig. 3. Light microscope photographs of leaf beetles (Chrysomelidae) associated with relict steppe habitats in northeast Siberia, Alaska and the Yukon Territory. Photos of *Galeruca interrupta*, *Hydrothassa hannoveriana*, *Phaedon concinnus*, *Phratora polaris* and *Phratora vulgatissima* courtesy of Dr Lech Borowiec, University of Wroclaw, Poland. Photo of *Phaedon armoraciae* courtesy of K. Makarov, Zoological Institute, Russian Academy of Sciences, St Petersburg.

long before the LGM. The bison (*Bison priscus*), another taxon with a broadly similar feeding preference to *Coelodonta*, managed to cross from Asia to Eastern Beringia before the LGM, sometime between MIS 8 and 6 (Shapiro et al., 2004).

Despite originating in northern China and subsequently spreading westwards through Eurasia, the woolly rhinoceros is not known from eastern Siberia before the last glacial episode (Valdai, Weichselian, Devensian). The precise nature of the barrier that prevented the entrance of *Coelodonta* into eastern Siberia prior to MIS 3 is uncertain. There was no extensive land ice in this region during the late Pleistocene (Brigham-Grette, 2001) but the Barents–Kara ice sheet extended as far east as the western margin of the Taymyr peninsula and south onto the Siberian landmass (Hubberten et al., 2004). The woolly rhinoceros was still present in China during the late Pleistocene (Deng, 2006), so if this moderate glaciation present in Taymyr offered any impediment to the eastward spread of European *Coelodonta* populations, there was no similar barrier to the Chinese populations aside from the Altai and Baikal mountains around Lake Baikal. The variability of the climate in this region was possibly a contributory factor, with full arid, glacial conditions reached only during the LGM (Hubberten et al., 2004).

There has been much debate centred around whether variation in vegetation across the BLB, caused by changes in micro-climate (Elias et al., 1997; Guthrie, 2001) together with frequent waterlogged ground, was a sufficient barrier to prevent the woolly rhinoceros from crossing the BLB. The extent of the mesic shrub tundra across the BLB is unknown, a factor largely attributed to incomplete sampling (Elias et al., 1997). The Last Glaciation was the first, and only, opportunity for *Coelodonta* to cross into the New World from Western Beringia, whereas the other components of

the *Mammuthus–Coelodonta* faunal complex had done so much earlier. Taking all the above into consideration leads to a supposition that the woolly rhinoceros arrived in Chukotka too late to take advantage of conditions that made crossing the BLB possible for the other (earlier) taxa. A similar scenario is proposed for the failure of the woolly rhinoceros to colonize Scandinavia, despite the woolly mammoth having already done so. Arriving when it did (>49,000 BP; Boeskorov, 2001), the woolly rhinoceros encountered more mesic and waterlogged conditions. These are the conditions that the woolly rhinoceros would have tried to avoid because of its long coat and gait that were better suited for firmer, flatter ground. The more mesic conditions would have had a corresponding effect on the dominant vegetation, which was unsuited to the derived feeding characteristics of the grazing woolly rhinoceros. The woolly rhinoceros would probably have avoided both deep snow and sodden ground in the same way as the Pleistocene musk ox (*Ovibos moschatus*) would have done (Kahlke, 1999) as their wool would have ceased to have been an effective insulator against the cold if wet and waterlogged. It is interesting to note therefore that the helmeted musk ox (*Bootherium*) had a similar pelage, stance and gait to that of the woolly rhinoceros and it also failed to cross the BLB. *Bootherium* is known from the Eastern Beringian region both before and after the last glacial maximum (Mead and Meltzer, 1984; Guthrie, 2001) but did not manage to cross the BLB to the Old World from America. It is likely that the same barrier of waterlogged ground prevented *Bootherium* from crossing the BLB in the same manner as prevented *Coelodonta*.

In summary, it is likely that *Coelodonta* arrived too late in northeastern Siberia to cross the BLB into the Americas. Restricted from entering the Beringian region prior to MIS 3, by the time the



Fig. 4. Map of the Arctic, showing the known modern distributions of three species of weevils (Curculionidae) associated with steppe-tundra environments in the Pleistocene. Data from Berman et al., 2001.

woolly rhinoceros finally arrived in Western Beringia the conditions on the bridge itself had worsened to such an extent as to make it broadly impassable for the woolly rhinoceros. These mesic conditions on the bridge would have made the ground too uneven and too wet for the stocky and woolly *Coelodonta* to cross.

3. Discussion

In attempting to reconstruct the glacial environments of the BLB, we are up against several thorny problems. The different lines of evidence (vertebrates, insects, plant macrofossils, and pollen; modern biogeographic patterns versus fossil data) do not always agree. In many ways we are like the committee of blind scientists, asked to describe an elephant. Each researcher gropes along one body part, and assumes that the whole beast is represented by that one part (the small tail, the massive legs, the long, flexible trunk, or the hard, curved tusks). In fact none of them is capable of describing the entire animal, because none of them has seen it in its entirety. This is certainly the case when we attempt to describe the BLB. None of us has enough evidence to get the job done. Nevertheless, we are slowly progressing, and enough has been done to foster a scientific debate.

Ager (2003) concluded that Guthrie's reconstruction of BLB environments (Guthrie, 2001), as well as Yurtsev's similar reconstruction of a band of mesic shrub tundra on the BLB (Yurtsev, 2001), "appear to be based on fossil evidence described by Elias et al. (1996)". In fact both Guthrie and Yurtsev gave careful consideration to several lines of evidence, past and present, when drawing their conclusions about a mesic environment on the land bridge. Guthrie (2001) pointed out that botanists such as Young (1971) commented on an apparent west-east moisture gradient effect in the zonation of the Arctic flora regions. Murray (1995) identified several plant species that have a limited distribution in the Bering Strait region, but are only found on one side or the other. A moisture gradient (higher moisture towards the BLB and lower moisture towards interior Alaska) was discussed by Young, 1982. Anderson and Brubaker (1994) also interpreted a significant east-west moisture gradient across Alaska during glacial intervals. Ironically, it may have been the relative wetness of western Alaska and the BLB that allowed lakes to persist in these regions through the LGM. These lakes, including Imuruk Lake on the Seward Peninsula, Kaiyak Lake and Squirrel Lake near Kotzebue, Zagoskin Lake on St Matthew Island, Flora Lake on St Lawrence Island, and Cagaloq Lake on St Paul Island, persisted through the LGM, yielding

the pollen used by Ager (2003) to argue *against* moist conditions in his study region. Guthrie (2001) noted that nearly all of the sediment cores taken from extant lakes in interior Alaska and the Yukon Territory have basal ages less than 15,000 years old. He concluded that the dry climate of these interior regions of Eastern Beringia made most lakes in this region dry up. Yurtsev (2001) argued that the exposed shelf of the Bering Strait and some adjacent regions received relatively high levels of precipitation, carried by moisture-laden winds from the North Pacific. He likened the spread of steppe–tundra vegetation across the BLB to the populating of an archipelago of small, dry islands.

3.1. Problems with pollen interpretation

Part of the difficulty in reconstructing ancient Beringian environments from pollen assemblages is the lack of ecological definition of pollen at the generic or family level. Grass pollen is extremely difficult to identify beyond the family level, and so it is generally reported as ‘Poaceae’ or ‘Graminaceae’ in pollen diagrams. But species within this large family have quite variable ecological requirements in Alaska today, and not all of them are indicative of dry environments. In fact, quite the opposite is true for some of the important Arctic grass species. For instance, the dominant Poaceae pollen in modern samples from Barrow, Alaska is *Dupontia fischeri* (Eisner and Peterson, 1998; Elias et al., unpublished). This species grows in wet tundra, often where there is standing water (Hultén, 1968). So arctic Poaceae pollen can be rightly considered just as much an indicator of wet tundra environments (such as on the Arctic coastal plain today) as it might be of dry steppe–tundra conditions. Oswald et al. (2003) were able to discriminate the modern pollen signatures of wet tundra and mesic shrub tundra on the Alaskan North Slope, based on the fact that the former plant community is dominated by the pollen of *Dupontia* and other grasses, while the latter community is dominated by pollen of dwarf shrubs. However, in fossil assemblages it would be impossible to separate *Dupontia* pollen from the pollen of dry-adapted grasses that might have formed part of a steppe–tundra community (see Table 1 for a list of typical steppe–tundra grasses).

Likewise, pollen from the family Cyperaceae is extremely difficult to distinguish at the genus or species level, so it is generally reported as Cyperaceae pollen, but how should this ‘signal’ be interpreted? Most members of this family are sedges (*Carex*), and most sedges grow in damp or waterlogged soils, but the dominant plant on the LGM landscape at Cape Espenberg, based on plant macrofossils, was *Kobresia myosuroides*. This is an upland, dry-adapted species, found today on dry mountain slopes and lichen tundra in Alaska (Hultén, 1968), but the pollen it produces is indistinguishable from that of aquatic sedges. Thus the palaeoenvironmental signals of sedges and grasses may be interpreted backwards from the normal method. At least in some contexts, Poaceae pollen may be taken as an indication of wet tundra and Cyperaceae pollen may be taken as an indication of dry tundra.

3.2. Steppe–tundra habitat islands on the land bridge?

As we have alluded to in this review, all of the LGM sites from which steppe–tundra or equivalent vegetation have been interpreted in the central region of Beringia are either on the Alaskan mainland, or on islands in the Bering Sea. The island localities would have been perched well above the elevation of the land bridge plains. Their height above the plain ranged from perhaps 75 to 200 m. These are not enormous heights, but there is at least a possibility that the environment of these uplands may have been sufficiently different to create habitat islands where relatively dry climate allowed steppe–tundra vegetation to persist. Yurtsev (2001) anticipated this reconstruction when he said that the spread

of steppe–tundra vegetation across the land bridge was like the populating of an archipelago of small, dry islands.

3.3. Abandoning the broad-brush approach

None of us should take the view that the BLB, or any other large geographic region, was completely dominated by a single type of biological community. All ecosystems, past and present, are made up of patches of varied communities. Certain community types may dominate, but not to the exclusion of others. Palaeoecologists (including Elias) who have attempted to reconstruct BLB environments for the Last Glaciation have too often fallen into the trap of attempting to reconstruct major portions of the land bridge from fossil data from just a few sites. At its height, the BLB covered about 1.5 million km²—a region about twice the size of Texas. During the LGM, the distance from the northern margin of the land bridge to the southern margin was 1800 km. Thus far, we have only got a handful of sites from the BLB region from which to draw conclusions. Whole sectors of the land bridge remain unstudied, including the Russian side of the Bering and Chukchi shelf regions. The Bering shelf region between the Pribilof Islands and the Alaskan Peninsula likewise remains unstudied. Parts of the Chukchi shelf have been studied (Elias et al., 1996, 1997), but thus far have not yielded organic-rich sediments dating as far back as the LGM. The few LGM samples from the land bridge plain are both quite near the shore of the Seward Peninsula. As discussed above, the island sites were all perched above this plain, and their fossil pollen signatures may or may not characterize the vegetation of the adjacent lowlands.

On biogeographic grounds, it appears that we can make a case for the presence of some kind of biological filter that blocked the movements of some steppe–tundra plants and animals across the BLB. Dry-adapted plants, some steppe weevils, and some megafaunal mammals failed to get established on one side or the other, and a land-bridge barrier seems the most likely cause.

Acknowledgements

Support for the preparation of this paper came from a grant from the Leverhulme Foundation, F/07 537/T. B.C. extends his thanks to NERC and the Natural History Museum for funding this research as part of a PhD titled ‘The Evolution and Palaeoecology of the Pleistocene woolly rhinoceros *Coelodonta antiquitatis* (Blumenbach, 1799)’ (ref: NER/S/C/2006/14279). Thanks also go to Dr Danielle Schreve (Department of Geography, Royal Holloway, University of London) and Mr Andrew Carrant (Department of Palaeontology, Natural History Museum) for their essential support in the supervision of this project.

References

- Ager, T.A., 1982. Vegetational history of western Alaska during the Wisconsin glacial interval and the Holocene. In: Hopkins, D.M., Matthews Jr., J.V., Schweger, C.E., Young, S.B. (Eds.), *Paleoecology of Beringia*. Academic Press, New York, pp. 75–93.
- Ager, T.A., 2003. Late Quaternary vegetation and climate history of the central Bering land bridge from St Michael Island, western Alaska. *Quaternary Research* 60, 19–32.
- Alfimov, A.V., Berman, D.I., 2001. On Beringian climate during the late Pleistocene and Holocene. *Quaternary Science Reviews* 20, 127–134.
- Anderson, P.M., 1985. Late Quaternary vegetational change in the Kotzebue Sound area, northwestern Alaska. *Quaternary Research* 24, 307–321.
- Anderson, P.M., Brubaker, L.B., 1994. Vegetation history of northcentral Alaska: a mapped summary of late-Quaternary pollen data. *Quaternary Science Reviews* 13, 71–92.
- Anderson, R.S., Peck, S.B., 1985. The Insects and Arachnids of Canada, Part 13. The Carrion Beetles of Canada and Alaska. *Biosystematics Research Institute, Research Branch, Agriculture Canada Publication* 1778.
- Bain, A.L., Morgan, A.V., Burns, J.A., Morgan, A., 1997. The palaeoentomology of Rat’s Nest Cave, Grotto Mountain, Alberta, Canada. In: Ashworth, A.C., Buckland, P.C., Sadler, J.P. (Eds.), *Studies in Quaternary Entomology—An Inordinate Fondness*

- for Insects. Quaternary Proceedings 5. Quaternary Research Association, Wiley, Chichester, pp. 23–33.
- Berman, D.I., Korotyaev, B.A., Alfimov, A.V., 2001. Contribution to the weevil fauna (Coleoptera: Apionidae, Curculionidae) of the mountain steppes in the Yukon Territory, Canada, with reference to the Pleistocene history of Beringia. *Entomological Review* 81, 993–998.
- Böcher, J., 1988. The Coleoptera of Greenland. *Meddelelser om Grønland Bioscience* 26, 1–100.
- Boeskorov, G.G., 2001. Woolly rhino (*Coelodonta antiquitatis*) distribution in northeast Asia. *Deinsea* 8, 15–20.
- Brigham-Grette, J., 2001. New perspectives on Beringian Quaternary paleogeography, stratigraphy and glacial history. *Quaternary Science Reviews* 20, 15–24.
- Brigham-Grette, J., Gualtieri, L.M., Glushkova, O.Y., Hamilton, T.D., Mostoller, D., Kotov, A., 2003. Chlorine-36 and ¹⁴C chronology support a limited last glacial maximum across central Chukotka, northeastern Siberia, and no Beringian ice sheet. *Quaternary Research* 59, 386–398.
- Colinvaux, P.A., 1964. The environment of the Bering Land Bridge. *Ecological Monographs* 34, 297–329.
- Colinvaux, P.A., 1967. A long pollen record from St Lawrence Island, Bering Sea (Alaska). *Palaeogeography, Palaeoclimatology, Palaeoecology* 3, 29–48.
- Colinvaux, P.A., 1981. Historical ecology in Beringia: the South Land Bridge coast at St Paul Island. *Quaternary Research* 16, 18–36.
- Cooper, D.J., Sanderson, J.S., 1997. A montane *Kobresia myosuroides* fen community type in the southern Rocky Mountains of Colorado. *U.S.A. Arctic and Alpine Research* 29, 300–303.
- Dall, W.H., Harris, G.D., 1892. Correlation papers, Neogene. U.S. Geological Survey Bulletin 84.
- Darwin, C., 1859. *The Origin of Species*. John Murray, London.
- Dawson, G.M., 1894. Geologic notes on some of the coasts and islands of Bering Sea and vicinity. *Geological Society of America Bulletin* 5, 117–146.
- Deng, T., 2006. The fossils of the Przewalski's horse and the climatic variations of the Late Pleistocene in China. 2005. In: Mashkour, M. (Ed.), *Equids in Time and Space: Papers in Honour of Vera Eisenmann*. Oxbow Books, Oxford, pp. 12–19.
- Deng, T., 2008. Comparison between woolly rhino forelimbs from Longdan, northwestern China and Tologoi, Transbaikalian region. *Quaternary International* 179, 196–207.
- Eisner, W.R., Peterson, K.M., 1998. High resolution pollen analysis of tundra polygons from the North Slope of Alaska. *Journal of Geophysical Research* 103 (D22), 28929–28937.
- Elias, S.A., 1992a. Late Wisconsin insects and plant macrofossils associated with the Colorado Creek mammoth, southwestern Alaska: taphonomic and paleoenvironmental implications. 22nd Arctic Workshop, Program and Abstracts, pp. 45–47.
- Elias, S.A., 1992b. Late Quaternary beetle fauna of southwestern Alaska: evidence of a refugium for mesic and hygrophilous species. *Arctic and Alpine Research* 24, 133–144.
- Elias, S.A., 2001. Mutual Climatic Range reconstructions of seasonal temperatures based on late Pleistocene fossil beetle assemblages in Eastern Beringia. *Quaternary Science Reviews* 20, 77–91.
- Elias, S.A., Brigham-Grette, J., 2007. Glaciations: Late Pleistocene events in Beringia. In: Elias, S.A. (Ed.), *Encyclopedia of Quaternary Science*. Elsevier, Amsterdam, pp. 1057–1066.
- Elias, S.A., Kuzmina, S., 2008. Palaeontology. In: Jolivet, P., Santiago-Blay, J., Schmitt, M. (Eds.), *Research on Chrysomelidae*. Brill Academic Publishers, Leiden, pp. 174–193.
- Elias, S.A., Short, S.K., Nelson, C.H., Birks, H.H., 1996. Life and times of the Bering land bridge. *Nature* 382, 60–63.
- Elias, S.A., Short, S.K., Birks, H.H., 1997. Late Wisconsin environments of the Bering Land Bridge. *Palaeogeography, Palaeoclimatology, Palaeoecology* 136, 293–308.
- Elias, S.A., Berman, D., Alfimov, A., 2000. Late Pleistocene beetle faunas of Beringia: where East met West. *Journal of Biogeography* 27, 1349–1364.
- Environment Canada, 1982. Canadian Climate Normals, Temperature and Precipitation. The North – Yukon Territory and Northwest Territories, 55 pp.
- Goetheus, V., Birks, H.H., 2001. Full-glacial upland tundra vegetation preserved under tephra in the Beringia National Park, Seward Peninsula, Alaska. *Quaternary Science Reviews* 20, 135–147.
- Guthrie, R.D., 2001. Origins and causes of the mammoth steppe: a story of cloud cover, woolly mammoth tooth pits, buckles, and inside-out Beringia. *Quaternary Science Reviews* 20, 549–574.
- Hoffecker, J.F., Elias, S.A., 2007. *Human Ecology of Beringia*. Columbia University Press, New York.
- Hoffecker, J.F., Powers, W.R., Goebel, T., 1993. The colonization of Beringia and the peopling of the New World. *Science* 259, 46–53.
- Hopkins, D.M., 1967. Introduction. In: Hopkins, D.M. (Ed.), *The Bering Land Bridge*. Stanford University Press, Stanford, California, pp. 1–6.
- Hopkins, D.M., 1988. The Espenberg Maars: a record of explosive volcanic activity in the Devil Mountain-Cape Espenberg area, Seward Peninsula, Alaska. In: Schaaf, J. (Ed.), *The Bering Land Bridge National Preserve: An Archaeological Survey*. National Park Service, Alaska Region Research/Management Report AR-14, pp. 262–321.
- Hopkins, D.M., Smith, P.A., Matthews, J.V., 1981. Dated wood from Alaska and the Yukon: implications for forest refugia in Beringia. *Quaternary Research* 15, 217–249.
- Hubbarten, H.W., Andreev, A., Astakhov, V.I., Demidov, I., Dowdeswell, J.A., Henriksen, M., Hjort, C., Houmark-Nielsen, M., Jakobsson, M., Kuzmina, S., Larsen, E., Lunkka, J.P., Lyså, A., Mangerud, J., Möller, P., Saarnisto, M., Schirmermeister, L., Sher, A.V., Siegert, C., Siegert, M.J., Svendsen, J.I., 2004. The periglacial climate and environment in northern Eurasia during the last glaciation. *Quaternary Science Reviews* 23, 1333–1357.
- Hughes, O., 1983. Quaternary geology, Yukon Territory and western District of Mackenzie. In: Thorson, R.M., Hamilton, T.D. (Eds.), *Glaciation*. University of Alaska, Fairbanks, Alaska Quaternary Center, pp. 51–56.
- Hultén, E., 1968. *Flora of Alaska and Neighboring Territories. A Manual of the Vascular Plants*. Stanford University Press, Stanford, CA, 1008 pp.
- Kahlke, R.-D., 1999. The history of the origin, evolution and dispersal of the late Pleistocene *Mammuthus-Coelodonta* faunal complex in Eurasia (large mammals). *Advances in Mammoth Research: Proceedings of the Second International Mammoth Conference, Rotterdam, 16–20 May 1999. The Mammoth Site of Hot Springs, South Dakota*, 219 pp.
- Kahlke, R.-D., Lacombe, F., 2007. Earliest occurrence of woolly rhinoceros (*Coelodonta antiquitatis*) in Europe. In: Boeskorov, G. (Ed.), *Abstracts of the Fourth International Mammoth Conference*. Ministry of Science and Professional Education of the Republic of Sakha, Yakutsk, pp. 141–142.
- Kuzmina, S., Elias, S.A., Matheus, P., Storer, J.E., Sher, A., 2008. Paleoenvironmental reconstruction of the Last Glacial Maximum, inferred from insect fossils from a tephra buried soil at Tempest Lake, Seward Peninsula, Alaska. *Palaeogeography, Palaeoclimatology, Palaeoecology* 267, 245–255.
- Lindroth, C.H., 1968. The ground beetles of Canada and Alaska, part 5. *Opuscula Entomologica Supplement* 33, 649–944.
- Lozhkin, A.V., Anderson, P.M., Vartanyan, S.L., Brown, T.A., Belaya, B.V., Kotov, A.N., 2001. Late Quaternary paleoenvironments and modern pollen data from Wrangel Island (Northern Chukotka). *Quaternary Science Reviews* 20, 217–233.
- Makarova, O.L., Bieńkowski, A.O., Bulavintsev, V.I., Sokolov, A.V., 2007. Beetles (Coleoptera) in polar deserts of the Severnaya Zemlya Archipelago. *Entomological Review* 87, 1142–1154.
- Mann, D.H., Hamilton, T.D., 1995. Late Pleistocene and Holocene paleoenvironments of the north Pacific coast. *Quaternary Science Reviews* 14, 449–471.
- Matthews Jr., J.V., 1974. Quaternary environments at Cape Deceit (Seward Peninsula, Alaska): evolution of a tundra ecosystem. *Geological Society of America Bulletin* 85, 1353–1384.
- Mead, J.L., Meltzer, D.J., 1984. North American late Quaternary extinctions and the radiocarbon record. In: Martin, P.S., Klein, R.G. (Eds.), *Quaternary Extinctions: A Prehistoric Revolution*. University of Arizona Press, Tucson, pp. 440–450.
- Miehe, G., 1996. On the connection of vegetation dynamics with climatic changes in High Asia. *Palaeogeography, Palaeoclimatology, Palaeoecology* 120, 5–24.
- Murray, D.F., 1995. The role of Arctic Refugia in the evolution of the Arctic vascular flora—a Beringian perspective. In: Scudder, G.G.E., Reveal, J.L. (Eds.), *Evolution Today. Proceedings of the Second International Congress of Systematic and Evolutionary Biology*. Hunt Institute of Botany Document, Pittsburgh, PA, pp. 11–20.
- NOAA, 2002. *Climatology of the United States No. 81. Monthly Station Normals of Temperature, Precipitation, and Heating and Cooling Degree Days 1971–2000, Alaska*. National Oceanic and Atmospheric Administration, Asheville, North Carolina, 35 pp.
- Shapiro, B., Drummond, A.J., Rambaut, A., Wilson, M.C., Matheus, P.E., Sher, A.V., Pybus, O.G., Gilbert, M.T.P., Barnes, I., Binladen, J., Willerslev, E., Hansen, A.J., Baryshnikov, G.F., Burns, J.A., Davydov, S., Driver, J.C., Froese, D.G., Harington, C.R., Keddie, G., Kosintsev, P., Kunz, M.L., Martin, L.D., Stephenson, R.O., Storer, J., Tedford, R., Zimov, S., Cooper, A., 2004. Rise and fall of the Beringian Steppe Bison. *Science* 306, 1561–1565.
- Thorson, R.M., Guthrie, R.D., 1992. Stratigraphy of the Colorado Creek mammoth locality, Alaska. *Quaternary Research* 37, 214–228.
- Tikhonov, A., Vartanyan, S., Joger, U., 1999. Woolly rhinoceros (*Coelodonta antiquitatis*) from Wrangel Island. *Darmstadter Beiträge zur Naturgeschichte* 9, 187–192.
- Wallace, A., 1876. *The Geographical Distribution of Animals*. Harper, New York.
- Wilmsen, E.N., 1965. *An outline of early man studies in the United States*. American Antiquity 31, 172–192.
- Young, S.B., 1971. The vascular flora of St Lawrence Island with special reference to floristic zonation in the Arctic regions. *Contributions from the Gray Herbarium of Harvard University* 201, 11–115.
- Young, S.B., 1982. The vegetation of the Bering Land Bridge. In: Hopkins, D.M., Matthews Jr., J.V., Schweger, C.E., Young, S.B. (Eds.), *Paleoecology of Beringia*. Academic Press, New York, pp. 179–191.
- Yurtsev, B.A., 1984. Problems of the Late Cenozoic paleogeography of Beringia in light of phytogeographic evidence. In: Kontrimavichus, V.L. (Ed.), *Beringia in the Cenozoic Era*. Amerind Publishing Co., New Delhi, pp. 129–153.
- Yurtsev, B.A., 2001. The Pleistocene 'Tundra-Steppe' and the productivity paradox: the landscape approach. *Quaternary Science Reviews* 20, 165–174.

Winter Biological Processes Could Help Convert Arctic Tundra to Shrubland

MATTHEW STURM, JOSH SCHIMEL, GARY MICHAELSON, JEFFREY M. WELKER, STEVEN F. OBERBAUER, GLEN E. LISTON, JACE FAHNESTOCK, AND VLADIMIR E. R OMANOVSKY

In arctic Alaska, air temperatures have warmed 0.5 degrees Celsius (°C) per decade for the past 30 years, with most of the warming coming in winter. Over the same period, shrub abundance has increased, perhaps a harbinger of a conversion of tundra to shrubland. Evidence suggests that winter biological processes are contributing to this conversion through a positive feedback that involves the snow-holding capacity of shrubs, the insulating properties of snow, a soil layer that has a high water content because it overlies nearly impermeable permafrost, and hardy microbes that can maintain metabolic activity at temperatures of -6°C or lower. Increasing shrub abundance leads to deeper snow, which promotes higher winter soil temperatures, greater microbial activity, and more plant-available nitrogen. High levels of soil nitrogen favor shrub growth the following summer. With climate models predicting continued warming, large areas of tundra could become converted to shrubland, with winter processes like those described here possibly playing a critical role.

Keywords: tundra, shrubs, snow, microbes, climate change

Transitions in vegetation are nothing new in the Arctic. The geologic record indicates that about 9000 years ago, the region underwent a widespread transformation from a grassland to a tundra ecosystem (Ager 1983). This resulted in the departure or extinction of the large Pleistocene megafauna (Owen-Smith 1987) and the exodus of Paleolithic humans from the Alaskan Arctic (Kunz and Reanier 1994). As recently as 8000 years ago, forests grew along the arctic coast (MacDonald et al. 2000), and the record also tells us that shrubs swept across the tundra several times during the Holocene (Anderson and Brubaker 1993). Now the abundance of arctic shrubs is again increasing, apparently driven by a warming climate. It is possible that we are witnessing the forerunner of another major transition in arctic vegetation.

The evidence for increasing shrub abundance is most comprehensive for northern Alaska. An extensive comparison of old (1940s) and modern photographs (figure 1; Sturm et al. 2001a, Stow et al. 2004) has shown that shrubs there are increasing in size and are colonizing previously shrub-free tundra. In western arctic Canada, increased shrub abundance is also indicated, but there the change has been inferred from the recollections of long-term residents (Thorpe et al. 2002). In central Russia, a transect along the Pechora River has shown a distinct decrease in tundra and a corresponding increase in shrubland (Shvartsman et al. 1999), but for the vast tundra regions of Siberia, there are currently no data on

which to make an assessment. Satellite remote sensing studies (Myneni et al. 1997, Silapaswan et al. 2001, Jia et al. 2003), however, greatly strengthen the case for a pan-Arctic expansion of shrubs. These studies indicate that over large regions of the tundra, leaf area has increased, a change one might expect if graminoids, lichen, and moss were giving way to shrubs.

The expansion of shrubs has coincided with three decades of rising arctic air temperatures. These are now at levels higher than any experienced in the last 400 years (Overpeck

Matthew Sturm (e-mail: mstur m@crrel.usace.army.mil) works at the US Army Cold Regions Research and Engineering Laboratory—Alaska, Fort Wainwright, AK 99703. Josh Schimel is with the Department of Ecology, Evolution and Marine Biology, University of California, Santa Barbara, CA 93106. Gary Michaelson works at the Agriculture and Forestry Experiment Station, and Vladimir E. Romanovsky is with the Geophysical Institute, at the University of Alaska Fairbanks (UAF), Fairbanks, AK 99775; Michaelson also works at the UAF Palmer Research Center, Palmer, AK 99645. Jeffrey M. Welker works in the Biology Department and Environment and Natural Resources Institute, University of Alaska Anchorage, Anchorage, AK 99510. Steven F. Oberbauer is with the Department of Biological Sciences, Florida International University, Miami, FL 33199. Glen E. Liston works at the Department of Atmospheric Science, Colorado State University, Fort Collins, CO 80523. Jace Fahnestock works at Northwind Inc., Idaho Falls, ID 83405. © 2005 American Institute of Biological Sciences.

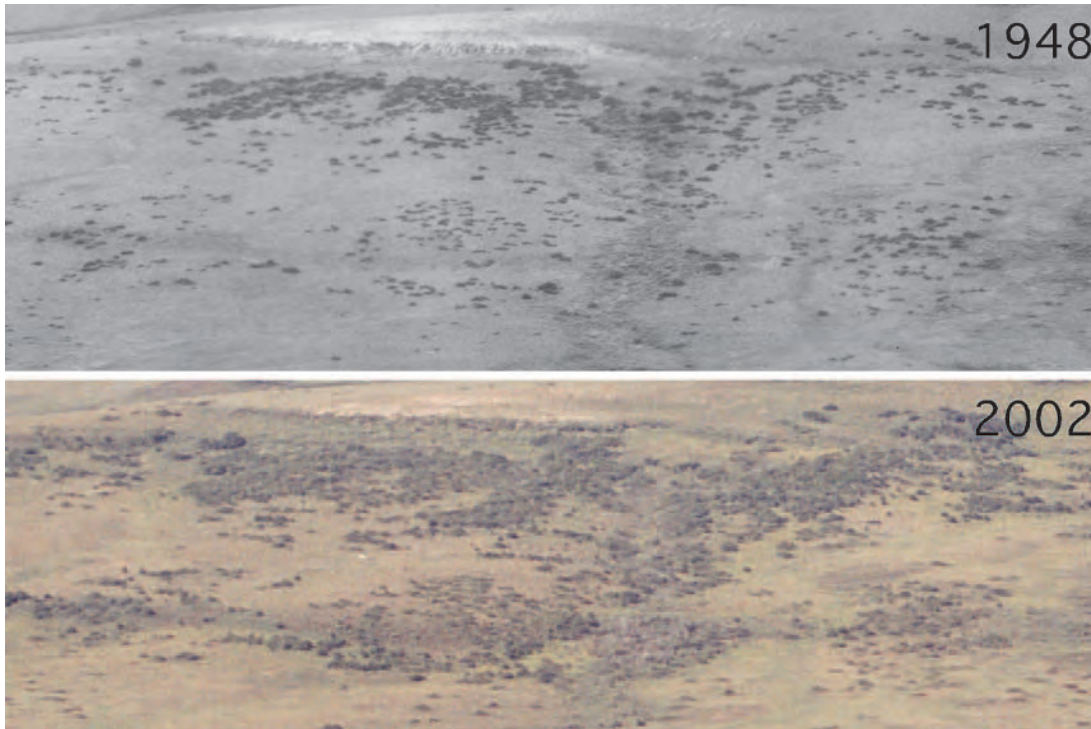


Figure 1. Increasing abundance of shrubs in arctic Alaska. The photographs were taken in 1948 and 2002 at identical locations on the Colville River (68° 57.9' north, 155° 47.4' west). Dark objects are individual shrubs 1 to 2 meters high and several meters in diameter. Similar changes have been detected at more than 200 other locations across arctic Alaska where comparative photographs are available. Photographs: (1948) US Navy, (2002) Ken Tape.

et al. 1997), and the rate, about 0.5 degrees Celsius (°C) per decade (Chapman and Walsh 1993, Serreze et al. 2000), is five times faster than the global rate of warming (Jones PD et al. 1999). A number of eye-catching environmental changes have been associated with this warming (Sturm et al. 2003), including (a) a reduction in the extent and thickness of sea ice (Parkinson et al. 1999), (b) the retreat of arctic and sub-arctic glaciers (Arendt et al. 2002), (c) increased annual discharge from large northward-flowing rivers (Peterson et al. 2002), and (d) an Arctic-wide increase in permafrost temperatures (Romanovsky et al. 2002).

With respect to the shrub expansion, it is surprising that most of the documented warming has taken place in winter (January–March; figure 2) and, to a lesser extent, in spring (April–June; Chapman and Walsh 1993, Serreze et al. 2000). Moreover, “spring” in this arctic context means freezing temperatures and a full snow cover through May and often into June. The conventional explanation for shrub expansion is accelerated summer growth, but with arctic warming predominantly affecting winter temperatures, processes outside the normal growing season are certain to be involved. Here we report how arctic soil microbes, buried under an insulating blanket of snow, remain surprisingly active during the frigid arctic winter, producing critical nutrients that the shrubs can utilize the following summer. As the shrubs grow, they trap and hold snow, which better insulates the soil and

the microbes, promoting even more winter activity. Combined, these two mechanisms form a winter feedback system that influences, and perhaps even controls, the transition of the arctic ecosystem from one state to another in response to a changing climate.

A conversion of arctic tundra to shrubland would have many ramifications. It would reduce forage quantity and quality for caribou, which prefer lichens and graminoids over shrubs. This would force the caribou to alter where they graze, which would affect subsistence hunters and the communities that rely on caribou for food. An extensive shrub canopy would also increase the summer sensible heat flux, perhaps by as much as 6 watts (W) per square meter (m^2) (Jason Beringer, School of Geography and Environmental Science, Monash University, Clayton, Australia, personal communication, 14 September 2004), more than twice the global impact of greenhouse gases, which are estimated to be approximately 3 W per m^2 (IPCC 2001). Dark shrubs protruding above the snow would reduce the winter albedo, increasing the solar energy absorbed at the surface. The increased production of woody material would affect the carbon budget. Shrubs allocate carbon to woody stems that have long turnover times compared with annual roots and the leaves of graminoids, so shrub-dominated tundra is likely to assimilate carbon in a different way and store it for a different length of time than shrub-free tundra. With the

Table 1. The five stages of arctic winter and their salient biophysical features (modified from Olsson et al. 2003).

Stage	Sensitivity to change	Salient features
Stage 1: Early snow	High (timing)	Maximum daily temperatures and active-layer temperatures above freezing, development of ephemeral snowpack
Stage 2: Early cold	High (timing and nature)	Daily average and maximum temperatures below freezing, rapid snow buildup, active layer beginning to freeze from the top down
Stage 3: Deep cold	Low	Little new snow accumulation, little or no solar radiation, active-layer temperatures falling, upper active layer completely frozen
Stage 4: Late cold	Low	Active-layer temperatures now in phase with air temperature, air temperature and active-layer temperatures beginning to rise, but active layer still frozen, with limited liquid water
Stage 5: Thaw	High (timing)	Minimum daily temperatures above freezing, snowpack melting, rapidly increasing soil temperatures

production of more woody material and the change in soil moisture levels due to shading, short- and long-term shifts in net carbon exchange and carbon storage would be set in motion (Oechel et al. 2000).

Winter, permafrost, and the active layer

The prolonged cold of arctic winter produces permafrost (perennially frozen ground) and snow that blankets the tundra for two-thirds of the year. These conditions constrain but do not stop biological activity. Significant plant and soil microbial activity continue during three of the five stages of winter that have been identified on the basis of surface and soil conditions (table 1; Olsson et al. 2003). The duration and starting date of these stages vary from year to year, with long-term shifts in stage timing being one of the ways winter can affect the ecosystem state. The asymmetry of winter also constrains above- and belowground biotic activity. The snow buildup is gradual over a period of several months, starting in September, but the melt is abrupt, taking as little as 5 days. As a consequence, the ground cools slowly but warms rapidly. The buildup is offset about 75 days after the summer solstice (June 21), but the melt occurs just a few weeks before the solstice. Plants emerge from the winter snow cover directly into an environment of near-maximum sunlight.

Because of the prolonged cold, permafrost (figure 3) forms a nearly continuous layer under the tundra regions of Alaska, Siberia, and northern Canada. Overlying the permafrost is the active layer, made up of strata of organic and mineral soil that thaw each summer and freeze the following winter. Depending on the location and year, maximum thaw depths range from 0.3 to more than 1.0 m. Because the permafrost is nearly impermeable to water infiltration, the active layer is often saturated, far more so than would be expected in the arid arctic climate. Stand-

ing surface water and lakes are ubiquitous. For example, more than 40% of the Arctic Coastal Plain of Alaska is covered by lakes (Sellman et al. 1975), despite low precipitation.

During summer, the active layer warms and thaws from the surface down. In winter, it cools and freezes from the surface down, as the winter cold wave penetrates through the snow and into the ground. It also freezes (albeit more slowly) from the bottom up, chilled by the underlying permafrost. The freezing process proceeds slowly, so it is not until the middle or even the end of winter that the layer is entirely frozen, and in mild winters it may not freeze completely. Even when a particular stratum in the active layer is described as “frozen,” a small amount of unfrozen water remains. Adsorption, water–soil particle interactions, and surface tension effects allow unfrozen water to exist at temperatures as low as -40°C (Anderson and Morgenstern 1973, Hinzman et al. 1991). The water is located in thin films (1 to 7 micrometers) that separate soil grains from the ice in pore spaces (Romanovsky and Osterkamp 2000). Depending on soil type, the films can occupy up to 10% of the soil by volume at temperatures between 0°C and -10°C , with thicker films found at higher temperatures and in soils

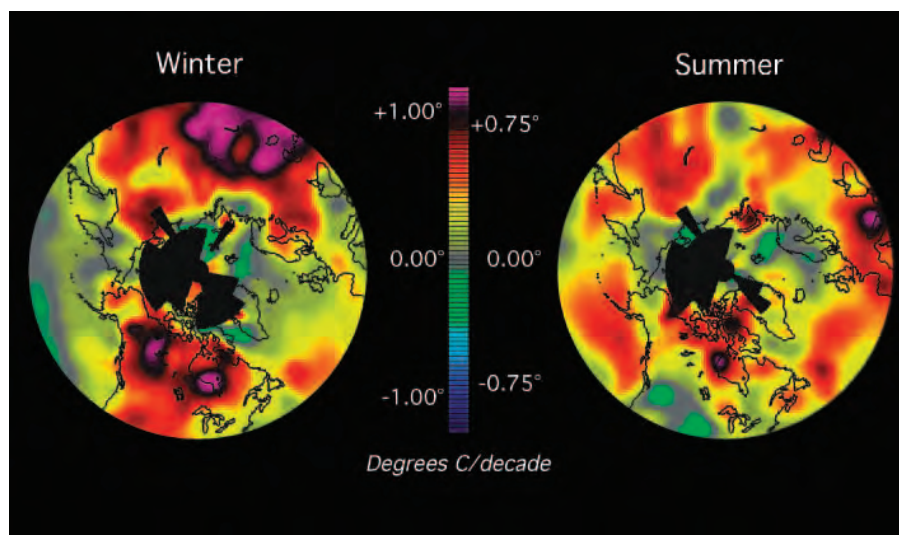


Figure 2. North polar view of the decadal warming in the Arctic in winter (left) and summer (right) for the period 1971 to 2000 (based on Chapman and Walsh 1993, updated at <http://faldo.atmos.uiuc.edu/ARCTIC>).



Figure 3. Soil pit profile from arctic Alaska, showing the active layer and the top of the permafrost, which is several hundred meters thick in this location. The hummocky, irregular nature of the interfaces between the layers is the result of cryoturbation, the slow convective overturning of the active layer. Photograph: Gary Michaelson.

with higher clay contents (Farouki 1981) and lower organic fractions (Hinzman et al. 1991). The presence of these unfrozen films produces a situation analogous to the one found in dry desert soils, where the bulk of the soil environment is inhospitable, but where niche environments are viable for microbes.

The buffered thermal environment of the active layer is, in part, a product of the latent heat barrier associated with soil water freezing. Until the abundant soil moisture trapped above the permafrost freezes, the soil temperature cannot drop below 0°C. This introduces delays in the downward propagation of the 0°C isotherm, which range from just a few days at the soil surface to several months near the base of the active layer (figure 4). For a typical active layer 0.4 m thick, with a liquid water content of 40% by volume, 5 kilojoules (kJ) of latent heat need to be removed from each square centimeter (cm²) of ground surface before the layer can freeze. Only 0.14 kJ of the heat that needs to be removed is due to the specific heat of dry soil. The snow cover also contributes to the buffered thermal environment in the active layer. Snow, a mixture of air and ice, is an excellent insulator. Its R-values (measuring resistance to heat flow) compare favorably with those of many manufactured insulating materials. For instance, the insulation provided by 0.5 m of arctic snow is equivalent to that of a fiberglass-insulated wall 6 inches (about 15 cm) thick, with an R-value of 20. Measurement and model results (Taras et al. 2002) show that, through its insulating properties, snow attenuates weekly winter air temperature fluctuations by about 40% and daily fluctuations by about 80%. At Franklin Bluffs, 50 kilometers (km) south of Prudhoe Bay,

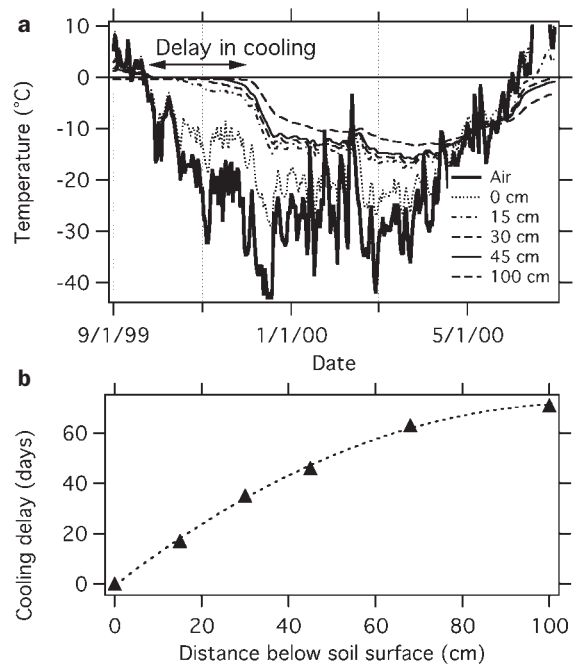


Figure 4. (a) A temperature record for the air and different depths of soil near Prudhoe Bay, Alaska. (b) The delay in cooling at depth in the soil due to latent heat storage in the ground and snow-cover insulation.

the average air temperature between 1 November 1999 and 1 May 2000 was -26°C, but the average temperature at 0.3 m depth in the soil was -10°C (figure 4a). The contrast in minimum temperatures was even greater: -45°C in the air compared with -16°C in the soil.

Snow cover, shrubs, and active-layer temperatures

On the windswept tundra, drifting snow is common, and deep drifts often surround and extend downwind from shrubs (figure 5). Where the snow is deeper, soil temperatures are higher because there is more insulation. In fact, as illustrated in figure 6, with sufficiently deep snow, subnivean temperatures can be elevated enough to convert a soil in which there is little or no unfrozen water into one in which unfrozen water films are widespread. In extreme cases, deep drifts can even prevent arctic soils from freezing. Organic debris and leaf litter also tend to concentrate in drifts (Fahnestock et al. 2000), potentially adding a nutrient boost to the same locations where there is a favorable thermal environment for soil microbes.

The snow depth enhancement effect is not limited to individual shrubs or patches of shrubs like those in figure 5. When snow depths from a 100-hectare shrubland in Alaska (1.5-m shrubs) were compared with depths from nearby shrub-free tundra, the snow in the shrubs was consistently deeper (17% to 48%). The deeper snow not only contained more water but also was less dense and therefore a better insulator than the snow on the tundra. The depth difference



Figure 5. A shrub patch that has created a snowdrift in and downwind of the patch. The snow on the tundra behind the patch was about one-fifth as deep as the drift. Photograph: Matthew Sturm.

reflects the enhanced capacity of the shrubs to trap snow, and also a reduction in the amount of sublimation the snow would otherwise have undergone had it been free to blow about (Sturm et al. 2001b, Liston et al. 2002). Up to 40% of the winter snow accumulation can be removed by sublimation if it is not trapped by shrubs (Liston and Sturm 2002).

We examined the effect of a widespread, climatically forced increase in shrub abundance on winter soil microbial activity using two coupled models, one that produces snow depth distributions based on topography and drift-trapping by vegetation (Liston and Sturm 1998) and another that simulates soil temperatures based on the snow depth (Taras et al. 2002). Using the models, we computed the expected number of winter days that microbes are active for a control winter (the present) and for a future state in which shrubs have increased in size and density. For simplicity, we assumed that soil microbes are active as long as the active-layer surface temperature is above -6°C , but that they shut down completely at lower temperatures.

Our focus was the 9000-km² Kuparuk Basin, which stretches from the Brooks Range (68.5° north [N]) to the Arctic Coast (70.5° N) near Prudhoe Bay, Alaska. From south to north across the basin, there is a 3°C decrease in winter air temperature (Haugen 1982, Olsson et al. 2002) and a pronounced decrease in snow depth (Liston and Sturm 2002, Taras et al. 2002). Winter lasts 15 days longer near the coast than it does near the Brooks Range (Taras et al. 2002), and the mean and peak wind speeds are also generally higher near the coast (Olsson et al. 2002). As a result, the snow cover in the north-

ern part of the basin is thinner, more windblown, less insulative, and longer lasting than the snow cover in the southern part. Under present-day conditions, temperatures at the top of the active layer decrease from about -6°C in the south to about -20°C in the north (Taras et al. 2002). Not surprisingly, a decrease in both shrub abundance (CAVM 2003) and

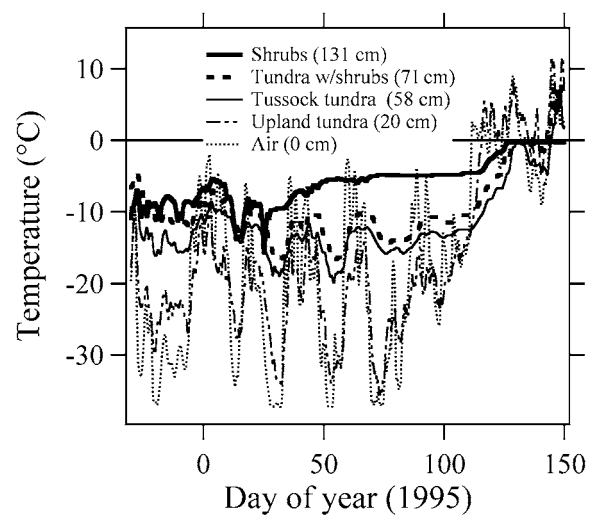


Figure 6. Active-layer surface temperatures as a function of vegetation type, including shrubs. The data are from the Kuparuk Basin in arctic Alaska. The average maximum winter snow depth for each type of vegetation is shown in the key.

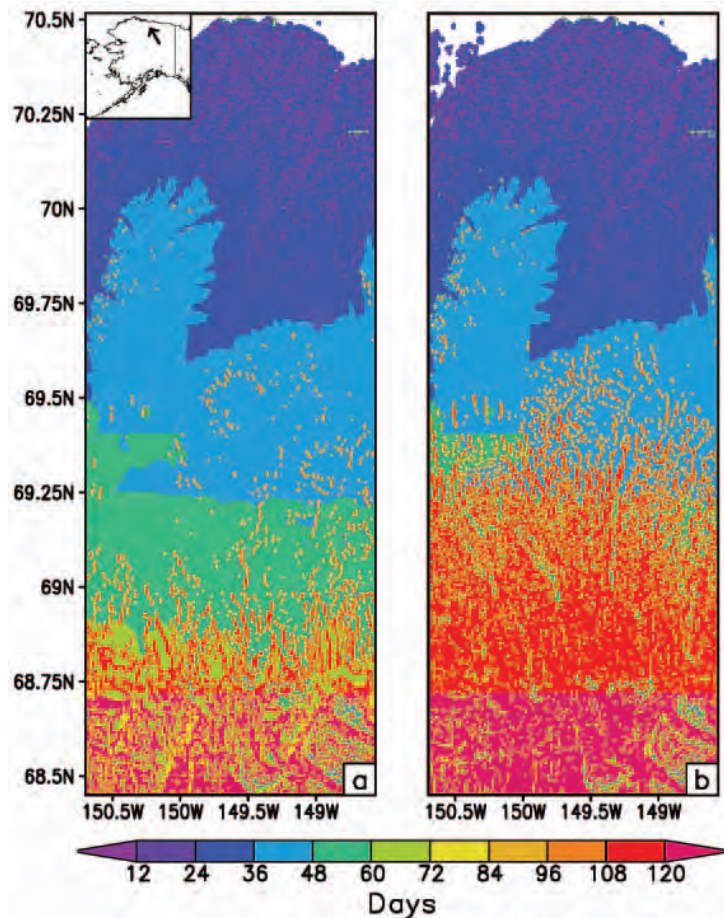


Figure 7. The Kuparuk Basin, showing a proxy index (number of days of microbial activity) for subsurface winter biological activity (a) under present conditions and (b) with projected increases in shrub growth. The index was computed by summing the number of days of the winter that the soil surface temperature is at or above -6 degrees Celsius (Taras et al. 2002). Note the strong latitudinal gradient in this index value. Snow depth increases as a function of vegetation growth, leading to significant increases in the index value, particularly in the middle and southern part of the basin.

winter microbial activity (as inferred from winter soil carbon dioxide [CO_2] efflux rates; Jones MH et al. 1999) are also observed along the same transect.

Model results (figure 7a) indicate under present-day conditions a tenfold decrease in the number of days that subsurface microbial activity takes place between the Brooks Range and the coast. This strong gradient is primarily the result of the snowfall gradient across the basin. Increasing the shrub height and abundance by 31% for moist tundra, 18% for moist-wet tundra, 6% for wet tundra, and 4% for shrublands (the amount of the increase dropping proportionately in those areas where shrubs are already affecting the snow depth or where the soil is too wet for shrubs; Liston et al. 2002) produced up to a 60-day increase in the number of days of winter soil microbial activity (compare figure 7a with figure 7b). The largest changes are in the middle of the basin. In the north, the change is limited because the soils are wet and

shrubs are unlikely to grow. In the south, they are limited because the shrubs are already tall and abundant. The results highlight that winter soil microbial activity is about equally sensitive to climate gradients and to changes in shrub cover. Changes in either factor can have a significant effect on the duration of winter activity and therefore affect the potential buildup of nutrients in winter.

Arctic microbial activity in winter

It is now well established that microbial (bacterial and fungal) respiration continues in arctic soils through the winter (Kelley et al. 1968, Zimov et al. 1993, Oechel et al. 1997, Fahnestock et al. 1999, Welker et al. 2000), along with nitrogen mineralization (Giblin et al. 1991, Grogan and Jonasson 2003, Weintraub and Schimel 2003). These activities are known to continue even in soils cooled to -10°C (Flanagan and Veum 1974, Clein and Schimel 1995, Mikan et al. 2002, Michaelson and Ping 2003), though for much of the winter the active layer is at a higher temperature (figures 4, 6, 7). Belowground plant biomass has been suggested as an alternate source of the observed respiration (Grogan et al. 2001), but this view is not widely held. Measured winter efflux rates range as high as 400 to 500 milligrams (mg) carbon as CO_2 per m^2 per day, though more typically they are 20 to 50 mg carbon as CO_2 per m^2 per day. Even the lower rates are sufficient to determine whether the ecosystem is a net sink (because of summer storage) or a net source to the atmosphere when extended over the long winter (Oechel et al. 1997). The efflux rates are closely linked to soil temperature (and unfrozen water content), and are higher where there are shrubs and deeper snow (Fahnestock et al. 1999).

An unusual shift in microbial substrate use takes place as arctic winter progresses and soil temperatures drop below freezing. The microbes living in the organic matter-rich surface soil begin to use less plant detritus and to rely more heavily on dissolved substrates and recycled microbial biomass and products. Our data indicate that the proportion of carbon respired from the microbial biomass and product pool roughly doubles, from 7% to 14% of the total respired carbon, as arctic soils freeze (figure 8a). Even though this substrate change is not very large in terms of carbon sourcing, it represents an important shift from nitrogen-poor plant detritus to nitrogen-rich microbial substrates of higher quality (Michaelson and Ping 2003) that may have bearing on the increasing abundance of shrubs. The shift helps ensure that higher rates of net nitrogen mineralization continue as soil temperatures drop (figure 8b). Interestingly, the shift occurs above 0°C (figure 8a).

The mechanism underlying the shift is not clear. We would have expected the shift to occur as the soil froze and the soil water system changed from a continuous water web to a set of discontinuous unfrozen water films. Following this transition, the microbes would have access only to (a) internal

resources, (b) dissolved substrate in the unfrozen films, and (c) substrate recycled from dying organisms (cryptic growth; Chapman and Gray 1986). Cut off from the plant and soil polymers they rely on during the summer (Michaelson and Ping 2003, Weintraub and Schimel 2003), the microbes would be expected to shift their use to the materials available in the water films. However, the shift occurs before the soil freezes, indicating that the change is due to some other physical or physiological mechanism, possibly one related to the dynamics of cellulolytic or lignolytic enzymes.

More directly related to shrubs, the substantial winter microbial respiration rates that have been observed are known to be aided by cryoturbation, the slow convective overturning of the active layer due to freeze–thaw heaving and settlement (figure 3). This process moves near-surface soil organic matter of relatively high quality into subsurface layers where it can be worked on by microbes during more of the winter. It is quite effective. Arctic Alaskan soils contain as much organic matter in subsurface layers as they do in surface organic horizons (Michaelson et al. 1996). Because these deeper layers stay warmer for a longer period of time (figure 4), and because they have a higher silt content, they contain unfrozen water films that are thicker and more abundant than those higher in the soil column (Romanovsky and Osterkamp 2000). The highest respiration rates in soil at below-freezing temperatures are found in subsurface layers containing the largest proportion of cryoturbated organic matter. Notably, the water-soluble organic substrates in mineral soils under shrubs are of higher quality than those found under tussock tundra (Michaelson and Ping 2003), one more reason why microbial action is enhanced where shrubs are more abundant.

A winter biophysical feedback loop

A positive feedback loop links snow, shrubs, soil, and microbes (figure 9). Active-layer temperatures in and around shrubs are higher than in shrub-poor locations (figure 6), resulting in enhanced winter microbial activity (figure 8) that persists through more of the winter. This results in more net nitrogen mineralization during winter (Schimel et al. 2004) and higher shrub leaf nitrogen content in summer. It also lowers the leaf carbon–nitrogen ratio, which may increase the decomposability of the leaf litter. For tundra, manipulation experiments (Chapin et al. 1995), point frame studies (Arft et al. 1999), and studies of latitudinal gradients in plant community composition (Bliss and Matveyeva 1992) indicate that where there are more nutrients, shrub growth is favored over that of other tundra plants. Larger and more abundant shrubs (figure 1) trap more snow (figure 5) and reduce winter sublimation losses, leading to deeper snow cover and still higher soil temperatures (figure 6).

The feedback loop was suggested (Sturm et al. 2001b) on the basis of colocated snow depth and shrub height measurements, but several links in the loop were speculative when it was first introduced. These links are now better established. They include evidence (a) that the microbes have access to substrate and unfrozen water through most of the

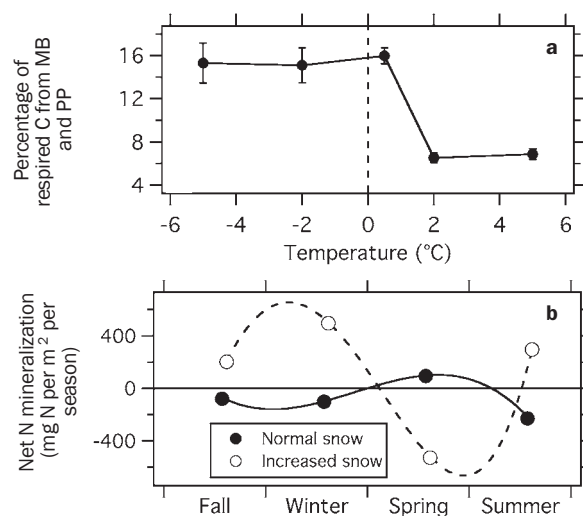


Figure 8. (a) Shift in microbial substrate use with temperature. Above 0 degrees Celsius ($^{\circ}\text{C}$), the microbes metabolize nitrogen-poor plant detritus, but below 0°C they rely more on nitrogen-rich microbial products. (b) Winter decomposition and nutrient mineralization for an area where the snow depth has been artificially enhanced compared with a control plot where it has not. Abbreviations: C, carbon; MB, microbial biomass; N, nitrogen; PP, product pool.

winter, (b) that as a result, microbial activity continues at below-freezing soil temperatures, (c) that the activity is due in part to a shift in substrate use by the microbes, (d) that even though winter rates of activity are lower than those of summer, the cumulative impact is a substantial contribution to the annual total because of the length the winter, and (e) that increasing the winter snow depth (i.e., accumulation in and around shrubs) produces greater net nitrogen nutrient mineralization (Schimel et al. 2004).

One link in the feedback loop remains untested. Does increased net winter nitrogen mineralization result in enhanced summer growth of shrubs? Summer fertilization of tundra leads to enhanced shrub growth (Chapin et al. 1995), so if winter-produced nutrients remain in place and are available to the plants the following growing season, the loop in figure 9 is closed. Do the nutrients stay put? During the spring thaw, active sheet wash and runoff could potentially strip or redistribute these nutrients. Because of the rapid nature of the thaw, however, arctic soils are typically still frozen during peak runoff. Moreover, most of the winter nutrient production takes place at depth in the active layer and is likely to be protected from redistribution. Initial indications based on studies using nitrogen-15 (Billbrough et al. 2000) also suggest that tundra plants can acquire soil nitrogen while the ground is still snow covered. We therefore think that the snow–shrub–soil–microbe feedback loop is contributing to the expansion of shrubs in the Arctic (figure 1; Sturm et al. 2001a) and may help explain why this expansion has coincided with winter warming (figure 2).

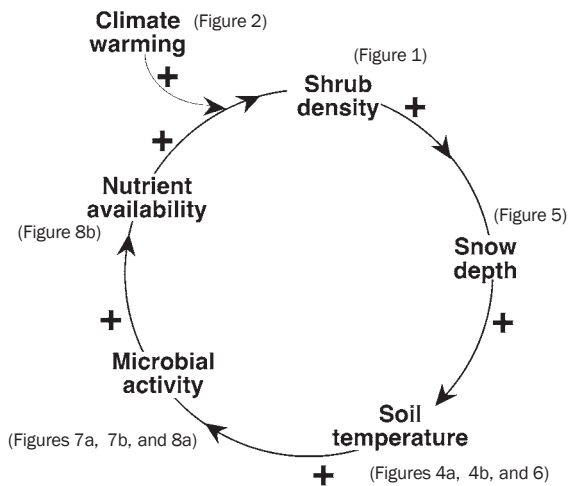


Figure 9. The snow–shrub–soil–microbe feedback loop (based on Sturm et al. 2001b).

Discussion and implications

Recent shrub expansion and invasion has been observed in semiarid grasslands and tallgrass prairies (Schlesinger et al. 1990, Archer et al. 2000, Lett and Knapp 2003, McCarron et al. 2003). While disturbance (grazing) or suppression of disturbance (fire) has played a role in establishing the shrubs in these lower-latitude ecosystems, climate-driven biological feedbacks similar to those described here have ensured that, once established, the shrubs have thrived. For example, Schlesinger and colleagues (1990) found that the introduction of shrubs in semiarid grasslands led to a localization of water and other soil resources under the shrubs, which had a positive feedback effect analogous to our results (figure 9). In a way that is eerily similar to the drifting of snow around shrubs on the tundra, they also found that the wind eroded material from the spaces between shrubs. This further differentiated the resources available to the vegetation. Lett and Knapp (2003) found that canopy shading, not soil source enrichment, maintained shrub dominance after shrubs were introduced to the tallgrass prairie. In both cases, however, positive feedbacks associated with a change in plant functional type (from low graminoids to erect and stiff shrubs) ensured the shrubs' success.

The competitive advantages of arctic shrubs are not limited to their physical architecture. They also have the highest potential for resource uptake of all the arctic plant functional groups, and they produce some of the most rapidly decomposable litter (Shaver et al. 1996). This is why within 10 years of a disturbance of the tundra by tracked vehicles, the disturbed areas are covered by shrubs, and why warmed and fertilized plots experience a relative explosion of shrubs (Chapin et al. 1995). With these attributes, shrubs are poised to take advantage of the current climate warming more readily than the other tundra plants. It may also explain why there have been several widespread expansions of shrubs

during the Holocene (Anderson and Brubaker 1993). What is less certain is how the current expansion might proceed, and whether it will actually convert the tundra into a shrubland. Shaver and colleagues (1992) have pointed out that the initial response of a tundra ecosystem to a change in climate is likely to be quite different from the response over decades or centuries. As the expansion of tundra shrubs continues and the shrubs occupy more of the landscape, canopies will thicken, leading to summer shading and a myriad of other effects that could produce fundamental changes in soil conditions. These could modify the winter feedback processes we have described here.

One aspect of the arctic tundra system that argues for more extensive rather than less extensive change is that the system is particularly susceptible to change because of the roles played by snow and permafrost in determining the soil conditions and microbial activity. Small shifts in ambient conditions (temperature, snow depth, or both) could produce large changes in the amount and distribution of unfrozen water in the soil and in the duration and timing of biological activity (figures 7, 8). This, in large measure, is because the system is balanced at the freezing point of water. This sensitivity is mirrored in Antarctica, where a whole cascade of terrestrial ecosystem changes has been observed in response to 20 years of cooling (Doran et al. 2002).

In table 2, by contrasting present-day tundra with shrubby tundra, we suggest some of the ecosystem changes that might ensue if shrub abundance continues to increase. The table is by no means comprehensive, but it does suggest that there would be important hydrologic, energy balance, and carbon budget ramifications. Changes in the carbon budget are likely to have global implications. Increased release of winter carbon due to greater soil microbial activity would compete with increased fixing of carbon in the form of woody plants to produce a balance that is difficult to predict. Of potentially greater impact, however, would be a secondary effect of a tundra-to-shrubland conversion: alteration of the thermal regime of the permafrost. This alteration could liberate large stores of carbon that are currently frozen and not participating in the carbon cycle (Michaelson et al. 1996). Not everything would change, of course. Wet meadow tundra is unlikely to turn shrubby, and places like Fenno-Scandia, where the tundra is already fairly shrubby, are likely to see only limited change. Still, a shrubby Arctic would be a markedly different place from the present-day Arctic covered by tundra.

The Arctic is locked in the grip of winter for two-thirds of the year, but biological activity continues to take place during that time. The results presented here suggest that these winter biological processes may be playing a crucial role in transforming the tundra landscape into shrubland. These results also challenge the view that plant community composition is controlled solely by competitive interactions during the growing season. If we want to predict how the current changes will play out in the future, and assess the ramifications of these changes, we are going to need year-round studies that link summer and winter biological activity.

Table 2. Key differences in properties between shrubby and nonshrubby tundra.

Properties	Nonshrub tundra	Shrub tundra
Snow depth/duration	Shallower/shorter	Deeper/longer; more snow runoff
Albedo	Higher	Lower
Summer active-layer depth	Deeper	Shallower (because of shading)
Summer active-layer temperature	Warmer	Cooler
Soil temperature	Higher in summer, lower in winter	Lower in summer, higher in winter
Nutrient (nitrogen) cycling	Faster	Slower
Carbon cycling	Faster	Slower
Caribou forage access and quality	Higher	Lower
Winter CO ₂ flux	Lower	Higher
Summer CO ₂ exchange	Lower	Higher

CO₂, carbon dioxide.

Acknowledgments

We thank Paul Brooks, Larry Hinzman, Jason Beringer, Terry Prowse, Walt Oechel, Michael Hunt-Jones, Terry Chapin, Gus Shavier, Chen Liu Ping, Chuck Racine, and others for helping us to refine our ideas concerning winter biological processes. Paul Grogan, Betsy Sturm, Skye Sturm, and Ken Tape made valuable suggestions on an earlier version of this paper. The comments of several anonymous reviewers greatly improved the manuscript. The ideas presented here are based on a series of studies supported by the Arctic System Science section of the National Science Foundation. Logistical support in the field was generously supplied by VECO Polar Resources and Toolik Lake Field Station (University of Alaska).

References cited

- Ager TA. 1983. Holocene vegetational history of Alaska. Pages 128–141 in Wright HE, ed. Late-Quaternary Environments of the United States, vol. 2: The Holocene. Minneapolis: University of Minnesota Press.
- Anderson DM, Morgenstern NR. 1973. Physics, chemistry and mechanics of frozen ground: A review. Pages 257–288 in Péwé TL, MacKay JR, eds. North American Contribution to the Proceedings of the Second International Conference on Permafrost, Yakutsk, USSR, July 1973. Washington (DC): National Academy of Sciences.
- Anderson PM, Brubaker LB. 1993. Holocene vegetation and climate histories of Alaska. Pages 386–400 in Wright HE, Kutzbach JE, Ruddiman WF, Street-Perrott FA, Bartlein P, eds. Global Climates since the Last Glacial Maximum. Minneapolis: University of Minnesota Press.
- Archer S, Boutton TW, Hibbard KA. 2000. Trees in grasslands: Biogeochemical consequences of woody plant expansion. Pages 115–137 in Schulze ED, Harrison SP, Heimann M, Holland EA, Lloyd J, Prentice IC, Schimel D, eds. Global Biogeochemical Cycles in the Climate System. San Diego: Academic Press.
- Arendt AA, Echelmeyer KA, Harrison WD, Lingle CS, Valentine VB. 2002. Rapid wastage of Alaska glaciers and their contribution to rising sea level. *Science* 297: 382–386.
- Arft AM, et al. 1999. Response patterns of tundra plant species to experimental warming: A meta-analysis of the International Tundra Experiment. *Ecological Monographs* 69: 491–511.
- Bilbrough C, Welker JM, Bowman WD. 2000. Early-spring N uptake by snow covered plants: A comparison of arctic and alpine plant function under snowpack. *Arctic, Antarctic, and Alpine Research* 32: 404–411.
- Bills LC, Matveyeva NV. 1992. Circumpolar arctic vegetation. Pages 59–89 in Chapin FS III, Jefferies RL, Reynolds JE, Shaver GR, Svoboda J, eds. Arctic Ecosystems in a Changing Climate: An Ecophysiological Perspective. San Diego: Academic Press.
- [CAVM] Circumpolar Arctic Vegetation Mapping Team. 2003. Circumpolar Arctic Vegetation Map. Anchorage (AK): US Fish and Wildlife Service. (16 November 2004; www.geobotany.uaf.edu/cavm/)
- Chapin FS, Shaver GR, Giblin AE, Nadelhoffer KJ, Laundre JA. 1995. Responses of arctic tundra to experimental and observed changes in climate. *Ecology* 73: 694–711.
- Chapman SJ, Gray TRG. 1986. Importance of cryptic growth, yield factors and maintenance energy in models of microbial growth in soil. *Soil Biology and Biochemistry* 18: 1–4.
- Chapman WL, Walsh JE. 1993. Recent variations of sea ice and air temperature in high latitudes. *Bulletin of the American Meteorological Society* 74: 33–47.
- Clein JS, Schimel JP. 1995. Microbial activity of tundra and taiga soils at sub-zero temperatures. *Soil Biology and Biochemistry* 27: 1231–1234.
- Doran PT, Prisou JC, Lyons WB, Walsh JE, Fountain AG, McKnight DM, Moorhead DL, Fritsen CH, McKay CP, Parsons AN. 2002. Antarctic climate cooling and terrestrial ecosystem response. *Nature* 415: 517–520.
- Fahnestock JT, Jones MH, Welker JM. 1999. Wintertime CO₂ efflux from arctic soils: Implications for annual carbon budgets. *Global Biogeochemical Cycles* 13: 775–779.
- Fahnestock JT, Povirk KL, Welker JM. 2000. Ecological significance of litter redistribution by wind and snow in arctic landscapes. *Ecography* 23: 623–631.
- Farouki OT. 1981. Thermal Properties of Soils. Hanover (NH): US Army Cold Regions Research and Engineering Laboratory. Monograph 81-1.
- Flanagan PW, Veum AK. 1974. Relationships between respiration, weight loss, temperature and moisture in organic residues on tundra. Pages 249–277 in Holding AJ, Heal OW, MacLean SF Jr, Flanagan PW, eds. Soil Organisms and Decomposition in Tundra. Stockholm: Tundra Biome Steering Committee.
- Giblin AE, Nadelhoffer KJ, Shaver GR, Laundre JA, McKerron AJ. 1991. Biogeochemical diversity along a riverside toposequence in arctic Alaska. *Ecological Monographs* 61: 415–435.
- Grogan P, Jonasson S. 2003. Controls on annual nitrogen cycling in the understorey of a sub-arctic birch forest. *Ecology* 84: 202–218.
- Grogan P, Illeris L, Michelsen A, Jonasson S. 2001. Respiration of recently-fixed plant carbon dominates mid-winter ecosystem CO₂ production in sub-arctic heath. *Climatic Change* 50: 129–142.
- Haugen RK. 1982. Climate of remote areas in north-central Alaska: 1975–1979. Washington (DC): US Army Cold Regions Research and Engineering Laboratory. CRREL Report 82-35.
- Hinzman LD, Kane DL, Benson CS, Everett KR. 1991. Hydrologic and thermal properties of the active layer in the Alaskan Arctic. *Cold Regions Science and Technology* 19: 95–110.

- [IPCC] Intergovernmental Panel on Climate Change. 2001. *Climate Change 2001: The Scientific Basis*. Geneva: UN Environment Programme–World Meteorological Organization.
- Jia GJ, Epstein HE, Walker DA. 2003. Greening of the Alaskan Arctic over the past two decades. *Geophysical Research Letters* 30: 2067.
- Jones MH, Fahnestock JT, Welker JM. 1999. Early and late winter CO₂ efflux from arctic tundra in the Kuparuk River watershed, Alaska, U.S.A. *Arctic, Antarctic, and Alpine Research* 31: 187–190.
- Jones PD, New M, Parker DE, Martin S, Rigor IG. 1999. Surface air temperature and its changes over the past 150 years. *Reviews of Geophysics* 37: 173–199.
- Kelley JJ, Weaver DF, Smith BP. 1968. The variation of carbon dioxide under the snow in the Arctic. *Ecology* 49: 358–361.
- Kunz ML, Reanier RE. 1994. Paleoindians in Beringia: Evidence from arctic Alaska. *Science* 263: 660–662.
- Lett MS, Knapp AK. 2003. Consequences of shrub expansion in mesic grassland: Resource alterations and graminoid responses. *Journal of Vegetation Science* 14: 487–496.
- Liston GE, Sturm M. 1998. A snow-transport model for complex terrain. *Journal of Glaciology* 44: 498–516.
- . 2002. Winter precipitation patterns in arctic Alaska determined from a blowing snow model and snow depth observations. *Journal of Hydrometeorology* 3: 646–659.
- Liston GE, McFadden JP, Sturm M, Pielke SRA. 2002. Modeled changes in arctic tundra snow, energy, and moisture fluxes due to increased shrubs. *Global Change Biology* 8: 17–32.
- MacDonald GM, et al. 2000. Holocene treeline history and climate change across northern Eurasia. *Quaternary Research* 53: 302–311.
- McCarron JK, Knapp AK, Blair JM. 2003. Soil C and N responses to woody plant expansion in a mesic grassland. *Plant and Soil* 257: 183–192.
- Michaelson GJ, Ping CL. 2003. Soil organic carbon and CO₂ respiration at subzero temperature in soils of Arctic Alaska. *Journal of Geophysical Research—Atmospheres* 108 (D2): 8164 (doi: 10.1029/2001JD000920).
- Michaelson GL, Ping CL, Kimble JM. 1996. Carbon storage and distribution in tundra soils of arctic Alaska, U.S.A. *Arctic and Alpine Research* 28: 414–424.
- Mikan CJ, Schimel JP, Doyle AP. 2002. Temperature controls of microbial respiration above and below freezing in arctic tundra soils. *Soil Biology and Biochemistry* 34: 1785–1795.
- Myneni RB, Keeling CD, Tucker CJ, Asrar G, Nemani RR. 1997. Increased plant growth in the northern high latitudes from 1981 to 1991. *Nature* 386: 698–702.
- Oechel WC, Vourlitis GL, Hastings SJ. 1997. Cold-season CO₂ emission from arctic soils. *Global Biogeochemical Cycles* 11: 163–172.
- Oechel WC, Vourlitis GL, Hastings SJ, Zulueta RC, Hinzman LD, Kane DL. 2000. Acclimation of ecosystem CO₂ exchange in the Alaskan Arctic in response to decadal climate warming. *Nature* 406: 978–981.
- Olsson PQ, Hinzman LD, Sturm M, Liston GE, Kane DL. 2002. *Surface Climate and Snow-Weather Relationships of the Kuparuk Basin on Alaska's Arctic Slope*. Fort Belvoir (VA): US Army Engineer Research and Development Center, Cold Regions Research and Engineering Laboratory. Technical Report 02-10.
- Olsson PQ, Sturm M, Racine CH, Romanovsky V, Liston GE. 2003. Five stages of the Alaskan Arctic cold season with ecosystem implications. *Arctic, Antarctic, and Alpine Research* 35: 74–81.
- Overpeck J, et al. 1997. Arctic environmental change of the last four centuries. *Science* 278: 1251–1256.
- Owen-Smith N. 1987. Pleistocene extinctions: The pivotal role of mega-herbivores. *Paleobiology* 13: 351–362.
- Parkinson CL, Cavalieri DJ, Gloersen P, Zwally HJ, Comiso JC. 1999. Arctic sea ice extents, areas, and trends. *Journal of Geophysical Research* 104: 20837–20856.
- Peterson BJ, Holmes RM, McClelland JW, Vörösmarty CJ, Lammers RB, Shiklomanov AI, Shiklomanov IA, Rahmstorf S. 2002. Increasing river discharge to the Arctic Ocean. *Science* 298: 2171–2173.
- Romanovsky VE, Osterkamp TE. 2000. Effects of unfrozen water on heat and mass transport processes in the active layer and permafrost. *Permafrost and Periglacial Processes* 11: 219–239.
- Romanovsky VE, Burgess M, Smith S, Yoshikawa K, Brown J. 2002. Permafrost temperature records: Indicators of climate change. *EOS, AGU Transactions* 83: 589–594.
- Schimel JP, Bilbrough C, Welker JM. 2004. The effect of increased snow depth on microbial activity and nitrogen mineralization in two Arctic tundra communities. *Soil Biology and Biochemistry* 36: 217–227.
- Schlesinger WH, Reynolds JF, Cunningham GL, Huenneke LF, Jarrell WM, Virginia RA, Whitford WG. 1990. Biological feedbacks in global desertification. *Science* 247: 1043–1048.
- Sellman PV, Brown J, Lewellen RI, McKim H, Merry C. 1975. *The Classification and Geomorphic Implications of Thaw Lakes on the Arctic Coastal Plain, Alaska*. Hanover (NH): US Army Cold Regions Research and Engineering Laboratory.
- Serreze MC, Walsh JE, Chapin FS, Osterkamp T, Dyrgerov M, Romanovsky V, Oechel WC, Morison J, Zhang T, Barry RG. 2000. Observational evidence of recent climate change in the northern high-latitude environment. *Climatic Change* 46: 159–207.
- Shaver GR, Billings WD, Chapin FS, Giblin AE, Nadelhoffer KJ, Oechel WC, Rastetter EB. 1992. Global change and the carbon balance of arctic ecosystems. *BioScience* 42: 433–441.
- Shaver GR, Giblin AE, Nadelhoffer KJ, Rastetter EB. 1996. Plant functional types and ecosystem change in arctic tundras. Pages 152–172 in Smith T, Woodward I, Shugart H, eds. *Plant Functional Types*. Cambridge (United Kingdom): Cambridge University Press.
- Shvartsman YG, Barzut VM, Vidyakina SV, Iglovsky SA. 1999. Climate variations and dynamic ecosystems of the Arkhangelsk region. *Chemosphere: Global Change Science* 1: 417–428.
- Silapaswan CS, Verbyla DL, McGuire AD. 2001. Land cover change on the Seward Peninsula: The use of remote sensing to evaluate potential influences of climate warming on historical vegetation dynamics. *Canadian Journal of Remote Sensing* 27: 542–554.
- Stow DA, et al. 2004. Remote sensing of vegetation and land-cover change in arctic tundra ecosystems. *Remote Sensing of Environment* 89: 281–308.
- Sturm M, Racine CR, Tape K. 2001a. Increasing shrub abundance in the Arctic. *Nature* 411: 546–547.
- Sturm M, McFadden JP, Liston GE, Chapin FS, Racine CH, Holmgren J. 2001b. Snow–shrub interactions in Arctic tundra: A hypothesis with climatic implications. *Journal of Climate* 14: 336–344.
- Sturm M, Perovich DK, Serreze M. 2003. Melt-down in the North. *Scientific American* (October): 60–67.
- Taras B, Sturm M, Liston GE. 2002. Snow–ground interface temperatures in the Kuparuk River Basin, Arctic Alaska: Measurements and model. *Journal of Hydrometeorology* 3: 377–394.
- Thorpe N, Eyegetok S, Hakongak N, Elders K. 2002. Nowadays it is not the same: Inuit Quajimajatuqangit, climate and caribou in the Kitikmeot region of Nunavut, Canada. Pages 198–239 in Krupnik I, Jolly D, eds. *The Earth Is Faster Now: Indigenous Observations of Arctic Environmental Change*. Fairbanks (AK): Arctic Research Consortium of the United States.
- Weintraub M, Schimel JP. 2003. Interactions between carbon and nitrogen mineralization and soil organic matter chemistry in arctic tundra soils. *Ecosystems* 6: 129–143.
- Welker JM, Fahnestock JT, Jones MH. 2000. Annual CO₂ flux from dry and moist arctic tundra: Field responses to increases in summer temperature and winter snow depth. *Climatic Change* 44: 139–150.
- Zimov SA, Zimova GM, Daviodov SP, Daviodova AI, Voropaev YV, Voropaeva ZV, Prosiannikov SE, Prosiannikova OV. 1993. Winter biotic activity and production of CO₂ in Siberian soils: A factor in the greenhouse effect. *Journal of Geophysical Research* 98: 5017–5023.